ChemMedChem

Review
doi.org/10.1002/cmdc.202400194

Chemistry
Europe
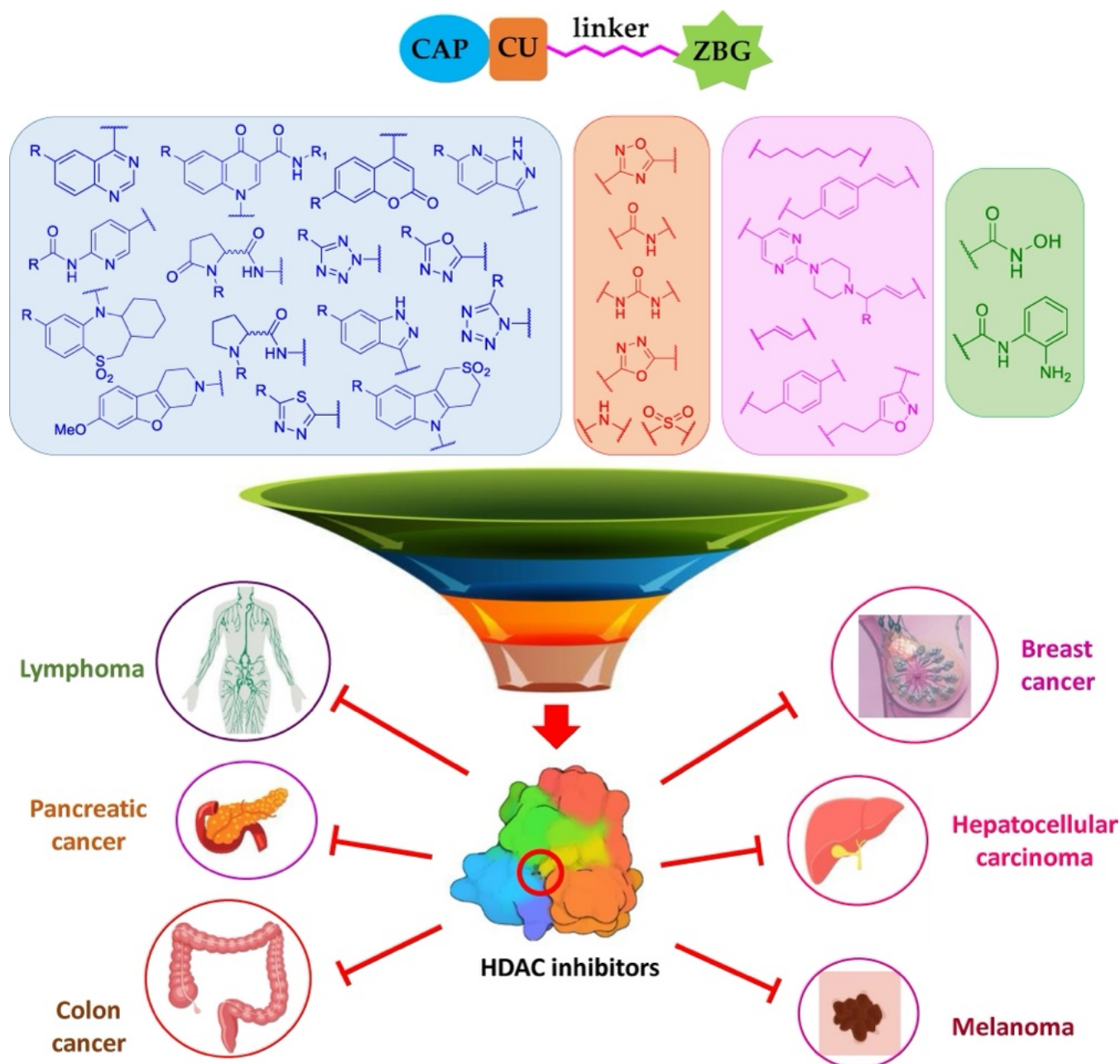European Chemical
Societies Publishing

www.chemmedchem.org

Heterocycles–Containing HDAC Inhibitors Active in Cancer: An Overview of the Last Fifteen Years

Alessia Raucci+,[a] Carola Castiello,[a] Antonello Mai,[a, b] Clemens Zwergel,*[a] and Sergio Valente*[a]

ChemMedChem

Review
doi.org/10.1002/cmdc.202400194

**Chemistry
Europe**
European Chemical
Societies Publishing

Cancer is one of the primary causes of mortality worldwide. Despite nowadays are numerous therapeutic treatments to fight tumor progression, it is still challenging to completely overcome it. It is known that Histone Deacetylases (HDACs), epigenetic enzymes that remove acetyl groups from lysines on histone's tails, are overexpressed in various types of cancer, and their inhibition represents a valid therapeutic strategy. To date, some HDAC inhibitors have achieved FDA approval. Nevertheless, several other potential drug candidates have been developed. This review aims primarily to be comprehensive of the studies done so far regarding HDAC inhibitors bearing heterocyclic rings since their therapeutic potential is well known and has gained increasing interest in recent years. Hence, inserting heterocyclic moieties in the HDAC-inhibiting scaffold can be a valuable strategy to provide potent and/or selective compounds. Here, in addition to summarizing the properties of novel heterocyclic HDAC inhibiting compounds, we also provide ideas for developing new, more potent, and selective compounds for treating cancer.

1. Introduction

The Post-translational modifications (PTMs) have now become increasingly important due to their dynamic role in defining an opened (euchromatin) or closed (heterochromatin) state of the chromatin,[1] thereby regulating its structure and functions.[2] These modifications can occur on histone or non-histone proteins, and among them, acetylation, and therefore deacetylation, are the most common and studied ones, playing a pivotal role in gene expression and regulation.[3] Consequently, the acetylation status of histones is of pivotal importance in investigating the potential role of (de)acetylating enzymes on the onset of various pathologies.

HDACs are a class of enzymes that catalyze the removal of the acetyl group from lysine residues in the histone tails, leading to chromatin remodeling.[3] In particular, the removal of the acetyl group causes chromatin condensation due to the interaction between the positive charge of the Nitrogen of the deacetylated histone amine and the negatively charged DNA strand.[4] This interaction hampers the access to transcription factors and ultimately leads to transcription repression. Therefore, HDACs are important enzymes that regulate gene expression.[5] Among HDAC substrates, there are not only lysines on histone tails but also non-histone proteins, such as transcription factors, cytoskeletal proteins, molecular chaperones, and nuclear import factors, covering a broad range of biological processes.[6]

HDAC family can be divided into four different classes: class I (HDAC 1, 2, 3, 8), class IIa (HDAC 4, 5, 7, 9) and IIb (HDAC 6, 10), class III and class IV (HDAC 11). The deacetylase members of class III are the non-canonical HDACs called Sirtuins, which consist of 7 isoforms and catalyze the deacetylation reaction in a different way. Indeed, the canonical HDACs operate with a Zn^{2+}-dependent mechanism to remove acetyl groups;[7] contrariwise, the Sirtuin family requires NAD^+ as a cofactor for their activity.[8]

HDACs are key enzymatic components of the transcription-silencing machinery, and their activity is crucial for cell proliferation, differentiation, and homeostasis.[3] For this reason, their dysregulation can lead to the insurgence of various diseases, including cancer, where HDACs altered expression is implicated in promoting migration, angiogenesis, proliferation, and resistance to chemotherapy, as well as preventing differentiation and apoptosis.[5b,9] It was also shown that HDACs play diverse roles in plenty of diseases, such as neurodegenerative diseases,[10] cardiovascular diseases,[11] inflammation, and innate immune response,[12] where the balance between these enzymes and their acetylating counterpart (histone acetylases, HATs) is impaired.[13] Therefore, HDACs currently represent potential therapeutics to be targeted in order to ameliorate patients' outcome.

Over the years, increasing interest has been shown towards the discovery of HDAC inhibitors,[14] and to date, several of them have entered clinical trials, and five compounds have been approved by the FDA. All inhibitors share the same pharmacophore structure, validated through the years via crystal structure analysis[15] and accepted as the lead to be followed to inhibit HDACs. The pharmacophore model is shown in Figure 1 and comprises a Zn^{2+} binding group (ZBG), which inserts in the catalytic cleft of the enzyme exerting its mechanism of action, a hydrophobic linker that places in the hydrophobic tunnel connecting the active site to the external part, a connecting unit (CU) that typically is represented by a carbonyl group or by a heterocyclic ring, and an aromatic or heteroaromatic cap group, the so-called surface recognition domain, which can either interact with the external part of the enzyme or be exposed to the solvent.[16]

[a] A. Raucci,[+] C. Castiello, A. Mai, C. Zwergel, S. Valente
    Department of Drug Chemistry and Technologies, Sapienza University of Rome, Piazzale Aldo Moro 5, 00185 Rome, Italy
    E-mail: clemens.zwergel@uniroma1.it
        sergio.valente@uniroma1.it

[b] A. Mai
    Pasteur Institute, Cenci Bolognetti Foundation, Sapienza University, Piazzale Aldo Moro 5, 00185, Rome, Italy

[+] *Equal contribution*

Figure 1. Pharmacophore model for HDAC inhibitors.

ChemMedChem

Review

doi.org/10.1002/cmdc.202400194

Chemistry
Europe
European Chemical
Societies Publishing

HDAC inhibitors can be classified according to their zinc-binding group into hydroxamic acids, 2-aminoanilides, aliphatic acids, electrophilic ketones, and more. The first two classes are the most common in both clinical and preclinical studies and show a high affinity for the zinc ion, thereby resulting in higher potency.[17] Nonetheless, they are non-selective over the different HDAC's isoforms as they share the catalytic site's sequence and structure. Hence, numerous efforts were made in order to investigate whether changes in the cap or in the linker could provide a better selectivity, as there are structural differences in the loop regions of the linker and in the external area around the entrance of the active site.[16a,18] Moreover, several investigations were made on the ZBG through computational studies in order to gain insights into the active site and develop non-hydroxamate zinc-binding groups bearing compounds with improved isoform selectivity while still maintaining their binding affinity.[16b,19]

In this review, we summarize some of the structural changes described in the scientific literature applied to the HDAC inhibiting moiety. In more detail, we analyzed numerous inhibitors bearing heteroaromatic rings occurring both in the cap and in the linker region, possessing one of the most promising ZBGs, either a hydroxamate or an anilide.

2. HDAC Inhibitors in Clinical Trials

To date, five HDAC inhibitors have been approved by the FDA for different therapies: Vorinostat (**1**), Romidepsin (**2**), Panobinostat (**3**), Belinostat (**4**), and the last approved Givinostat (**5**). Tucidinostat (**6**) has been approved by the China Food and Drug Administration (CFDA) and the Japanese Pharmaceuticals and Medical Devices Agency (PMDA) (Figure 2).

Vorinostat (**1**) (Zolinza®), also known as SAHA, was the first HDAC inhibitor with hydroxamate-based ZBG approved by the FDA in 2006 for the treatment of patients with cutaneous T-cell lymphoma (CTCL) that were refractory or intolerant to other treatments.[20] Vorinostat is a pan-HDAC inhibitor that inhibits all Zn^{2+}-dependent HDACs with nanomolar activity, impairing tumor cell growth in a wide range of tumor cells and inducing cellular differentiation;[21] this non-selectivity is probably due to its very simple structure with a linear aliphatic linker and an aromatic ring cap (Figure 3). Moreover, it belongs to class IV of the Biopharmaceutical Classification System, being low water soluble and low cell-permeable, and it is highly metabolized by glucuronidation and oxidative cleavage, thereby having a low oral bioavailability. For this reason, in the beginning, it was
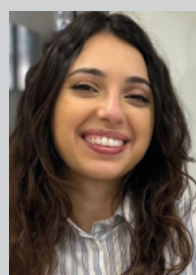
Alessia Raucci graduated from Sapienza University of Rome (Italy) with a degree in Medicinal Chemistry in 2022. Her thesis, under the supervision of Prof. Antonello Mai, focused on the synthesis and biological evaluation of dual inhibitors of epigenetic enzymes and immunological targets. She is currently in her second year as research assistant in the same research group where she works on developing small-molecule compounds for epigenetic and immunological targets.

Carola Castiello graduated from Sapienza University of Rome (Italy) with a degree in Medicinal Chemistry in 2020. Her thesis, under the supervision of Prof. Antonello Mai, focused on the synthesis and biological evaluation of dual inhibitors that target epigenetic enzymes. In 2021, she worked in the same group as a research assistant. She is now a Ph.D. student in Pharmaceutical Sciences under the supervision of Prof. Mai and works on the design and synthesis of multitarget small-molecule compounds for epigenetic targets.

Antonello Mai graduated from Sapienza University of Rome (Italy) with a degree in Pharmacy in 1984. He received his Ph.D. in Pharmaceutical Sciences in 1992. In 1998, he was appointed Associate Professor of Medicinal Chemistry and to Full Professor in 2011 at the same university. He published more than 300 papers in peer-reviewed high-impact-factor journals. His research interests include the synthesis and biological evaluation of new bioactive small-molecule compounds, in particular epigenetic modulators with applications in cancer, metabolic disorders, neuro-degenerative diseases, and parasitic infections. In addition, he works in the fields of anti-bacterial or antimycobacterial, antiviral, and CNS agents.

Clemens Zwergel is currently Assistant Professor at the Department of Drug Chemistry and Technologies, Sapienza University of Rome. In the last years, he proved to be a true European citizen: he moved after his license to practice as a Pharmacist in Germany to Exeter (UK) for a Diploma in Pharmaceutical Sciences. Before moving to Italy, he was then a Marie Curie fellow in France (Metz), where he obtained his EuroPhD within the RedCat network. Since 2010, his main research interest lies mainly in the drug design of epigenetic and non-epigenetic enzymes with potential applications in cancer, neurodegenerative, metabolic, and infectious diseases.
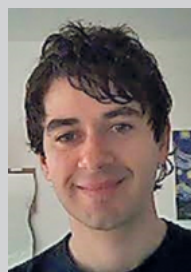
Sergio Valente is currently Associate Professor at the Department of Drug Chemistry and Technologies, Sapienza University of Rome. He received a degree in Pharmacy and obtained his Ph.D. at the same university. He completed his postdoctoral research period in medicinal chemistry within the REDCAT Marie Curie project at the University of Lorraine-Metz, France. Back in Italy, from 2011 to 2020, he was an Assistant Professor in Medicinal Chemistry at Sapienza University. His main research activities focus on the design and synthesis of small molecules as epigenetic target modulators. Recently, he started working on novel chemical probes for chemo-proteomic studies.
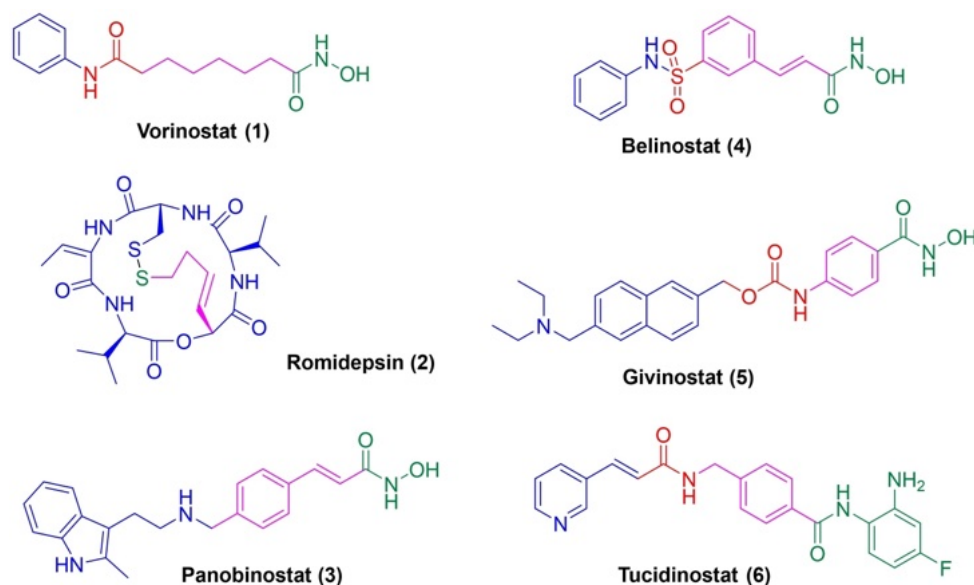
ChemMedChem

Review
doi.org/10.1002/cmdc.202400194

Chemistry
Europe
European Chemical
Societies Publishing

Figure 2. The five approved HDAC inhibitors and Tucidinostat. The different colors refer to the pharmacophore model shown above in Figure 1: cap is blue, CU is red, linker is pink, and ZBG is green.
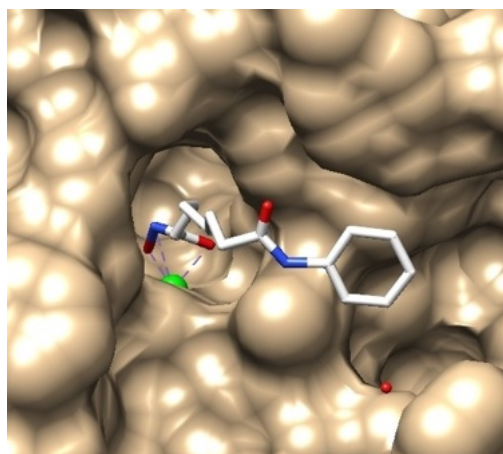

Figure 3. Representation of Vorinostat binding mode in HDACs active site. The hydroxamate group coordinates the Zn^{2+} ion (green) at the end of the cavity.[16c] Carbon atoms are colored in grey, oxygen in red, and nitrogen in blue.

administered intravenously, while later on, an oral formulation was developed that is currently used.[14,22]

Subsequent to Vorinostat, various hydroxamate-based HDAC inhibitors have been developed and are promising candidates to enter clinical trials, following the aliphatic and non-rigid linker lead. Among them, there are inhibitors bearing heterocyclic moieties in the cap region, as shown in Figure 4.

Ricolinostat (**7**), investigated for its activity in multiple myeloma (MM), where it ameliorated the patients' survival, deferring the progress of the disease, has a bulky cap moiety containing a diphenylamine pyrimidine connected to the aliphatic linker with an amide group.[23] Citarinostat (**8**), in phase 1b clinical trial for the treatment of MM, bears the same structure as Ricolinostat with the addition of a chlorine atom, which enhances the solubility and the bioavailability of the

compound.[24] The pharmacophoric moiety of Vorinostat (**1**)was also crucial in the development of dual targeting molecular hybrids.[25] CUDC-101 (**9**) is an HDAC/EGFR-HER2 dual-targeting hybrid containing a 3-ethynylphenylamino-7-methoxyquinazoline structure resembling the scaffold of the drug Erlotinib.[26] Tinostamustine (**10**) is another example of a Vorinostat-based dual inhibitor, representing the combination of Vorinostat and the well-known alkylating agent Bendamustine,[27] approved for the treatment of leukemia and non-Hodgings lymphomas. It has the classical alkylating agent moiety with the bischloroethyl amine, connected to the methylene chain with a methyl benzimidazole. All these molecules represent a good example of how using heterocyclic and more constrained moieties can be a potential approach for designing novel, efficient molecules for treating cancer.

Romidepsin (**2**) (Istodax®), a natural cyclic depsipeptide, was the second HDAC inhibitor approved by the FDA for the treatment of CTCL and peripheral T-cell lymphoma (PTCL). It is specific for the nuclear HDAC1-3 at nanomolar levels, and it is activated *in vivo* by the reduction of the dithiol to its active form.[28]

In 2015, the FDA approved Panobinostat (**3**) (Farydak®), an orally active pan-HDAC inhibitor for the treatment of Relapsed and Refractory Multiple Myeloma (RRMM).[29] Panobinostat is the only HDAC inhibitor approved for RRMM so far, and it is used in combination with other agents in multiple clinical studies.[20] It is a cinnamic hydroxamate-based inhibitor bearing a 2-methyl-3-ethylamine indole in the cap region, demonstrated to be a very efficient compound in several cancer cell lines.[30] The structurally related Belinostat (**4**) (Beleodaq®) was approved for the treatment of PTCL.[31] Other cinnamyl hydroxamate derivatives structurally similar to Panobinostat are in clinical trials (Figure 5): Resminostat (**11**),[32] a low micromolar class I, IIb, and IV selective inhibitor, has been used in clinical
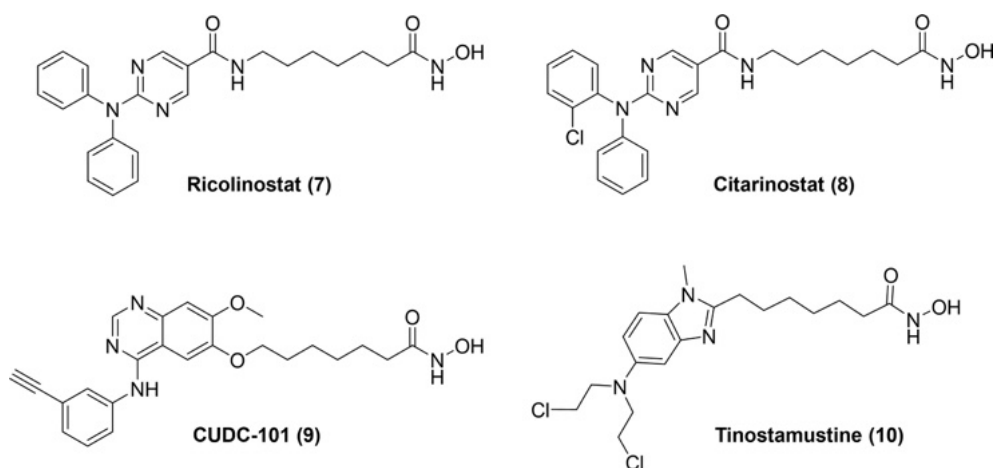
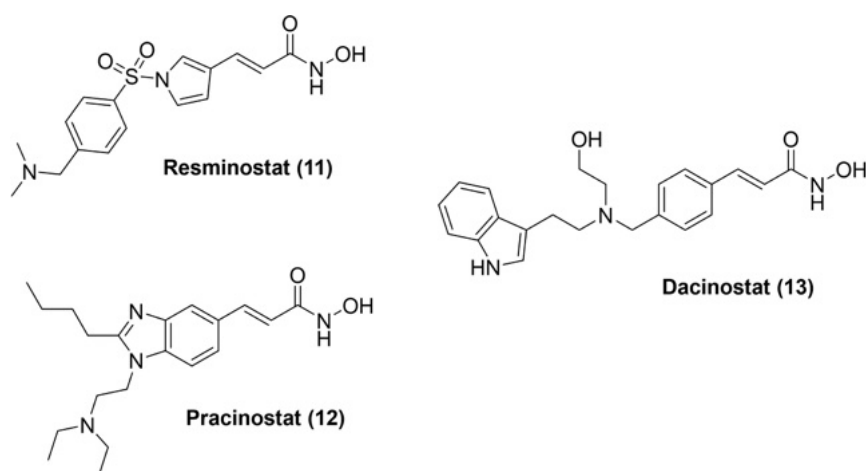**Figure 4.** Vorinostat-based HDAC inhibitors with heterocyclic cap.

Figure 5. Cinnamic hydroxamate-based HDAC inhibitors in clinical trials.

trials for hepatocellular carcinoma and Hodgkin's lymphoma;[33] Pracinostat also known as SB939 (**12**), used for patients with solid tumors and hematologic malignancies[34] has favorable pharmacokinetic properties and leads to a strong hyperacetylation induction in tumor models, as a result of its notable HDAC inhibitory effect.[34a] Dacinostat (**13**) is a submicromolar pan HDAC inhibitor against multiple myeloma.[35] In **11** and **12**, the polymethylene spacer of Vorinostat is replaced with a cinnamoyl group in the linker region, and the cap bears bulkier moieties.

After Vorinostat, which has a rather simple structure, more hydroxamate-based inhibitors, now clinical candidates containing more complicated and rigid heterocyclic moieties, were developed to explore the binding pockets of the various HDAC isoforms with the goal of gaining more selectivity. Some of these compounds are shown in Figure 6.

Of note, Givinostat (**5**) (Duvyzat®) was recently approved by the FDA, unlike the other approved HDACi for the non-cancerous disease Duchenne muscular dystrophy (DMD).[37] **5** is a pan HDACi that bears a hydroxamate as a ZGB linked by a carbamate moiety to a diethylamino naphthyl ring. The drug led to decreased inflammatory infiltration and reduced fibrotic scars in a mouse model of Duchenne muscular dystrophy.[38] Considering the good results of a phase 2 trial, givinostat increased the fraction of muscle tissue and reduced the portion of fibrosis and necrosis.[39] The drug was approved by the FDA after a phase III trial in 179 DMD patients, during which a marked deceleration of the spread of the disease was observed.

Tucidinostat (**6**) (Epidaza®), approved by the CFDA and the Japanese PDMA for the treatment of PTCL,[40] is an orally bioavailable drug containing a pyridine acrilamide moiety in the cap region while presenting an aminobenzamide group as Zn^{2+}-coordinator. It has a submicromolar inhibiting activity, weaker in comparison with the hydroxamate binding group, probably due to a tighter and slower binding of the aminobenzamide group within the HDAC's active pocket respect to the fast interaction displayed by the hydroxamate group.[41] Indeed, the ortho-aminoanilides show a slow-on/slow-off kinetic with a tight-binding mechanism. This class of HDAC inhibitors is selective for the isoforms 1–3 while being poorly active against HDAC6 and −8.[22] Entinostat (MS-275) (Figure 7, **20**) was the first molecule of this class to reach clinical trials. It is a class I-
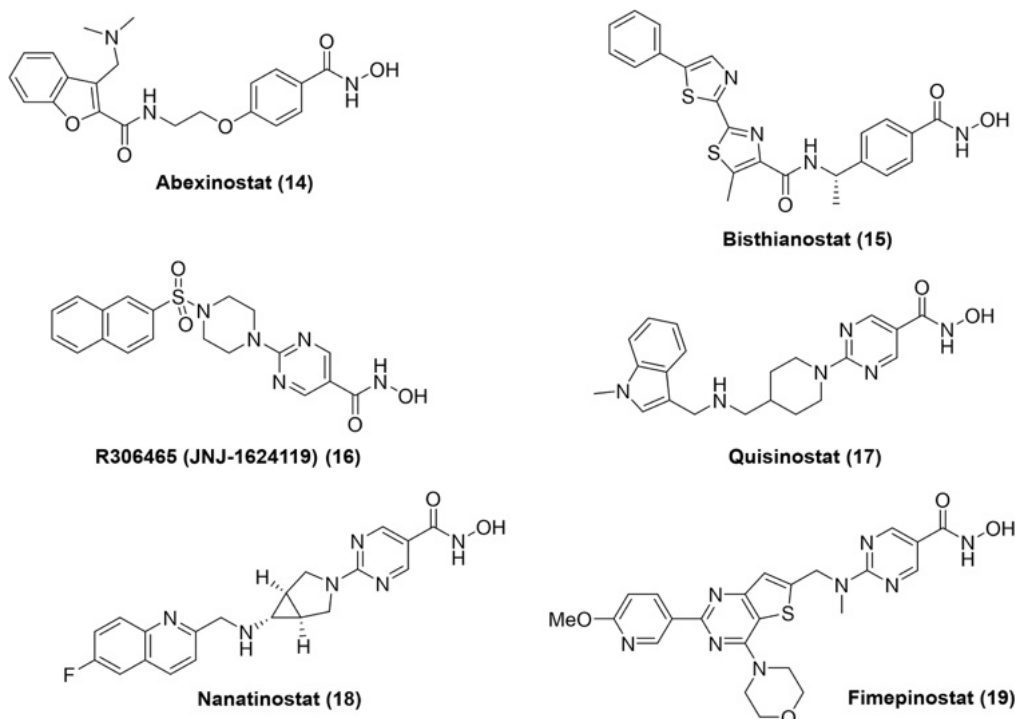
Figure 6. Clinical candidates HDAC inhibitors: **14** and **15** with a phenylhydroxamic acid; **16**, **17**, **18**, and **19** containing a pyrimidinyl hydroxamic acid.[14,36]
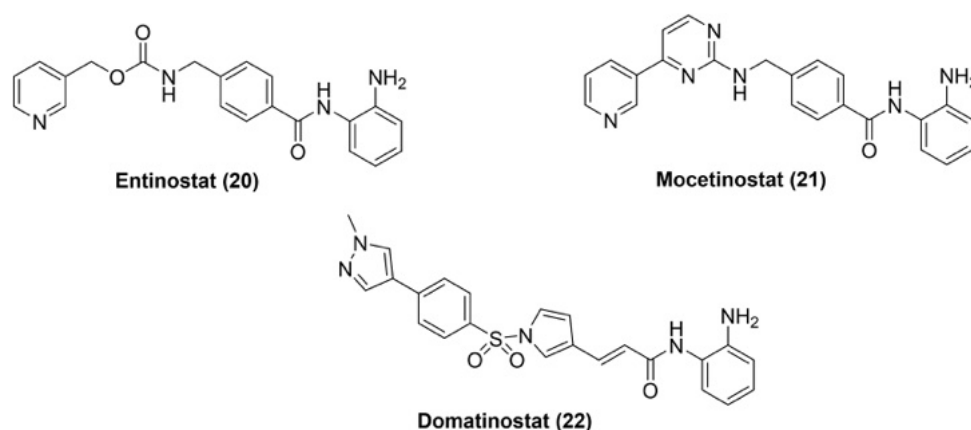

Figure 7. 2-aminoanilides HDAC inhibitors in clinical studies.

selective inhibitor with an inhibitory activity in the low micro-molar (IC$_{50}$ = 2 μM) range in clinical studies for patients with advanced and refractory solid tumors or lymphoma.[42] It has been demonstrated to hamper tumor cell proliferation in different xenograft models; nevertheless, it has a low therapeutic index, probably due to off-target effects or poor pharmacokinetic properties.[22,42] This class also includes Mocetinostat (**21**)[43] and Domatinostat (**22**),[44] both showing good antiproliferative activities in a wide range of tumors.[14]

3. HDAC inhibitors with Heterocyclic Scaffold

Nowadays, heterocyclic compounds have gained increasing interest in medicinal chemistry for their therapeutic potential. Indeed, various heterocyclic moieties are included in well-known drugs, such as antimicrobial or antitumor agents. Moreover, the presence of a heteroatom in the scaffold can influence the pharmacodynamic and pharmacokinetic properties of the drug, giving more opportunities to medicinal chemists to investigate the interaction and, therefore, the specificity of the molecule. Substituting carbon rings with bioisosteric heterocyclic ones can lead to more active and less toxic molecules, amplifying the possibilities for finding new

ChemMedChem

Review
doi.org/10.1002/cmdc.202400194

Chemistry Europe
European Chemical
Societies Publishing

therapeutic agents with increased bioavailability and reduced side effects.[45]

To date, many HDAC inhibitors with heterocyclic moieties have been synthesized in order to explore the enzyme's regions and gain more selectivity and potency. Here, we focus on the changes in the cap and linker regions, differentiating the newly developed molecules by their ZBG.

3.1. Hydroxamic Acid–based HDAC Inhibitors

The hydroxamic acid is the most common ZBG used in HDAC inhibitors. It has a strong binding affinity for the zinc ion, resulting in a potent inhibitory activity with IC_{50} values in the low nanomolar range.[20,46] HDAC inhibitors bearing this ZBG can strongly chelate the metal in the catalytic cleft, forming a pentacoordinate stable adduct that hampers the deacetylating activity of the enzyme. The crystallographic analysis showed that the usual coordination for HDAC inhibitors occurs in a bidentate manner,[15,47] with the zinc ion forming metal bonds with the carbonyl group (C=O) and the oxyanion (N–O⁻) of the hydroxamate. However, a monodentate coordination was also observed for inhibitors bearing phenyl linker units,[48] where only the N–O⁻ group coordinates the zinc ion, which in turn forms a hydrogen bond with a catalytic molecule of water (Figure 8).

This monodentate coordination may result from the steric hindrance of phenyl hydroxamate inhibitors with bulky caps or linkers, which cannot go deep inside the catalytic cleft. Nonetheless, this does not influence the inhibitory affinity of the inhibitor to the enzyme but may be selective for HDAC6 isoform, as stated by Porter et al..[48b] Despite its strong inhibitory potency, the hydroxamic acid has some negative aspects that prompt medicinal chemists to investigate other safer and more selective ZBGs, as reported later in this review. Indeed, it can lead to undesirable effects, such as binding to other enzymes that depend on the zinc ion for their catalytic activity (e.g., metalloproteinases, carbonic anhydrase, etc.)[50], therefore being poorly selective, or its extensive metabolism into glucuronate products, may result in scarce pharmacokinetic properties and in vivo efficacy.[51]

For these reasons, linker and cap region changes are necessary to improve hydroxamic acids' safety and selectivity. Recently, QSAR-based studies revealed the importance of hydrophobic and bulky groups for HDAC inhibitory activity.[51–52] In this paragraph, we summarize the latest developments in the search for better HDAC inhibitors bearing a hydroxamate binding group and investigate the potential of these compounds bearing a heterocycle in the linker or cap region.

Several research groups investigated the role of quinazoline moieties in the cap region to improve the binding affinity with the amino acids in the outside area of the enzyme. Quinazolines have been studied for years for their therapeutic potential by medicinal chemists,[53] as they possess a plethora of pharmacological applications such as antimicrobial, anti-fungal, anti-malarial, anti-inflammatory, anti-diabetic, or anti-cancer ones.[54] Zhang and coworkers[55] synthesized a series of novel compounds starting from the Vorinostat structure via the replacement of the benzamide cap with a differently substituted 4-aminoquinazolinyl moiety exploring the SAR and the inhibitory activity of these compounds (Table 1). They also changed the length of the linker at five methylene units, but there was no significant difference in the activity, as also reported by other research groups.[56] Hence, here we only discuss the 6-methylene units linker compounds. As shown in Table 1, electron-donating groups such as methyl (**23 a**) or amino (**23 b**) result in a decreased inhibitory activity ($IC_{50} = 20$ nM and 22 nM, respectively) in comparison with electron-withdrawing halogen groups (compound **23 c**, $IC_{50} = 8$ nM, and compound **23 d**, $IC_{50} = 3$ nM). Moreover, the 6-position substituent provides the most potent inhibitory activity related to substituents in position 7 (compounds **23 e** and **23 f**).[55]

The most potent compound, **23 d**, was selected for docking studies in order to elucidate the favorable interactions of the quinazoline moiety with the external aminoacidic residues surrounding the enzyme active pocket. Indeed, adding this heterocycle might influence the binding affinity through its various Wan der Waals interactions. Moreover, compound **23 d** was selective for HDAC1 and −6 over HDAC8 (IC_{50} against HDAC8 1.97 μM), displaying good pharmacokinetic properties and a tumor growth inhibition capacity in vivo.[55] Following this lead, Hieu and colleagues,[57] synthesized N-hydroxybenzamide compounds incorporating a variously substituted quinazoline
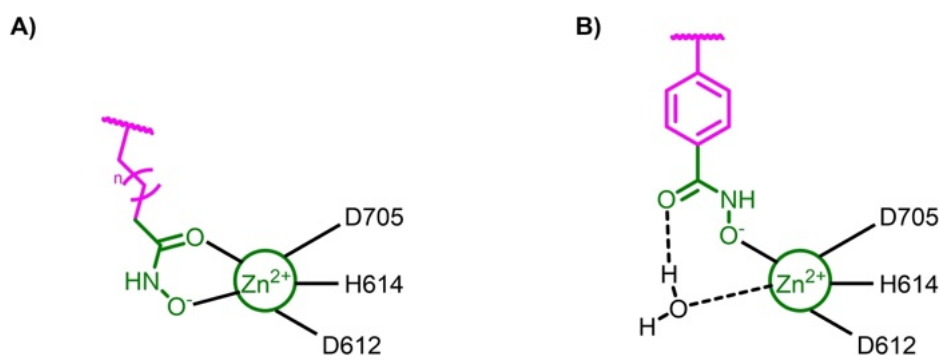

Figure 8. Representation of the (A) bidentate and (B) monodentate HDAC inhibitors zinc coordination. In green the ZBG, in pink the linker region, hydrogen bonds in dashed lines, and metal coordination in solid lines.[48b,49]

moiety. Among them, of note is compound **24 d** (Table 2), bearing a chloro substituent at the sixth position of quinazoline, with low micromolar IC_{50} values (0.12 μM), assessed using HeLa cell nuclear extract assay, confirming the results by Zhang et al. about the favorable Cl-substituent in the 6-position.

From the IC_{50} values shown in Table 2, the compounds are more potent than the positive control Vorinostat. The inhibitory activity correlated well with the cytotoxicity against three cancer cell lines (SW620, PC3, and NCI–H23) except for compound **24 b** bearing a 6,7-dimethoxy substituent, probably due to its poor solubility. Furthermore, **24 d** was docked in the active site of HDAC2 to gain insights about its binding mode. It chelates the zinc ion in a bidentate fashion with a strong binding affinity, as its benzene ring in the linker can have a π-π stacking interaction with Phe155 or Phe210 residues.[57a] Therefore, adding a phenyl linker can improve the binding affinity and, consequently, the inhibitory activity of the compounds. The quinoxalinones class represents an important heterocycle in the chemical and pharmaceutical field due to its broad spectrum of biological properties such as anti-viral,[58] anti-diabetic,[59] anti-bacterial,[60] anti-fungal,[61] anti-malarial, and anti-tumor ones.[62] Considering this, Hieu et al.[63] investigated the role of quinazolinones in the cap region by synthesizing compounds bearing the quinazolin-4(3H)-one heterocycle with a 6- or 7-carbon methylene spacer (**25 a**–**f, 26 a**–**e**; Table 3).

As shown in Table 3, compounds **25 a**–**f** have a lower IC_{50} average than compounds **26 a**–**e**, confirming that the favorable length of the linker is with six methylene units, except for compound **26 e**, with an $IC_{50} = 0.09$ μM, being the most potent. The different substitutions do not particularly influence the inhibitory potency of the compounds; however, some substituents seem to be preferred, such as the chlorine in the 6-position (**25 c**, $IC_{50} = 0.22$ μM and **26 c**, $IC_{50} = 0.29$ μM) or the methoxy

Table 1. Structures and inhibition data of the quinazoline-containing hydroxamate derivatives.[55]

Compound	R	Inhibition activity IC_{50} (μM) HDAC (HeLa extract)
23 a		0.020
23 b		0.022
23 c		0.008
23 d		0.003
23 e		0.020
23 f		0.024

group in the 7-position (**25 e**, $IC_{50} = 0.28$ μM and **26 c**, $IC_{50} = 0.09$ μM). Moreover, adding a further methyl group in the 2-position of compound **25 a** ($IC_{50} = 0.56$ μM) resulted in compound **25 f** with a better inhibitory activity ($IC_{50} = 0.16$ μM). The most potent compounds were also docked in the active site of HDAC1, and various Van der Waals interactions and hydrogen bonds were outlined, deducing that the quinazolin-4(3H)-one moiety in the cap region can be a valuable alternative for novel HDAC inhibitors. According to this statement, the same research team[57a] explored the linker region maintaining the same quinazolin-4(3H)-one moiety in the cap and synthesized novel N-hydroxybenzamides and N-hydroxypropenamides derivatives (Table 4).

From the IC_{50} values, we can obtain some important information regarding the SARs. First, the 6- or 7-position and the nature of the substituent influence the HDAC inhibitory potency. For example, the methyl group is preferred in the 6-position rather than in the seventh in both series of compounds (**27 a** and **28 a** being more potent than compounds **27 d** and **28 b**), except from the quinazolin-4(3H)-one bearing a 2-methyl substituent, in which the effect is inverted (**27 f** more potent than **27 g**). On the contrary, the fluoro substituent leads to better IC_{50} when in the 7-position (**27 e**, $IC_{50} = 0.86$ μM, against **27 b** with $IC_{50} = 1.50$ μM). Of the N-hydroxybenzamides, **27 h**, bearing a 6,7-dimethoxy substitution, resulted in the best inhibitory activity (IC_{50} value of 0.37 μM). However, the most active compounds were in the series of N-hydroxypropenamides **28 a**–**c**, with **28 a** being the most potent ($IC_{50} = 0.09$ μM). Every compound was also tested against three different cancer cell lines (SW620, PC3, and NCI-H23) to evaluate their cytotox-

Table 2. Structures and inhibition data of novel N-hydroxybenzamide with quinazoline cap (**24 a**–**d**).[57a]

Compound	R	Inhibition activity IC_{50} (μM) HDAC (HeLa extract)
24 a		0.020
24 b		0.022
24 c		0.008
24 d		0.003
Vorinostat		0.020

Table 3. Inhibition data of novel quinazolin-4(3H)-one derivatives (**25a–f**; **26a–e**).[63]

n=4 (**25a-f**)
n=5 (**26a-e**)

Compound	R	Inhibition activity IC$_{50}$ (µM) HDAC (HeLa extract)
25a		0.56
25b		0.55
25c		0.22
25d		0.30
25e		0.28
25f		0.16
26a		0.91
26b		0.78
26c		0.29
26d		0.50
26e		0.09
26c		0.29

icity, and it was found that their inhibitory potency translated well into cytotoxicity. Additionally, the binding mode of the most promising compounds was assessed. The differences among the series of compounds were due to their different linker. Indeed, while the N-hydroxybenzamides form the classical interactions as previously seen with the other synthesized compounds[57b,63] with hydrogen bonds in the outside area of the enzyme and the π-π stacking interaction with Phe155 or Phe210, the N-hydroxypropenamides form additional hydrogen bonds and π-π stacking with both the Phenylalanine residues, conferring increased inhibitory potency.[57a]

Chen et al.[64] also explored the cap region and performed various docking analyses that resulted in the synthesis and biological evaluation of a series of compounds bearing the quinazoline moiety, which was shown to be the most prone to occupying and suiting the cap area. The most potent compound (**29**, Figure 9) has a 3-carbon spacer unit, which was shown to be the optimal length for the inhibitory activity and a methoxyl group in the 4-position of the aromatic ring. This combination of substituents resulted in the best inhibition over HDAC6 (IC$_{50}$ = 0.017 µM), being selective over the other isoforms.[64]

Prompted by these results, the same research team[65] investigated the SAR of compound **29** in order to identify a potent dual inhibitor of HDAC1 and HDAC6 and synthesized a series of compounds (**30a–g**) depicted in Table 5.

As the lead compound **29** had an antiproliferative activity against HCT116 cells, the inhibitory potency of the newly synthesized compounds was assessed with MTT tests in the same cell line. First of all, Chen and colleagues explored the substituent R$_1$, which was a methyl group in the lead compound. They replaced it with larger linear or branched substituents (compounds **30a** and **30b**), which resulted in less potency than the lead compound **29**. Therefore, maintaining the methyl group at the R$_1$ position, they explored the substitutions in the aromatic ring, with the linker either in the para (R$_2$) or in the meta (R$_3$) position of the aromatic ring. Compound **30c**, with the inverted substitutions respect compound **29**, exhibited a loss of potency compared to **29**. Moreover, compounds **30d** and its para-counterpart **30e**, bearing the amide hydrocarbon chain as R$_2$ or R$_3$ substituent respectively, exhibited less potency than **29**, leading to the conclusion that, even if the amide chain is preferred in the R$_3$ position (**30d** more potent than **30e**) and to the ether group (**30d** more potent than **30c**), the methoxy group at R$_2$ is still needed. Accordingly, compounds **30f** and **30g**, with the methoxyl substituent at R$_2$ and the amide chain at R$_3$, exhibited better antiproliferative activity than the other compounds, with **30f** being the most potent, as a spacer with 3-carbon length, it is more favorable than a longer chain. In addition, compounds **30f** and **30g** were assessed for their activity over HDAC isoforms, and both were selective over isoform 1 (IC$_{50}$ = 0.031 µM and 0.037 µM, respectively) and 6 (IC$_{50}$ = 0.016 µM and 0.035 µM respectively), being promising dual inhibitors.[65] Several dual HDAC inhibitors containing the quinazoline moiety were developed and are very well summarized in two recent reviews,[66] highlighting the importance of hybrid molecules
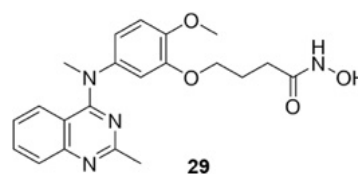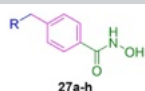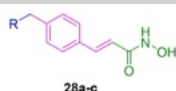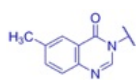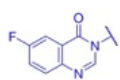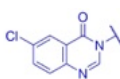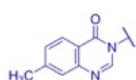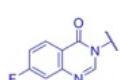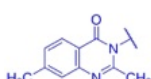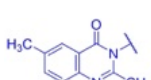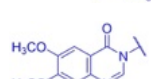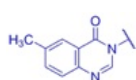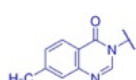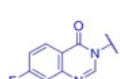

Figure 9. The most potent compound synthesized by Chen et al.[64]

ChemMedChem

Review
doi.org/10.1002/cmdc.202400194

Chemistry Europe
European Chemical
Societies Publishing

Table 4. Structure and inhibition data of N-hydroxybenzamides and N-hydroxypropenamides derivatives (**27a–h**; **28a–c**).[57a]

Compound	R	Inhibition activity IC$_{50}$ (µM) HDAC (HeLa extract)
27a		0.49
27b		1.50
27c		0.61
27d		0.91
27e		0.86
27f		0.62
27g		0.71
27h		0.37
28a		0.09
28b		0.15
28c		0.17
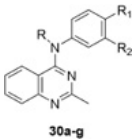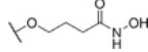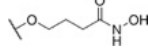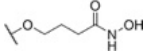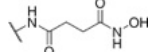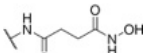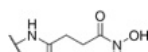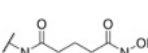
that can exert multiple anticancer properties without resulting in drug resistance.[66b]

In the search for novel HDAC inhibitors with different cap groups, Balasubramanian and coworkers[67] explored various amide substituents on the quinolone scaffold, maintaining the linear linker with five methylene spacers (Table 6). The quinolone moiety has been extensively studied for its therapeutic potential as an antibiotic, and recently, a quinolone derivative named Voreloxin has entered a phase II clinical trial for cancer treatment.[68] Therefore, it is worth investigating this moiety for further developing new HDAC inhibitors. Moreover, this lipophilic portion can occupy and make interactions in the cap region, leading to more potent inhibitory activity. Consequently, Balasubramanian et al. developed a set of compounds varying the amide substituent in the 3-position of the

quinolone ring (R) and, in a second round, adding a methoxyl group in the 6-position (R$_1$).[67]

As shown in Table 6, the IC$_{50}$ values are very diverse and give us some insights into the SAR of this cap group. With a phenyl or a para-methoxyphenyl as substituents, the IC$_{50}$ values do not differ from each other, but with the addition of a further methylene, which results in a benzyl group, the inhibitory potency is strongly decreased (compounds **31a** and **31b** in comparison with **31c** and **31d**, respectively). Moreover, the presence of a thiazole ring seemed to recover the inhibitory activity (**31e**, IC$_{50}$ = 42 nM), which was further improved with the addition of a methyl group on the thiazole ring, with IC$_{50}$ value in the low nanomolar (**31f**, IC$_{50}$ = 0.1 nM). In addition, compound **31h**, bearing a 1-methyl-3-phenyl-pyrazolyl substituent, showed comparable inhibitory results (IC$_{50}$ = 95 nM). All the compounds were also tested for their antiproliferative

ChemMedChem

Review
doi.org/10.1002/cmdc.202400194

Chemistry
Europe
European Chemical
Societies Publishing

Table 5. Structure of novel quinazoline-based compounds (**30a–g**).[65]

Compound	R	R$_1$	R$_2$
30a	$-CH_2CH_3$	$-OCH_3$	(O-linked hydroxamic acid chain)
30b	$-CH_2CH(CH_3)_2$	$-OCH_3$	(O-linked hydroxamic acid chain)
30c	$-CH_3$	(O-linked hydroxamic acid chain)	$-OCH_3$
30d	$-CH_3$	$-H$	(N-linked succinyl hydroxamic acid chain)
30e	$-CH_3$	(N-linked succinyl hydroxamic acid chain)	$-H$
30f	$-CH_3$	$-OCH_3$	(N-linked succinyl hydroxamic acid chain)
30g	$-CH_3$	$-OCH_3$	(N-linked glutaryl hydroxamic acid chain)

activities against three cell lines (NCIH460, HCT116, and U251), and compounds **31a–e** exhibited good anticancer activities, which were increased in compounds **31f–h**. The addition of a methoxyl group in the 6-position of the quinolone ring did not lead to significant changes in the HDAC inhibitory potency of compounds **31i** and **31j** (IC$_{50}$ = 32 nM and IC$_{50}$ = 75 nM) but slightly decreased or increased the inhibition capacity for compounds **31k** and **31l**, respectively (IC$_{50}$ = 10 nM and IC$_{50}$ = 28 nM). Again, the antiproliferative activity was retained.[67]

Prompted by the efficacy given by the introduction of a quinolone moiety as a cap group in HDACi, Relitti *et al.* developed a library of quinolone-based HDAC6 selective inhibitors,[69] which are based on Viridicatin, a natural alkaloid found in *Penicillium genus* which has gained much interest in the pharmaceutical field (Figure 10).[70] All the developed compounds were assayed against HDAC1 and HDAC6 isoforms. The chemical modification introduced in the lead compound **32a**, together with a computational analysis based on molecular docking calculations, allowed to draw up the SAR analysis for the corresponding developed HDACi (**32a–d, 33a–i; 34a**).

In this **32** series, the alkylation of the hydroxy group based in the C3 position led to an improvement of the potency. **32b** and **32c** displayed more potent HDAC6 inhibition properties
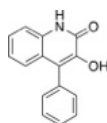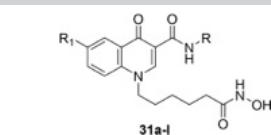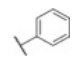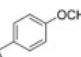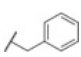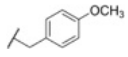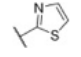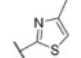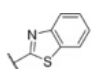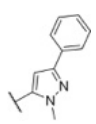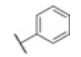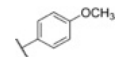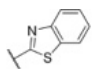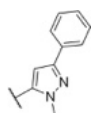

Figure 10. Viridicatin chemical structure.

than the corresponding compound **32a** (Table 7). Relitti *et al.* also investigated the effects of switching the ZBG from the N1 to the C3 position by developing the **33** series. These compounds displayed good inhibiting properties against HDAC6 being almost 100 times more selective over HDAC1 (**33f**). When a basic lateral chain was introduced, such as a 4-pyridyl (**33d**) or N,N-diethylaminomethylbenzyl moiety (**33e**), in order to reach polar contacts in HDAC6 binding site together with an improvement of the water solubility, a strong increase in HDAC6 inhibition was observed. **33e** exhibited the best HDAC6 inhibiting properties of the whole developed series (IC$_{50}$ = 7 nM) via the introduction of a flexible and protonatable moiety (N,N-diethylaminomethylbenzyl group) that established a salt bridge and a polar contact with D567 residue in HDAC6. The insertion of a bulky alkylated group generated less potent compounds against HDAC6 (**33b** and **33c**). Differently from the **32** series (**32d**), the introduction in the **33** series of a pyridin-3-yl group in the C4 position (**33f–i**) instead of the phenyl ring (**33a–e**) led to higher potency than the corresponding N1-ZBG substituted compound (**32d**) together with a higher selectivity ratio observed towards HDAC6 instead of HDAC1. Considering the good inhibitory activities showed by compounds **33a–i**, C4 position replacement with an aliphatic cycle led to compound **34a**, which displayed both a high HDAC6 inhibitory activity (IC$_{50}$ = 33 nM) and a good selectivity over HDAC1. The best HDAC6 inhibiting compounds highlighted from the previously discussed enzymatic assays (**33e** and **33i**) were performed in cell-based MTT assays against a colon cancer cell line (HCT-116) and a histiocytic lymphoma cell line (U937). **33i** and **33e** displayed the best cytotoxic activities in HCT-116 cancer cell

ChemMedChem

Review
doi.org/10.1002/cmdc.202400194

Chemistry
Europe
European Chemical
Societies Publishing

Table 6. Structure and inhibition data of novel quinolone-based HDAC inhibitors (31 a–l).[67]

31a-l

Compound	R	R_1	Inhibition activity IC$_{50}$ (µM) Mouse liver HDACs
31a	(benzyl)	–H	0.032
31b	(4-methoxybenzyl)	–H	0.039
31c	(phenethyl)	–H	0.120
31d	(4-methoxyphenethyl)	–H	0.410
31e	(thiazolyl)	–H	0.042
31f	(methylthiazolyl)	–H	0.0001
31g	(benzothiazolyl)	–H	0.0015
31h	(1-methyl-3-phenylpyrazolyl)	–H	0.095
31i	(benzyl)	–OCH$_3$	0.032
31j	(4-methoxybenzyl)	–OCH$_3$	0.075
31k	(benzothiazolyl)	–OCH$_3$	0.010
31l	(1-methyl-3-phenylpyrazolyl)	–OCH$_3$	0.028
Vorinostat			0.110

activity. The **31 a–f** series inhibited HDAC6 from the submicro-molar (**35 a**) to the nanomolar (**35 e**) range. Compound **35 e** exhibited an HDAC6 selectivity, which is 1000 times higher over HDAC4 and more than 38-fold selectivity over the other HDAC isoforms tested. The nicotinic derivative series (**36 a–f**) displayed higher potency than the pyridylacrylic series (**35 a–f**), where the compounds exhibited an inhibition potency against HDAC6 from dual-digit to single-digit nanomolar range. In particular, compound **36 d** displayed the best IC$_{50}$ value (IC$_{50}$ = 0.5 nM) against HDAC6 and the best selectivity rate for HDAC6 over the other HDAC isoforms recruited. Further SAR analysis underlines that bulky or branched substituents at the phenylacetyl chain (**35 b–d** and **36 b–d**) conferred higher inhibition potency and selectivity for HDAC6 when compared with derivatives **35 a** and **36 a**, which displayed a no-substituted phenylacetyl chain. In granulocytic cytodifferentiation assays conducted in human U937 leukemia cell lines, compounds **32 b** and **33 c** exhibited high cytodifferentiating properties.

Based on the previously discussed findings obtained in 2021, Di Bello *et al.* designed and developed a regioisomer series of the latter compounds[72] by synthesizing novel 5-acylamino-2- pyridylacrylic hydroxamates and novel 5-acylami-no-2- picolinic hydroxamates (**37 a–f** and **38 a–f**) containing the same acyl-substituent of the reference compounds[72] but inserted in different pyridine ring positions.[73] The research group also developed the corresponding derivatives bearing 2-aminoanilide in parallel, such as ZBG (**98 a–f, 99 a–f**), which will be discussed later in paragraph 3.2.

Each compound was tested for its inhibitory activity against HDAC1, −3, −4, −6, and −8, and some of them were also tested against HDAC10. As shown in Table 9, the compounds exhibited, in most cases, good IC$_{50}$ values, preferring some HDAC isoforms over others and showing a selectivity profile that depends on the substituent in the cap group. For the series of 5-acylamino-2-pyridylacrylic-hydroxamates (**37**), both the substitution at the Cα of the benzyl substituent of **37 a**, with an ethyl (**37 b**), isopropyl (**37 c**) or benzyl (**37 d**), and the introduction of bulkier substituents, such as 1- (**37 e**) or 2-naphthyl (**37 f**), decreased the inhibitory potency of the resulted compounds against HDAC1, in comparison with **37 a**. Regarding HDAC3 inhibition, some of the compounds (**37 b,c,e**) exhibited increased potency in comparison with **37 a**, while **37 f** did not show as low IC$_{50}$ values as the other compounds. HDAC6 was inhibited by the compounds with IC$_{50}$ values in the low micromolar range, except for **37 f**, with a slightly higher inhibitory potency, while for HDAC4, only compound **37 e** (IC$_{50}$ = 2.73 µM) resulted in a good inhibition. Regarding HDAC8, the ethyl (**37 b**) and the 1-naphthyl (**37 e**) increased the inhibitory activity; instead, the benzyl (**37 d**) and 2-naphthyl (**37 f**) decreased it. Moreover, **37 e** was the best among the compounds tested against HDAC10 (IC$_{50}$ = 0.071 µM). Collecting all these data, the introduction of a benzyl in the Cα (**37 d**) led to a discrete selectivity for HDAC3/6, while the 2-naphthyl substituent (**37 f**) resulted in a general decrease of potency. For the series of the picolinic hydroxamates (**38**), we notice a general decrease in potency against all the HDAC isoforms tested. Nonetheless, the introduction of a bulkier substituent in

lines, with **33 e** being the most cytotoxic compound after 48 h of induction at the tested concentration.

Pyridine-based HDACi represented an active moiety in preclinical settings.[71] Based on this evidence, Zwergel and colleagues developed a novel 2-acylamino-5-(3-oxoprop-1-en-1-yl)pyridine hydroxamates (**35 a–f**) and 2-aminoanilide series (**96 a–f**) and the corresponding nicotinic derivative series (**36 a–f** and **97 a–f**, respectively) to be tested in enzymatic and antiproliferative assays.[72] The 2-aminoanilide derivatives (**96 a–f** and **97 a–f**) will be opportunely discussed in paragraph 3.2.
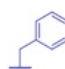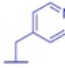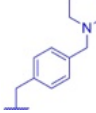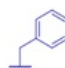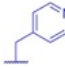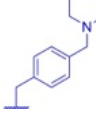
In Table 8, the biochemical data about HDAC1, −3, −4, −6, and −8 inhibition activity of **35 a–f** and **36 a–f** are reported. All the synthesized compounds possessed high HDAC6 inhibition

Table 7. Structure and inhibition data of the quinolone-based HDAC inhibitors **32 a–d**; **33 a–i** and **34 a**.[69]

Inhibition activity
IC$_{50}$ (μM)

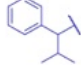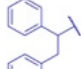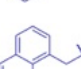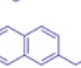| Compound	R	X	HDAC1	HDAC6
32 a	—H	CH	11.0	0.301
32 b	—CH$_3$	CH	4.5	0.062
32 c	(benzyl)	CH	5.5	0.085
32 d	H	N	50.0	0.296
33 a	H	CH	6.6	0.147
33 b	—CH$_3$	CH	50.0	0.519
33 c	(benzyl)	CH	50.0	0.176
33 d	(pyridylmethyl)	CH	1.2	0.084
33 e	(4-(diethylaminomethyl)benzyl)	CH	0.322	0.007
33 f	—CH$_3$	N	5.01	0.046
33 g	(benzyl)	N	2.5	0.026
33 h	(pyridylmethyl)	N	1.7	0.045
33 i	(4-(diethylaminomethyl)benzyl)	N	0.319	0.012
34 a	–	–	3.0	0.033
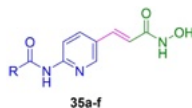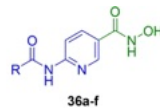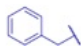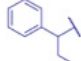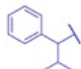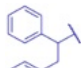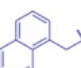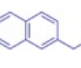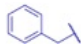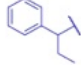
the Cα of the benzyl substituent increased the inhibitory activity against HDAC1 and −3, in comparison with **38 a**, except for **38 e**, which resulted in a good IC$_{50}$ value (IC$_{50}$ = 0.058 μM), and therefore selective, for HDAC6. Indeed, the 1-naphthyl substituent (**38 e**), and not the 2-naphthyl (**38 f**), increased both the potency and selectivity versus HDAC6. Generally, picolinic hydroxamates showed a better potency for HDAC6, with **38 d** being the most potent (IC$_{50}$ = 0.016 μM). Furthermore, compounds were evaluated for their ability to impair cell proliferation using three cancer cell lines (HCT116, K562, and A549), and compounds **37 d** and **37 e** resulted in the best IC$_{50}$ values in the range of nanomolar, while the series of picolinic hydroxamates was less potent. Therefore, **37 d** and **37 e** were selected to assess their target engagement, and both induced hyper-

acetylation of α-tubulin and histone H3, confirming their HDAC inhibitory activity. In addition, their role in cell cycle regulation and apoptosis induction was demonstrated, being able to modulate the expression of pro- and anti-apoptotic factors in U937 cells.[73] Considering all these promising data, it might be interesting to investigate the pyridine scaffold further for novel potent and selective HDAC inhibitors.

Oanh *et al.*[74] investigated the cap region, developing two series of novel compounds obtained by substituting the aromatic ring of Vorinostat with a variously decorated benzothiazole ring (Table 10).

As shown in Table 10, the series of **40** mimics the linker of Vorinostat having the same number of methylene spacer units, while the series of **39** is shorter. All the compounds were tested

Table 8. Structures and inhibition data against HDAC1, −3, −6,–8 of 2-acylamino-5-(3-oxoprop-1-en-1-yl)pyridine hydroxamate (**35a–f**) and the related nicotinic derivative series (**36a–f**).[72]

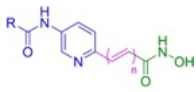| Compound	R	Inhibition activity IC$_{50}$ (μM)				
		HDAC1	HDAC2	HDAC3	HDAC6	HDAC8
35a		7.08	6.30	155	0.164	2.94
35b		1.56	1.23	31.7	0.012	1.15
35c		2.26	2.19	39.4	0.016	1.45
35d		2.02	0.781	27.3	0.022	1.41
35e		0.271	0.351	7.05	0.007	0.352
35f		0.425	0.581	10.7	0.013	0.552
36a		2.42	2.71	26.0	0.017	0.386
36b		1.12	0.917	28.8	0.006	0.277
36c		1.0	0.665	46.6	0.006	0.357
36d		0.117	0.056	17.2	0.0005	0.643
36e		1.03	0.765	14.4	0.007	0.40
36f		0.784	0.301	6.0	0.019	1.0
Vorinostat	–	0.31	0.13	8.8	0.06	0.31

NA = not active.

for their antiproliferative activity against five cancer cell lines, including SW620, MCF-7, PC3, AsPC-1, and NCI-H460 (here are shown only the results regarding the activity against SW620, colon cancer cell line). Generally, the series of **40** resulted in better anticancer activity compared to the **39** series, suggesting that the number of methylene spacers is vital for the activity of the compounds. In particular, compounds **40b–d** exhibited a good inhibitory activity derived from increased histones H3 and H4 acetylation, while compounds **40e** and **40f** did not affect the acetylation status. Therefore, we can deduce that it is not important if the compound is an electron-donating group
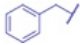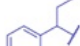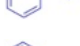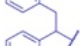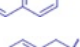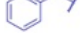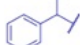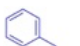
(−OCH$_3$, compound **40d**) or electron-withdrawing group (−NO$_2$, compound **40c**), but the size of the substituents (−OC$_2$H$_5$ or −SO$_2$CH$_3$, compounds **40e** and **40f** respectively) influences the compounds' inhibitory potency. Moreover, compounds **40b** and **40d** were selected for docking studies in the active site of HDAC8, for which they have high affinity, but further experiments have to be done.[74]

Through fragment-based virtual screening, which has become increasingly important in recent years as a valuable technique for identifying potential drug candidates,[75] Liu et al.[76] designed and synthesized novel indazole and

Table 9. Structures and inhibition data against HDAC1, −3, −4, −6, −8, −10 isoforms of pyridylacrylic- (**37 a–f**) and picolinic-hydroxamate (**38 a–f**) novel compounds.[73]

n=0 (37a-f)
n=1 (38a-f)

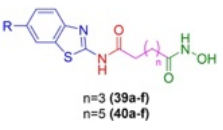| Compound	R	Inhibition activity IC$_{50}$ (μM)					
		HDAC1	HDAC3	HDAC4	HDAC6	HDAC8	HDAC10
37 a		0.068	0.078	19.3	0.013	0.183	–
37 b		0.077	0.036	17.1	0.011	0.104	–
37 c		0.081	0.028	16.0	0.010	0.168	–
37 d		1.42	0.080	11.7	0.011	0.612	1.80
37 e		0.098	0.039	2.73	0.015	0.047	0.071
37 f		0.376	0.168	17.6	0.112	1.01	–
38 a		3.43	2.06	82.4	0.174	1.09	–
38 b		1.49	0.777	77.9	0.051	0.964	–
38 c		1.01	0.681	63.2	0.041	0.882	–
38 d		0.783	0.153	39.2	0.016	1.09	–
38 e		2.85	1.39	30.7	0.058	1.81	–
38 f		0.394	0.207	15.8	0.123	0.976	–
Vorinostat		0.077	0.064	76.0	0.010	0.306	0.198

pyrazolo[3,4-b]pyridine derivatives from Vorinostat structure (Table 11) as HDAC inhibitors with potential further interactions in the cap region.

Each compound in Table 11 was tested against HDAC1, −2, and −8, and exhibited IC$_{50}$ values in the nanomolar range, generally better than Vorinostat used as positive control. For the series of **41**, the addition of substituents on the aromatic ring in the 6-position of the indazole/pyrazolo[3,4-b]pyridine scaffold (**41 b–l**), gave compounds more potent in comparison with compound **41 a** without substituents (e.g., **41 d** HDAC1 IC$_{50}$ = 2.7 nM, HDAC2 IC$_{50}$ = 5.2 nM, HDAC8 IC$_{50}$ = 4 nM). How-

ever, the nature of the substituent on the aromatic ring influenced the inhibitory potency: electron-withdrawing substituents, such as fluoro (**41 c**, HDAC1 IC$_{50}$ = 1.8 nM, HDAC2 IC$_{50}$ = 4.4 nM, HDAC8 IC$_{50}$ = 2.4 nM) or chloro (**41 d**, HDAC1 IC$_{50}$ = 2.7 nM, HDAC2 IC$_{50}$ = 5.2 nM, HDAC8 IC$_{50}$ = 4 nM) or, had better IC$_{50}$ values than compound **41 b** (HDAC IC$_{50}$ = 4.6 nM, HDAC2 IC$_{50}$ = 5.4 nM, HDAC8 IC$_{50}$ = 4.2 nM) with a methoxy electron-donating substituent in the same position. Comparing the *ortho*, *meta*, and *para* positions of the different substituents, we do not notice particular differences in the potency but slight changes in the selectivity. Moreover, the bulkier the substituent

Table 10. Structure and inhibition data in SW620 cancer cell line of novel benzothiazole-based HDAC inhibitors (**39a–f; 40a–f**).[74]

n=3 (39a-f)
n=5 (40a-f)

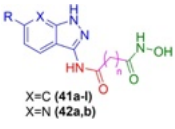| Compound	R	Inhibition activity IC$_{50}$ (μM) HDAC (SW620 extract)
39a	−H	7.85
39b	−CH$_3$	4.69
39c	−NO$_2$	>30
39d	−OCH$_3$	9.07
39e	−OC$_2$H$_5$	9.26
39f	−SO$_2$CH$_3$	>30
40a	−H	4.01
40b	−CH$_3$	0.56
40c	−NO$_2$	0.29
40d	−OCH$_3$	0.96
40e	−OC$_2$H$_5$	10.43
40f	−SO$_2$CH$_3$	5.42

in the *meta* position, the less is the inhibitory activity of the compound (**41f** bearing an ethoxy substituent showed higher IC$_{50}$ values than **41e**). In order to further explore the SAR, the research team replaced the aromatic ring with a pyridine, which led to **41j** with less potency compared to **41a** (HDAC1 IC$_{50}$= 23 nM, HDAC2 IC$_{50}$=25.9 nM, HDAC8 IC$_{50}$=24.5 nM). Therefore, the aromatic ring was preferred as a substituent in the 6-position of the 1H-indazole moiety. In addition, the length of the linker was evaluated, and two compounds with fewer methylene units, **41k** and **41l**, with three and five methylene units, respectively, were synthesized. As shown in Table 11, both compounds were less potent than **41e**, therefore deducing that the 6-methylene spacer is preferred. Regarding the series of **42**, obtained by bioisoter strategy from the indazole scaffold, compound **42b** showed better IC$_{50}$ values (HDAC1 IC$_{50}$=6 nM, HDAC2 IC$_{50}$=9 nM, HDAC8 IC$_{50}$=7.2 nM) than **42a**, but was less potent than the bioisoster **41i**. Subsequently, the antiproliferative activity of the synthesized compounds was assessed against three cancer cell lines, HCT-116, MCF-7, and HeLa, and compounds **41h**, **41i**, and **42b** were the most promising. These compounds were, therefore, selected for further evaluations using the HCT-116 cell line, such as target engagement through the analysis of the tubulin's acetylation status via western blot or the cell cycle analysis. In both experiments, the indazole compounds **41h** and **41i** showed a better profile, in terms of increase in tubulin's acetylation status, than compound **42d**, confirming the antiproliferative results. Moreover, **41h** and **41i** induced HCT-116 cell cycle arrest in the G2/M phase, while **42b** did not affect it. From molecular docking analysis, the three of the compounds placed in the active site of HDAC2 in a similar conformation of the control
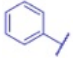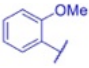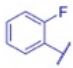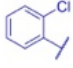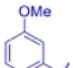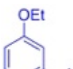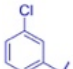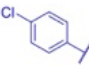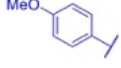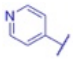
Vorinostat, making several hydrophobic interactions between the indazole/ pyrazolo[3,4-b]pyridine cap moieties and the aminoacids in the outside area of the enzyme.[76] Consequently, it is worth further investigating this scaffold to obtain more information on the SAR and thereby develop potent and selective HDAC inhibitors.

Recently, intending to target hepatocellular carcinoma (HCC), which is a high cause of mortality and whose therapies are not efficacious for tumor remission,[77] Lai and coworkers[78] developed a series of novel 1,2,3,4-tetrahydrobenzofuro[2,3-c]pyridine derivatives. They started from the structure of the known inhibitor Abexinostat in a phase III clinical trial for the treatment of renal carcinoma and lymphoma and applied a multicomponent synthetic approach to incorporate its benzofuran scaffold, which could represent a valuable alternative for novel effective HDAC inhibitors.

As seen in Table 12, the compounds were tested for their inhibitory activity against HDAC1 (IC$_{50}$) and for their antiproliferative activity against three human HCC cells (Bel-7402, HepG2, and Huh-7) and a healthy liver cell line (AML12) to assess their cytotoxicity. Among compounds **43a–d**, the unsaturated hydroxamate **43d** resulted in the best inhibitory activity with an IC$_{50}$ value of 8.9 nM and significantly hampered Bel-7402 cell proliferation (IC$_{50}$=2.38 μM) without affecting the other cell lines. Furthermore, the length of the linker chain was important, and the 6-methylene spacer was preferred (compare **43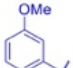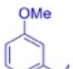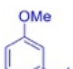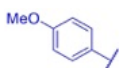a** with **43b**). The addition of an aromatic ring increased the potency (compound **43c**, IC$_{50}$=0.175 μM), which was further enhanced by introducing an unsaturated bond (compound **43d**). As the antiproliferative activity of these compounds was not significant against the HCC cell lines, they further synthesized compounds **43e–g**, which have an amide as a connecting unit and variously substituted aromatic linkers. As expected, the inhibitory potency increased in comparison with **43d**. For compounds **43h–i**, instead, the introduction of an unsaturated bond decreased the inhibitory potency and lowered the antiproliferative activity. Compound **43f** resulted to be the best among all synthesized compounds, inhibiting cell proliferation in all the cell lines tested more than Vorinostat and Abexinostat. Moreover, it showed lower toxicity (IC$_{50}$=3.69 μM) against AML12 cells than Abexinostat, and resulted selective for isoforms −1, −2, −3, and −6, having a better profile than Abexinostat. In addition, **43f** could inhibit colony formation and migration of three of the HCC cells, it induced apoptosis and autophagy in Bel-7402 and HepG2 cells, and it increased the acetylation status of α-tubulin and histone H3 both *in vitro* (Bel-7402 and HepG2) and *in vivo* (Bel-7402-derived xenografts), where showed a therapeutic effect without significant toxicity. Of note is the binding mode of **43f** in the active site of HDAC1. The docking studies revealed a T-conformation of **43f** (in its S-absolute configuration), which could make many interactions with residues in the linker and cap region, such as π-π stacking with Phe205 and Phe150 or the Hydrogen bond with Asp99, the most important. This particular binding mode might be of interest for further studies on potent HDAC inhibitors.[78]
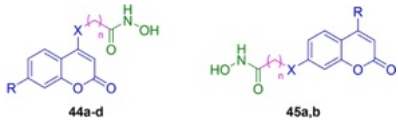
Coumarins, classified as 2H-1-benzopyran-2-one or 2H-chromen-2-one, represent a significant bicyclic heterocycle within

Table 11. Structure and inhibition data against HDAC1, −2, −8 of novel indazole- and pyrazolo[3,4-b]pyridine-based HDAC inhibitors (**41 a–l; 42 a,b**).[76]

X=C (41a–l)
X=N (42a,b)

Compound	R	n	Inhibition activity IC$_{50}$ (μM)		
			HDAC1	HDAC2	HDAC8
41 a		6	0.0096	0.0131	0.0126
41 b		6	0.0046	0.0054	0.0042
41 c		6	0.0018	0.0044	0.0024
41 d		6	0.0027	0.0052	0.004
41 e		6	0.0019	0.0039	0.003
41 f **41 i**		6	0.0021	0.0042	0.0034
41 g **41 f**		6	0.0037	0.004	0.0038
41 h **41 g**		6	0.0031	0.0036	0.0033
41 i **41 h**		6	0.0027	0.0042	0.0036
41 j		6	0.023	0.025	0.024
41 k		3	0.076	0.168	0.054
41 l		5	0.0026	0.0063	0.0045
42 a		6	0.0024	0.0053	0.0033
42 b		6	0.006	0.009	0.0072
Vorinostat			0.013	0.070	0.044

the flavonoid group of plant metabolites. They constitute a diverse group of natural and synthetic compounds, showcasing a broad spectrum of beneficial properties. These compounds have been demonstrated to be potential anticancer,[79] anti-HIV,[80] anti-Alzheimer[81] and antimicrobial[82] agents. Notably, coumarin and its derivatives exhibit rare instances of neph-rotoxicity, hepatotoxicity, cardiotoxicity, dermal toxicity, and other adverse effects.[83] In recent years, the development of

Table 12. Structures, inhibition data against HDAC1, and antiproliferative activity in human HCC cell lines (Bel-7402, HepG2, Huh-7) and regular liver cell line (AML12) of **43a–i** compounds.[78]

Compound	R	Inhibition activity IC$_{50}$ (µM)	Antiproliferative activity IC$_{50}$ (µM)			
		HDAC1	Bel-7402	HepG2	Huh-7	AML12
43a		0.058	>5	>5	>5	>5
43b		0.030	>5	>5	>5	>%
43c		0.175	>5	>5	>5	>5
43d		0.0089	2.38	>5	>5	>5
43e		0.0023	0.81	0.52	1.79	3.27
43f		0.0031	0.03	0.12	0.24	3.69
43g		0.0021	0.56	0.14	0.38	3.40
43h		0.061	>5	>5	>5	>5
43i		0.15	1.27	1.47	2.49	>5
Vorinostat		0.013	1.80	1.14	1.65	>5
Abexinostat		0.007	0.37	0.21	1.01	1.82

coumarin-based anticancer agents has gained considerable attention in the pharmaceutical field.[84] For these reasons, Yang et al.[85] hybridized the coumarin moiety with the classical pharmacophore of the HDAC inhibitors, in order to increase its therapeutic potential and find novel and effective anticancer agents. Novel compounds bearing a coumarin cap group were synthesized and tested against HDAC1 to assess their inhibitory activity. First, they synthesized the series of **44**, with a substituent in the 7-position of the coumarin ring and a linear linker in position 3 connected to the ring through a heteroatom, such as nitrogen or oxygen. Then, to explore the SAR, they moved the linker to the 7-position of the coumarin ring and put a hydrogen or a methyl group in the 3-position, obtaining two compounds (**45a,b**, Table 13).

For the series of **44**, increasing the length of the methylene units in the linker increased the inhibitory potency, resulting in compound **44c** with an IC$_{50}$ in the low nanomolar range (IC$_{50}$ = 2.4 nM). Moreover, the introduction of a methoxyl group in the 7-position did not significantly change the activity (compare **44a**, IC$_{50}$ = 9.1 nM, with **44b**, IC$_{50}$ = 6.4 nM). The replacement of the connecting secondary amine with an oxygen, led to the ether **44d** with comparable IC$_{50}$ value (1.8 nM). Compounds **45a,b**, having the linker in the 7-position of the coumarin ring, exhibited less potency than compound **44c**, suggesting that having the linker in that position might influence HDAC inhibitory activity. The most potent compounds **44c,d** were tested against HeLa and A549 cancer cell lines and resulted in better antiproliferative activity than Vorinostat, inducing cell cycle arrest and enhancing their apoptosis. In addition, **44c,d** inhibited the other HDAC isoforms similarly to Vorinostat, thereby being pan-HDAC inhibitors, displayed the same interactions and binding mode in the active site of HDAC1 and

Table 13. Novel coumarin-based HDAC inhibitors (**44a–d; 45a,b**) and related inhibition data against HDAC1.[85]
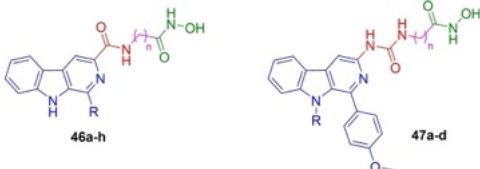

44a-d   45a,b

Compound	X	n	R	Inhibition activity IC$_{50}$ (μM) HDAC1
44a	–NH	5	–H	0.0091
44b	–NH	5	–OCH$_3$	0.0064
44c	–NH	7	–OCH$_3$	0.0024
44d	–O	7	–OCH$_3$	0.0018
45a	–O	7	–H	0.0087
45b	–O	7	–CH$_3$	0.0069
Vorinostat				0.0211

increased the acetylation status of histone H3 and H4, confirming their target engagement.[85] Therefore, coumarin-based HDAC inhibitors might be promising anticancer agents to be further investigated.

A few years before, Ling and colleagues[86] synthesized novel hybrid compounds containing the HDAC pharmacophore and the β-carboline scaffold in order to study the synergistic effect of the natural alkaloid in inhibiting HDACs, and therefore becoming an effective anticancer agent. β-carboline has various anticancer properties: it can inhibit cancer cell growth, induce apoptosis,[87] and, due to its planar tricyclic pyrido-[3,4-b]indole

ring, can intercalate into the DNA strands hampering the replication.[88] Therefore, Ling et al. prepared two series of compounds merging the hydroxamate ZBG for the HDAC inhibitory activity with a β-carboline moiety as the cap group through a linear linker and a carboxyl or uramido connecting unit (Table 14).

The compounds were tested for their inhibitory activity using nuclear extract of HeLa cells, rich in HDAC1 and –2, and the related IC$_{50}$ values are shown in Table 14. For the series of **46** with an amide as a connecting unit, 3 or 4-methylene spacers resulted in the best inhibitory activity for each
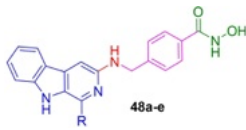
Table 14. Structure and inhibition data of novel β-carboline/hydroxamate hybrid compounds (**46a–h; 47a–d**).[86]

46a-h   47a-d

Compound	R	n	Inhibition activity IC$_{50}$ (μM) HDAC (HeLa extract)
46a	–H	3	1.56
46b	–H	4	1.43
46c	–H	5	1.81
46d	–CH$_3$	3	1.21
46e	–CH$_3$	4	1.26
46f	–CH$_3$	5	1.43
46g	p-MeOPh	3	0.67
46h	p-MeOPh	4	0.81
47a	–H	3	0.27
47b	–H	4	0.35
47c	–CH$_3$	3	0.51
47d	–CH$_3$	4	0.86
Vorinostat			0.56

compound with a different substituent in the 1-position of the pyrido-[3,4-b]indole ring (R=-H, -CH₃, p-MeOPh). Moreover, the substitution of the hydrogen with a methyl group did not particularly influence the potency (e.g., compared **46b**, IC₅₀= 1.43 μM, with **46e**, IC₅₀=1.26 μM), while the substitution with the *para*-methoxyphenyl group resulted in compounds with better IC₅₀ values (**46g** and **46h**, IC₅₀ values of 0.67 and 0.81 μM, respectively). The compounds were also tested against three human colorectal cancer cell lines (HCT116, LOVO, SW620), and their antiproliferative activity correlated well with their inhibitory activity, with compounds **46g** and **46h** being the most potent and effective in the cells. Afterwards, as the *para*-methoxyphenyl group resulted important for both potency and antiproliferative activity of compounds, Ling and coworkers synthesized the series of **47**, with an ureido group as connecting unit, maintaining the paramethoxyphenyl in 1-position of the pyrido-[3,4-b]indole ring. Accordingly, compounds of series **47** showed better IC₅₀ values than series **46**, suggesting that this substituent might be important for the activity. They also investigated the substitution of the N9 replacing the hydrogen with a methyl group, which did not particularly influence the inhibitory potency, showing a slight decrease (compare **47b**, IC₅₀=0.35 μM, with **47d**, IC₅₀= 0.86 μM). Again, 3- or 4-methylene units were optimal for the inhibitory activity, following the same trend as the previous series. Regarding the antitumor activity, all the compounds inhibited cancer cell proliferation, with compound **47a** being the most potent. It is important to notice that the inhibitory activity of **47a** resulted only two-fold better than Vorinostat (IC₅₀=0.56 μM), while its antiproliferative activity was greater, suggesting that the β-carboline moiety might play an important role in the anticancer activity. Compound **47a** was selected for further evaluation, and it was demonstrated that it induces DNA damage through increased phosphorylated H2AX and p53 at Ser15, both markers of DNA damage. Moreover, **47a** induced apoptosis in HCT116 cells and inhibited cancer cell growth *in vivo*.[86] Prompted by these results, the same research group[89] further investigated the β-carboline scaffold and synthesized novel β-carboline/hydroxamate hybrid compounds with a benzylic linker and an amine as connecting unit (**48a–e**, Table 15).

Compounds were tested for their inhibitory activity against HDAC1 and showed IC₅₀ values in the nanomolar range. In particular, we notice that the substitution in C1 of the pyrido-[3,4-b]indole ring with aryl electron-donating groups, such as *p*-tolyl (**48a**, IC₅₀=2.8 nM) or trimethoxyphenyl (**48e**, IC₅₀= 4.7 nM), increased the potency in comparison with electron-withdrawing groups such as nitro (**48b**, IC₅₀=65 nM). Moreover, the potency was retained with an aromatic linker, suggesting that this is the optimal distance between the cap group and the hydroxamate portion, as it happened with the substitution of the amide into an amine as a connecting unit. The antiproliferative activity was evaluated against five cancer cell lines (HepG2, SMMC-7721, Huh7, HCT116, and Mcf-7), and it proved a correlation with HDAC inhibition. The most potent compound, **48a**, enhanced the acetylation level of both α-tubulin and histone H3, confirming its target engagement for HDAC1 and

Table 15. Structure and inhibition data against HDAC1 of novel β-carboline/hydroxamate hybrid compounds with aromatic linker (**48a–e**).[89]
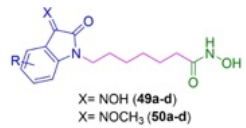

Compound	R	Inhibition activity IC₅₀ (μM) HDAC1
48a	*p*-MePh	0.0028
48b	*p*-NO₂Ph	0.065
48c	*m*-MeOPh	0.0071
48d	*p*-MeOPh	0.0093
48e	3,4,5-(MeO)₃Ph	0.0047
Vorinostat		0.142

induced G2/M phase cell cycle arrest in HepG2 cells. In addition, **48a** significantly inhibited HepG2 cell migration and invasion, resulting in a promising drug candidate for the treatment of hepatocellular carcinoma (HCC).[89]

Nam et al.[90] replaced the phenyl ring of Vorinostat with isatin derivative rings, such as isatin-3-oximes and isatin-3-methoximes, in order to find novel HDAC inhibitors that can make further interactions with the aminoacidic residues in the outside area of the enzyme catalytic site. The newly synthesized compounds are shown in Table 16.

Compounds were tested for their inhibitory activity by evaluating the histone acetylation status. For both the isatin-3-oxime hydroxamic acids (**49**), obtained as *Z* thermodynamically stable isomers, and the isatin-3-methoxime hydroxamic acids (**50**), obtained as *E*-isomers, the nitro group in 5-position led to histones deacetylation, suggesting that compounds **49c** and **50c** did not inhibit HDAC enzyme. Moreover, compounds were

Table 16. Structures and antiproliferative activity of novel isatin-hydroxamic acid derivatives (**49a–d**; **50a–d**).[90]

X= NOH (**49a-d**)
X= NOCH₃ (**50a-d**)

Compound	R	Antiproliferative activity IC₅₀ (μM) SW620
49a	–H	0.64
49b	5-Cl	0.65
49c	5-NO₂	3.39
49d	7-Cl	1.05
50a	–H	0.73
50b	5-Cl	0.49
50c	5-NO₂	1.35
50d	-7-Cl	0.26
Vorinostat		3.70

evaluated for their antiproliferative activity against SW620 cells. The compounds' anticancer activity was consistent with their target engagement; indeed, compounds with a nitro group showed the least potency. Of note, 5-Cl substitution was preferred to the 7-Cl for the series of **49** (compare **49b**, $IC_{50} =$ 0.65 μM, with **49d**, $IC_{50} = 1.05$ μM), while it was the opposite for the series of **50** (compare **50b**, $IC_{50} = 0.49$ μM, with **50d**, $IC_{50} =$ 0.26 μM). In addition, compounds **49a** and **50a**, without substituents in the isatin ring, were docked into the active site of HDAC8, and it was found that they bound with more stable energy than Vorinostat, making several interactions between the isatin ring and hydrophobic residues in the cap and at the entrance of the linker region.[90]

Similarly, Anh and colleagues[91] synthesized novel indirubin-based hydroxamates, hybridizing the HDAC-inhibiting moiety with the indirubin scaffold. They investigated both the substitution in the indirubin ring and the nature of the linker, obtaining indirubin-3'-oxime N-hydroxybenzamides (**51**), indirubin-3'-oxime N-hydropropenamides (**52**), and indirubin-3'-oxime N-hydroxyheptanamides (**53**, Table 17).

The compounds were tested for their inhibitory activity using nuclear extract of HeLa cells, and they all showed better potency than Vorinostat. These IC_{50} values give us important information regarding the SAR: for the series of **51**, the 7-Cl substitution is preferred to the 5-Cl (**51e** with an IC_{50} value lower than **51d**, 0.071 and 0.174 μM respectively), while for the series of **52**, the effect is the opposite (**52d** more potent than **52e**, IC_{50} values of 0.318 and 0.604 μM respectively). Moreover, substitution with electron-donating groups, such as methyl or methoxy, increased the inhibitory potency in both series, suggesting that these substituents are preferred to the electron-withdrawing groups. The series of **53**, instead, did not show particular changes in the activity with the various substitutions, except for a slight decrease in potency for compounds **53b** and **53c** bearing electron-donating substituents. The indirubin-based N-hydroxyheptanamides generally showed better potency, suggesting that the linear linker is preferred in this kind of scaffold. In addition, compounds were tested against SW620 cells to assess their capacity to inhibit cancer cell proliferation, and all the compounds were more potent than Vorinostat, with IC_{50} values in the low micromolar range.[91] Considering these results, hybridization of the HDAC-inhibiting scaffold with heterocyclic compounds might be a promising strategy to target solid tumors that are resistant to other therapies.

Regarding the influence of the various cap groups in the HDACi development, the spiroindoline role was investigated by Brindisi et al. Spiro-fused moieties showed promising properties

Table 17. Structure and inhibition data of indirubin-based hydroxamate derivatives (**51a–e**; **52a–e**; **53a–e**).[91]

Compound	R	Inhibition activity IC_{50} (μM) HDAC (HeLa extract)
51a	—H	0.195
51b	5–CH_3	0.005
51c	5–OCH_3	0.025
51d	5–Cl	0.174
51e	7–Cl	0.071
52a	—H	0.095
52b	5–CH_3	0.020
52c	5–OCH_3	0.005
52d	5–Cl	0.318
52e	7–Cl	0.604
53a	—H	0.022
53b	5–CH_3	0.018
53c	5–OCH_3	0.021
53d	5–Cl	0.003
53e	7–Cl	0.007
Vorinostat		1.12

to be used in drug development. Recent literature reported that their achiral properties and their conformational restriction, together with related minor off-target effects, may contribute to improving the pharmacodynamic and pharmacokinetic properties of the corresponding compounds.[92] Considering the docking studies conducted by the research group, a series of HDAC6i bearing a spiroindoline as a cap group was developed (**54a–g**).[93] All the compounds were assayed in vitro against HDAC1 and HDAC6 isoforms showing micromolar inhibiting values towards HDAC1 and from micromolar to double-digit nanomolar IC_{50} values against HDAC6 (Table 18). **54a** and **54b**, which differ from each other in the tert-butyl carbamate moiety at N-piperidine, showed both high HDAC6 inhibition properties due to the similar chemical interactions established with the latter enzyme. The replacement of the carbamate of **54b** with a methyl group (**54c**) generated a derivative markedly less potent against HDAC6. The insertion of an in vivo positively charged group (N-Me) is not well tolerated in HDAC6 inhibiting terms for the presence of positive enzymatic residues in the enzyme active pocket. The same trend was observed with compound **54f** which showed a decreased affinity and a reduced selectivity for HDAC6 due also to the replacement, in the linker, of the benzyl group with a thienyl ring. **54g**, which retained the thienyl group but presented the same carbamate as **54b**, confirmed the previous trend displaying better HDAC6 inhibiting properties than **54f** (IC_{50} [HDAC6] = 0.719 μM and 1.78 μM, respectively). **54b** and **54e**, which also displayed good physiochemical properties (data not discussed), were assayed in acute promyelocytic leukemia (NB4) and glioblastoma (U87)

cancer cell lines. Both compounds were highly cytotoxic due to the arrest of the cell cycle progression in the G1-phase.

Considering the previously discussed study, the latter research group extended their investigations about the spiroindoline cap group role in the development of HDAC6 selective inhibitors. Specifically, taking into consideration the good antitumoral properties shown by compound **54b**,[93] Sharaswati et al. studied the influence of the p-benzyl hydroxamate linker shift from the indoline nitrogen to the piperidine one in order to obtain derivatives **55a–j**[94] exhibiting better biological properties than the latter developed compounds **54a–g**. Considering the good inhibiting properties shown by the prototype **55a** (IC_{50} [HDAC6] = 0.265 μM) and the available crystal structure of the latter with the zfHDAC6 enzyme, Swaraswati and colleagues investigated the interaction occurring with the enzyme active pocket to develop a series of derivatives with improved interactions. The first series of developed derivatives (**55b–g**) present bulkier cap groups. In the enzymatic assays performed against HDAC1, HDAC6, and HDAC8 isoforms, **55a–g** showed IC_{50} values against HDAC6 in the low micromolar range (Table 19). The research group also investigated the influence, in HDAC6 inhibitory terms, given by different groups placed between the cap group and the ZBG. The corresponding synthesized compounds **55h–j**, which presented an amide, an urea, and a carbamate group between the cap group and the ZBG, respectively, showed good inhibiting properties against HDAC6, whereas **55j** displayed the best inhibitory behavior among all the synthesized compounds (IC_{50} [HDAC6] = 0.049 μM) together with a 140-fold selectivity for HDAC6 over HDAC1. Complementary docking studies

Table 18. Structure and inhibition data of HDACi bearing a spiroindoline as cap group (**54a–g**).[93]
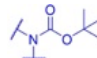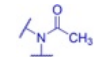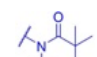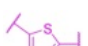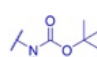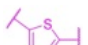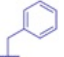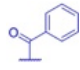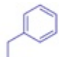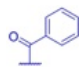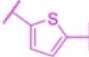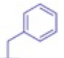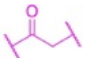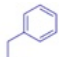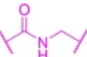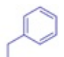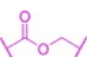
Compound	X	Ar	Inhibition activity IC_{50} (μM) HDAC1	HDAC6
54a	CH_2	benzyl	6.79	0.041
54b	N-Boc carbamate	benzyl	4.00	0.042
54c	$N-CH_3$	benzyl	11.71	0.204
54d	N-acetyl	benzyl	7.29	0.063
54e	N-isobutyryl	benzyl	4.47	0.060
54f	$N-CH_3$	thienyl	11.44	1.780
54g	N-Boc carbamate	thienyl	10.87	0.719

ChemMedChem

Review
doi.org/10.1002/cmdc.202400194

Chemistry Europe
European Chemical
Societies Publishing
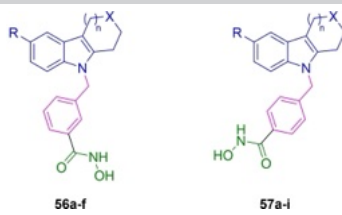
Table 19. Structure and inhibition data of HDACi bearing a spiroindoline as cap group (55 a–j).[94]

Inhibition activity
IC_{50} (μM) or inhibition % at 1 μM

Compound	R_1	R_2	X	Ar	HDAC1	HDAC6
55 a	H	—CH_3	—CH_2—	(phenyl)	22.4	0.264
55 b	H	(benzyl)	—CH_2—	(phenyl)	6.5	0.561
55 c	H	(benzoyl)	—CH_2—	(phenyl)	10.1	0.155
55 d	C_6H_5	—CH_3	—CH_2—	(phenyl)	8.5 %	50.0 %
55 e	C_6H_5	(benzyl)	—CH_2—	(phenyl)	2.9 %	29.7 %
55 f	C_6H_5	(benzoyl)	—CH_2—	(phenyl)	4.7	0.465
55 g	H	—CH_3	—CH_2—	(thiophene)	6.6 %	51.3 %
55 h	H	(benzyl)	(ketone linker)	(phenyl)	10.2	0.227
55 i	H	(benzyl)	(amide linker)	(phenyl)	3.6	0.110
55 j	H	(benzyl)	(ester linker)	(phenyl)	6.8	0.049

confirmed that the bulkier cap group of the synthesized compounds allowed to gain a better fit into the HDAC6 active pocket than the HDAC1 one, confirming the spiroindoline moiety as an effective group in HDAC6 selective inhibitors. The selected compounds **55 b**,**55 h**, and **55 j** were next tested to evaluate their antiproliferative properties against U937 and NB4 cancer cell lines. The latter compounds showed good cytotoxic properties together with promising effects in various oral and esophageal cancer cell lines (KYSE520, OE33, Ca9-22, TR- 146, and U266B) (data not shown).

In the search for highly selective HDAC inhibitors, De Vreese et al.[95] focused on the HDAC6 isoform, as it is involved in the development of neurodegenerative[96] and immunological diseases,[97] besides from cancer, becoming a target of growing importance. The research group synthesized a series of novel sulfur analogs of Tubastatin A, a well-studied HDAC6 inhibitor, called Tubathians, and investigated their activity towards HDAC6 through several modifications and substitutions in the tetrahydrothiopyranoindole cap group.

As shown in Table 20, De Vreese and colleagues synthesized both the *para-* and the *meta-*substituted benzohydroxamic acids in order to have a clear insight into which structural variation would be more effective over HDAC6 isoform. From the results obtained after a preliminary *in vitro* study, the *meta-*substituted compounds showed a moderate inhibition percentage against HDAC6 (**56 a–f**, 34–74 % inhibition at 10 μM), with compound **56 e**, bearing a phenyl substituent being the most potent (74 % inhibition). While the *para-*substituted tubathians (**57 a–i**) resulted in a high inhibition percentage, around 99 %, and were selected for further modifications. Therefore, the research team explored the oxidation status of the sulfur atom and obtained sulfides, sulfoxides, and sulfons, which differ in their inhibitory activity due to the number of oxygen atoms present able to create additional interactions with the surrounding residues in the cap region, as demonstrated by the in silico docking studies. In fact, comparing compounds **57 b** (sulfide), **57 d** (sulfoxide), and **57 h** (sulfon), the latter showed a slightly better inhibitory potency ($IC_{50} = 3.7$ nM) than the others. Moreover, they showed the importance of the thioring size for the

Table 20. Structure of novel tubathian compounds and in vitro enzyme inhibition data (IC$_{50}$ values) toward HDAC6 (**56a–f; 57a–i**).[95]

56a-f   57a-i

Compound	X	n	R	% Inhibition[a,b] HDAC6	Inhibition activity IC$_{50}$ (µM) HDAC6
56a	S	1	–H	34	–
56b	S	1	–F	53	–
56c	SO$_2$	1	–H	65	–
56d	SO$_2$	1	–F	65	–
56e	SO$_2$	1	–Ph	74	–
56f	SO$_2$	0	–F	40	–
57a	S	1	–H	–	0.015
57b	S	1	–F	–	0.022
57c	SO	1	–H	99	0.014
57d	SO	1	–F	100	0.0094
57e	SO$_2$	0	–H	99	0.0082
57f	SO$_2$	0	–F	100	0.016
57g	SO$_2$	1	–H	–	0.0019
57h	SO$_2$	1	–F	–	0.0037
57i	SO$_2$	1	–Br	100	0.0034
Tubastatin A	NCH$_3$	1	–H	–	0.015

[a]% inhibition of control values with regard to HDAC6 inhibitory activity. [b]Test concentration: 10 µM.

potency. Comparing the thiolanes **57g** and **57h** with the corresponding thianes **57e** and **57f**, the 6-atom ring is favored in terms of potency (IC$_{50}$=1.9 and 3.7 nM, against 8.2 and 16 nM, respectively). Moreover, the series of **57** was tested against the other HDAC isoforms in order to depict a selectivity profile for these compounds, which resulted in selective over HDAC6, with IC$_{50}$ values in the low nanomolar, but in some extent displayed some moderate affinity for class IIa HDAC, too. De Vreese and coworkers carried out not only western blot analysis to confirm the compounds' target engagement but also investigated ADME properties. The *para*-substituted compounds showed an effective target engagement leading to hyperacetylation of α-tubulin, and, in particular, the sulfones **57g** and **57h** displayed a promising ADME profile, which suggests a further scaffold optimization for future inhibitors development.

The same research group[98] identified and selected the 1,5-benzothiazepine unit as a starting scaffold for the development of novel and potent inhibitors, as it is a well-known pharmacophore contained in several approved drugs, such as diltiazem or clotiapine. Therefore, they synthesized novel hydroxamic acids containing the 1,5-benzothiazepine ring merged with a cyclohexane or cycloheptane, obtaining new octahydrodibenzo-

and octahydro-*6H*-benzocycloheptathiazepine-based HDAC6 inhibitors, respectively.

In Table 21 are represented the synthesized novel compounds and the corresponding inhibitory activities. As we can notice, in the series of octahydrodibenzothiazepines (**58**), the sulfones (**58f–g**) and the sulfoxide **58e** have lower IC$_{50}$ values than the non-oxidized compounds **58a–c**, resulting in a better HDAC6 inhibition. This higher potency can be explained by an additional hydrogen-bond interaction between one of the oxygens in the sulfone group and a serine residue at position 564, as outlined by a molecular dynamic simulation. Moreover, the non-substitution (**58a, 58f**) is preferred over the trifluoromethyl (**58b,58g**) and chlorinated compounds (**58c, 58h**), with higher HDAC6 inhibitory activity. In addition, the seven-membered ring (**58h**) showed a better potency than its six-membered counterpart (**59a**) did (IC$_{50}$=33 nM and 36 nM, respectively), while its diastereoisomer **59c** showed a weaker potency (IC$_{50}$=92 nM). The most active compounds (**58a, 58f, 58g, 58e, 58d**) were tested against the other HDAC isoforms and resulted in selective over HDAC6 with a lesser extent over HDAC8 and 11 in the submicromolar level. Moreover, these compounds not only induced a significant increase in α-tubulin acetylation without affecting acetylation of histone H3, confirming their target engagement and selectivity over HDAC6, but

ChemMedChem

Review
doi.org/10.1002/cmdc.202400194

Chemistry
Europe

European Chemical
Societies Publishing

Table 21. Structure and inhibition data of novel octahydrodibenzo- and octahydro-6H-benzocycloheptathiazepine-based HDAC6 inhibitors (**58a–h**; **59a,b**).[98]

58a-h   59a,b

Compound	X	n	R	Inhibition activity IC$_{50}$ (μM) HDAC6
58a	S	1	—H	0.036
58b	S	1	—CF$_3$	0.200
58c	S	1	—Cl	0.650
58d	S	2	—H	0.033
58e	SO	1	—H	0.0063
58f	SO$_2$	1	—H	0.0083
58g	SO$_2$	1	—CF$_3$	0.011
58h	SO$_2$	1	—Cl	0.068
59a	S	1	—Cl	0.160
59b	S	2	—H	0.092

also resulted negative in the Ames mutagenicity test, confirming their potential for further optimization studies.

Ressing and colleagues[99] worked on the development of HDAC6 inhibitors, too. They synthesized novel hydroxamic acids bearing a bifurcated cap group containing a bioisosteric tetrazole ring, replacing the commonly used amide as CU.

The synthesized compounds were tested for their inhibitory activity in enzymatic assays against HDAC1 and 6, and the selectivity index (SI) was calculated as follows: IC$_{50}$ $\frac{(HDAC1)}{(HDAC6)}$. As shown in Table 22, N-acylated compounds (**60a–d**) displayed a slightly better inhibitory potency and selectivity than compounds **60e,f**. Moreover, the benzyl derivatives **60b** and **60e** resulted in lower IC$_{50}$ values than the cyclohexyl derivatives **60e** and **60a** (IC$_{50}$ = 0.10 and 0.03 μM versus IC$_{50}$ = 0.12 and 0.07 μM), maintaining a similar selectivity index. Of note, comparing **60a** with **60b** and **60d**, a further substituent on the 2-position of the benzamide group increased the potency and the selectivity, especially for compound **60d**, which resulted in the most effective one. Consequently, it was selected for additional screenings. The crystal structure of HDAC6 in complex with compound **60f** showed that its bifurcated capping group occupied both different pockets (called loop L1 and L2) of the enzyme in the cap region, with the tetrazole ring forming hydrogen bonds with external residues. These steric complementarity features could explain the selectivity over the HDAC6 isoform.

Furthermore, compound **60d** was demonstrated to be selective over HDAC class I and IIa and induced acetylation of α-tubulin without affecting the acetylation of H3. In particular, **60d** exhibited synergistic antiproliferative activity in a leukemia cell line (HL60), increasing apoptosis induction in combination with Bortezomib, a clinically used proteasome inhibitor, as
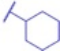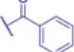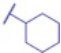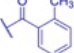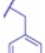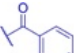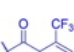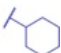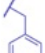
described in the literature.[100] Therefore, compound **60d** is a valuable hit compound that needs to be further optimized in order to increase the cytotoxic properties of HDAC6 inhibitors used in combination with other agents.[101]

Guan and colleagues[102] inserted a thiadiazole moiety in the cap region and synthesized several compounds as potential HDAC inhibitors. At the 5-position of the 1,3,4-thiadiazole moiety, the research group inserted various substituents, such as phenyl, benzyl, phenethyl, and (E)-styryl, which resulted in a progressive general decrease of inhibitory potency (compare for example compound **61e** with **61f–h**) except for compound **61d** (IC$_{50}$ = 0.16 μM). Moreover, compounds having a linker of 5 or 6 methylene units were preferred, with IC$_{50}$ values in the nanomolar range (compounds **61e–g** and **61i–k**, Table 23).[102]

The most potent compound **61e** was also tested in MTT assays for its antiproliferative activity against two cancer cell lines (MDA-MB-231 and K562) and effectively inhibited cell proliferation. In addition, its binding mode was evaluated in the HDAC1 binding site, and it was shown to form the canonical hydrogen bonds in the active site and two further hydrogen interactions between the nitrogen atom of the thiadiazole ring with the Phe197.[102]

Vergani et al.[103] used various pentaheterocyclic rings in the cap region, such as 1,2,4-triazole, tetrazole (both 1,5- and 2,5-disubstituted), 1,3,4-oxadiazole, 1,2,4-oxadiazole, and 1,3,4-thiadiazole, which replaced the connecting unit amide while maintaining the potency and selectivity. Using a ligand-based approach, they synthesized N-hydroxybenzamide compounds with the aromatic linker and explored the substitutions on the heterocyclic ring, obtaining important SAR information regarding the selectivity for HDAC6 isoform.

ChemMedChem

Review

doi.org/10.1002/cmdc.202400194

Chemistry
Europe
European Chemical
Societies Publishing

Table 22. Structure and IC$_{50}$ values (μM) of novel tetrazole-capped HDAC6 inhibitors (**60 a–f**).[99]

60a-f

Compound	R$_1$	R$_2$	R$_3$	Inhibition activity IC$_{50}$ (μM) HDAC1	Inhibition activity IC$_{50}$ (μM) HDAC6	SI IC$_{50}$ $\frac{HDAC1}{HDAC6}$
60 a		—H		2.37	0.07	34
60 b		—H		3.03	0.06	50
60 c		—H		1.24	0.03	41
60 d		—H		5.18	0.03	173
60 e		—Ph	—H	4.06	0.12	34
60 f		—Ph	—H	3.37	0.10	34
Nexturastat A				0.50	0.02	24
Tubastatin A				2.49	0.014	178

Compounds **62 a–c** and **62 g–i** (Table 24), bearing different heterocycles, showed a good inhibitory potency in the nanomolar range with also good selectivity over HDAC3. Consequently, we can deduce that the isosteric replacements of the heteroatoms in the pentacycle are well tolerated for potency and selectivity. Moreover, comparing the tetrazole compounds **62 c** and **62 d**, the latter, with a benzyl group instead of a phenyl, decreases potency (IC$_{50}$ values of 3 nM and 52 nM, respectively). The distance between the aromatic linker and the heterocycle is also important: the direct connection of the heterocycle to the aromatic ring results in a significant loss of potency (compare **62 e** to **62 b**). The methylation at position 4 of the 1,2,4-triazole ring resulted in compound **62 f**, which, in comparison to the free —NH compound **62 a**, slightly lost its inhibitory potency (IC$_{50}$ = 17 nM instead of 5 nM of **62 a**) while increasing its HDAC6 selectivity. Further investigations on the bioisosteric replacement of the connecting methylene unit between the aromatic linker and the heterocycle gave compounds **63 a,b** with a sulfur-connecting atom, which exhibited still high potency (IC$_{50}$ values of 6 nM for both compounds) but a reduced selectivity, which was more evident for the 1,2,4-oxadiazole **63 a** (Table 25).
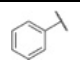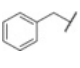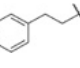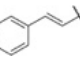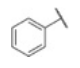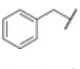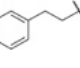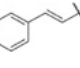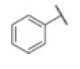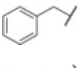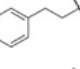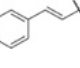
Vergani and colleagues also investigated in more detail the substitution pattern of the 1,3,4-triazole, adding substituents on the N1 and N2 of the cycle, as the substitution on N4 did not influence the potency and selectivity, as previously seen

comparing compounds **62 f** and **62 a**. The resulting compounds **64 a–c** (Table 26) retained the selectivity for HDAC6 but displayed a strong decrease in inhibitory potency. Therefore, substitutions on the nitrogen atoms of the 1,3,4-triazole ring are not favored, and it might be due to the loss of additional interactions they would have made without substituents.

Furthermore, the research group studied the SAR for the aryl substituent on the tetrazole ring and synthesized the series of **65**. Substitution in both *meta* and *para* position with an electron-withdrawing group, such as SF$_5$, reduced the potency and the selectivity (compare compounds **65 a–b** with **62 c**). Contrariwise, the amide substituent in the *para* position of the phenyl ring retained the selectivity while improving the inhibitory potency (compound **65 c**, IC$_{50}$ = 1 nM), which was also maintained in compound **65 d** with an aminomethylphenyl (IC$_{50}$ = 2 nM). Replacing the phenyl ring with either a pyridyl (compound **65 e**) or pyrimidinyl (compound **65 f**) moiety strongly increased the selectivity of the compounds, maybe due to possible further interactions of the additional nitrogen atom in the external area of the enzyme catalytic site. The substitution of the aromatic ring with a larger moiety, such as quinoline (compound **65 h**) and isoquinoline (compound **65 i**), slightly reduced the potency (IC$_{50}$ = 20 nM for both) but increased the selectivity only for **65 h** (Table 27).

Conclusively, Vergani *et al.* provided some insightful SAR information regarding HDAC6 selective inhibition: the introduc-

Table 23. Structures and inhibition data of novel 1,3,4-thiadiazole hydroxamic acid derivatives (**61 a–l**).[102]

61a-l

Compound	R	n	Inhibition activity IC$_{50}$ (µM) HDAC (HeLa extract)
61 a		3	> 5
61 b		3	1.87
61 c		3	2.71
61 d		3	0.16
61 e		5	0.089
61 f		5	0.22
61 g		5	0.33
61 h		5	> 5
61 i		6	0.27
61 j		6	0.26
61 k		6	0.32
61 l		6	3.21
Vorinostat			0.15

tion of the previously discussed substituted rings in the cap group allowed additional interactions within the HDAC6 active pocket thus obtaining derivatives with a better inhibiting spectrum in potency and selectivity terms. Moreover, they tested the compounds against the other HDAC isoforms, and most of them were selective over HDAC6. The selectivity *in vivo* was investigated by measuring the tubulin acetylation status in mice injected intraperitoneally with two of the synthesized compounds (not shown here), which resulted in high selectivity for HDAC6 with an increased degree in tubulin acetylation.[103] These data offer a good starting point for further evaluations on HDAC inhibitors with pentaheterocycles as capping groups.

Several research groups investigated the role of oxadiazole isomers into HDACi scaffold. The ability of oxadiazole and its isomers to interact with biological targets through hydrogen bonds allowed them to gain significant interest in chemical and pharmaceutical research. Oxadiazole has four isomers, and among them, the 1,3,4-oxadiazole isomer is widely known and used in several chemical and pharmaceutical applications[104] thanks to its antimicrobial, anti-inflammatory, antibacterial,

antifungal, and antitumor properties.[105] In the literature, its use in HDACi development is extensively reported.

Indeed, this heterocycle was used as a connecting unit in a research work by Valente *et al.*,[106] where the authors synthesized 1,3,4-oxadiazole-containing derivatives as HDAC inhibitors (**67 a–c** and **68 a,b**, Table 28). The work of the latter research group was based on acylamino- cinnamyl hydroxamates and 2-aminoanilides (**66**), developed by Valente and coworkers, which displayed higher pro-apoptotic and/or cytodifferentiating effects than Vorinostat and Entinostat in human leukemia U937 cells.[107] More specifically, the amide group of **66** was replaced with a C5-substituted 1,3,4-oxadiazole to analyze the consequence of variations at CU (Figure 11). The corresponding 2-aminoanilides derivatives (**80 a–d, 81 a,b**) will be discussed in paragraph 3.2.

Among the synthesized compounds, the selected ones shown in Table 28, when tested against HDAC1 and −6, resulted in a potent inhibitory activity in the low micromolar range. Moreover, the 1-naphthyl substituent at the 5-position of the oxadiazole, connected with a methylene unit, showed the best results from preliminary studies. The introduction of a further methylene unit between the 2-position of the oxadiazole and the aril linker improved the inhibitory activity (compare **67 a** with **67 c** and **68 a** with **68 b**). In addition, the removal of the cinnamic double bond and its replacement with the benzoic moiety decreased the selectivity over HDAC6 (compare **67 c**, IC$_{50}$ HDAC6 = 0.03 µM, with **68 b**, IC$_{50}$ HDAC6 = 1.2 µM). **67 c** and **68 b** were also evaluated for their antiproliferative capacity, and both of them induced cell cycle arrest, apoptosis as well as cytodifferentiation in a dose-dependent manner in human leukemia U937 cells. In addition, they showed a better anticancer activity than Vorinostat in SW620 cells and in five AML cell lines (U937, HL60, HEL, KG1, and MOLM13).[106]

Cai *et al.* investigated the role of 1,2,4-oxadiazole isomers in HDACi structure.[108] This research group has focused on developing HDACi derivatives by replacing the carbamate moiety of Entinostat with a C3-substituted 1,2,4-oxadiazole, as a heterocyclic isostere to analyze the consequence of variations at CU. The latter research group synthesized the anilide analogs
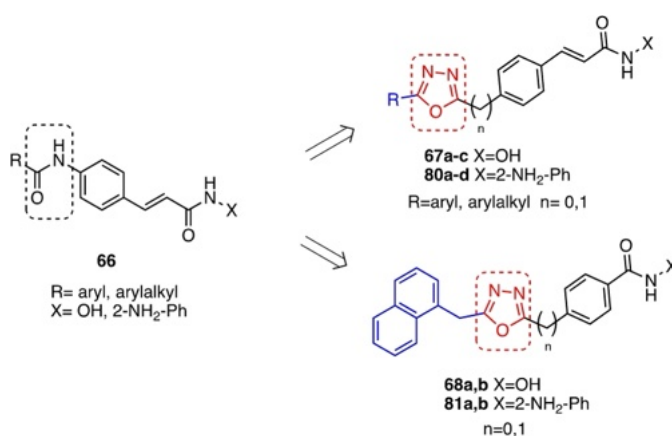

Figure 11. Design of hydroxamate and 2-aminoanilide HDACi bearing 1,3,4-oxadiazole.

ChemMedChem

Review
doi.org/10.1002/cmdc.202400194

Chemistry Europe
European Chemical
Societies Publishing

Table 24. Structures, inhibition data against HDAC6, and selectivity data of aromatic heterocycle derivatives (**62a–i**).[103]

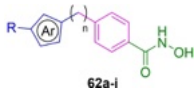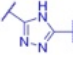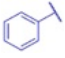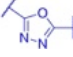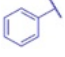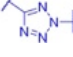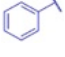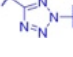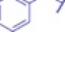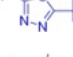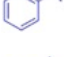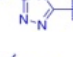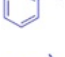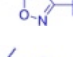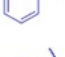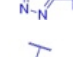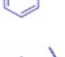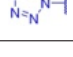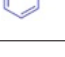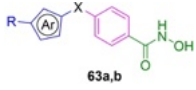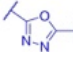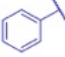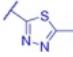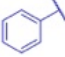| Compound	Ar	n	R	Inhibition activity IC$_{50}$ (µM) HDAC6	HDAC6 selectivity (HDAC3/HDAC6)
62a		1		0.005	21
62b		1		0.004	32
62c		1		0.003	72
62d		1		0.052	26
62e		0		0.660	3
62f		1		0.017	129
62g		1		0.006	50
62h		1		0.016	105
62i		1		0.009	83

Table 25. Structures, inhibition data against HDAC6, and selectivity data of aromatic heterocycle derivatives (**63a,b**).[103]

Compound	Ar	X	R	Inhibition activity IC$_{50}$ (µM) HDAC6	HDAC6 selectivity (HDAC3/HDAC6)
63a		S		0.006	17
63b		S		0.006	62

83a–j, which are discussed later in paragraph 3.2, too. Additionally, they also developed compounds **69a–d** by replacing the ZBG of entinostat with the hydroxamate group (Table 29).

The compounds were tested for their inhibitory activity against HDAC1, −2, and −8, and all of them exhibited low IC$_{50}$ values except for HDAC8, resulting in being more potent than Vorinostat. Therefore, in this case, the electronic nature of the substituents did not influence the activity of the compounds, whereas the unsubstituted one (**69a**) was the most potent. **69a** was docked into the active site of HDAC8, pointing out various further interactions with the oxadiazole moiety, which might have enhanced its inhibitory activity. In addition, when tested against

different cancer cell lines (U937, A549, NCI–H661 MDA-MB-231, HCT116), these compounds exhibited good anticancer activity only against U937 cells without being effective on solid tumor cell lines.[108] The same research group[109] further investigated the SAR of these compounds and synthesized 1,2,4-oxadiazole analogs containing a linear linker (**70a–g**, Table 30).

In this case, the nature of the substituent R was relevant for the inhibitory potency of these compounds. Indeed, the nitro group, especially in the para position (**70c** preferred over **70b**), was favored, and heterocycles such as thiophene and pyridine rings (compounds **70f** and **70g**, respectively) led to lower IC$_{50}$ values in comparison with **70a**. Moreover, the compounds

Table 26. Structures, inhibition data against HDAC6, and selectivity data of 1,3,4-triazole derivatives (**64a–c**).[103]
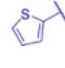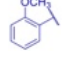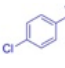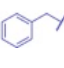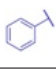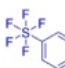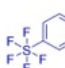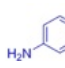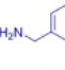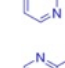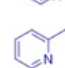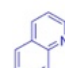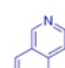

Compound	X	R	R$_1$	R$_2$	Inhibition activity IC$_{50}$ (μM) HDAC6	HDAC6 selectivity (HDAC3/HDAC6)
64a	CH$_2$	(thiophene)	–	(2-methoxyphenyl)	0.333	16
64b	CH$_2$	(4-chlorophenyl)	–	(benzyl)	0.368	24
64c	S	(cyclopropyl)	(benzyl)	–	0.162	12

Table 27. Structures, inhibition data against HDAC6, and selectivity data of tetrazole derivatives (**65a–i**).[103]

Compound	R	Inhibition activity IC$_{50}$ (μM) HDAC6	HDAC6 selectivity (HDAC3/HDAC6)
65a	(3-SF$_5$-phenyl)	0.026	35
65b	(4-SF$_5$-phenyl)	0.025	50
65c	(4-aminophenyl)	0.001	75
65d	(4-aminomethylphenyl)	0.002	30
65e	(pyridin-2-yl)	0.009	189
65f	(pyrimidin-2-yl)	0.007	126
65g	(pyridin-2-ylmethyl)	0.025	157
65h	(quinolin-2-yl)	0.020	7
65i	(isoquinolin-3-yl)	0.020	132

showed a better inhibitory activity for HDAC1 and −2, confirming the selectivity profile of Vorinostat derivatives with a linear linker. Again, they exhibited a better anticancer activity towards U937 cells without affecting lung carcinoma cells (A549 and NCI–H661) in a significant way.[109]

A different oxadiazole isomer, the 1,2,5-oxadiazole, was included in the development of HDAC-based dual hybrid inhibitors. Fang *et al.* designed a series of HDAC-indoleamine 2,3-dioxygenase 1 (IDO1) dual inhibitors by merging Mocetinostat and INCB024360 (IDO1 inhibitor, Figure 12) structures using aryl and heterocyclic moieties as linker groups.[110] The research group focused on developing derivatives bearing hydroxamate (**71a–h**) and 2-aminoanilide (**82a–d**) as ZBG, and the latter will be discussed later in paragraph 3.2.

Considering the impact of the carbon chain length (**71a–c**) on HDAC1 inhibiting properties, **71b** and **71c**, bearing a five and a six-carbon chain, respectively, exhibited a relevant inhibition activity against HDAC1, with compound **71b** being the most potent compound of the whole synthesized series **71a–h** (IC$_{50}$ = 9.2 nM). Compounds **71d** and **71e**, bearing a double bond between the phenyl group and the hydroxamate, exhibited strong HDAC1 inhibiting properties, showing an IC$_{50}$ value in the double-digit nanomolar range (46.2 nM and 70.5 nM, respectively). The insertion of the 1,2,3-triazole ring in compounds **71f–h** led to good inhibiting HDAC1 properties when the carbon chain length was four (**71g**) or five (**71h**) membered instead of three carbons (**71f**). The latter evidence explains how increasing the carbon chain length influences the inhibiting properties of **71f–h**, with compound **71h** being the strongest of these series (IC$_{50}$ = 23.5 nM). The antiproliferative assays were conducted in LLC (Lewis lung cancer), CT-26 (mouse colon cancer), A549 (human lung cancer), HCT-116 (human colon cancer) and HT-29 (human colon cancer) cell lines and a great part of **71a–h** compounds (Table 31) exhibited good antitumor suppressing activities, specifically against HCT-116 cell line where compound **71c** and **71e** exhibited a cytotoxic activity similar to the Vorinostat one, showing IC$_{50}$ values in the submicromolar range (IC$_{50}$ = 4.70 μM and IC$_{50}$ = 5.89 μM, respectively).
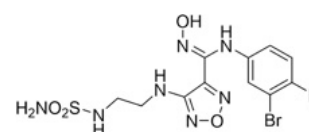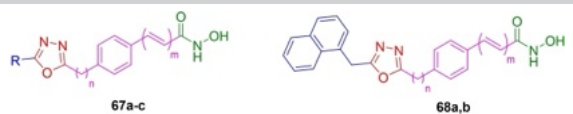
Figure 12. INCB024360 chemical structure.

ChemMedChem

Review
doi.org/10.1002/cmdc.202400194

Chemistry
Europe
European Chemical
Societies Publishing

Table 28. 1,3,4-oxadiazole derivatives as HDAC inhibitors (**67a–c; 68a,b**) and relative inhibition data against HDAC1 and HDAC6.[106]
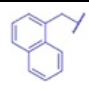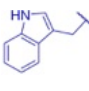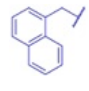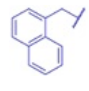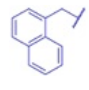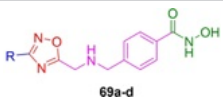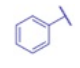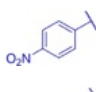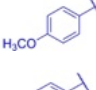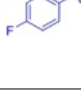
| | | | | Inhibition activity IC$_{50}$ (µM) | |
Compound	R	n	HDAC1	HDAC4	HDAC6
67a		0	0.8	>20	0.06
67b		0	0.6	15.2	0.03
67c		1	0.2	>20	0.03
68a		0	9.9	>20	4.1
68b		1	0.2	7.8	1.2
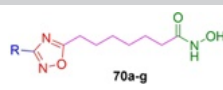
Table 29. Structure and inhibition data against HDAC1, −2, −8 of novel 1,2,4-oxadiazole hydroxamate derivatives (**69a–d**).[108]
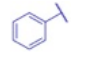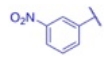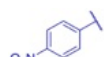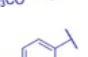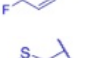
| | | Inhibition activity IC$_{50}$ (µM) | | |
Compound	R	HDAC1	HDAC2	HDAC8
69a		5.73	>10	0.20
69b		2.67	9.23	0.38
69c		8.32	>10	0.86
69d		3.53	7.69	0.23
Vorinostat		0.15	0.28	1.68

Shen *et al.*,[111] consequently to the identification of a lead compound in a previous study,[112] introduced an isoxazole ring in the linker region and obtained isoxazole-3-hydroxamates derivatives with different cap groups, which are essential for driving the selectivity toward HDAC6 isoform, as recently stated by Zhang and colleagues.[113] Therefore, they synthesized various compounds in order to achieve selectivity as well as potency (**72a–f**).

As seen in Table 32, bulkier substituents increased the inhibitory potency (**72c** and **72d** more potent than **72a** and **72b**) but decreased the selectivity towards HDAC6. Moreover, the replacement of the amide as a connecting unit with an ether (**72e**) or an alkyl chain (**72f**) was detrimental for both HDAC1 and −6 inhibition, suggesting that the amide group is necessary for both potency and selectivity. The selected compound **72b** was docked into HDAC6 active site, and it was found to form a bidentate coordination with the Zn^{2+} ion, differently as it is reported for hydroxamates with an aryl linker in HDAC6 catalytic cleft. Indeed, the isoxazole moiety slightly shifts the distances between the atoms, creating a more stable conformation that consequently binds in a bidentate fashion. Furthermore, **72b** did not affect cell cycle arrest, apoptosis, and differentiation of human and murine melanoma cells but

ChemMedChem

Review
doi.org/10.1002/cmdc.202400194

Chemistry Europe
European Chemical
Societies Publishing
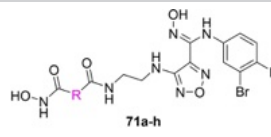
Table 30. Structure and HDAC1, −2, −8 inhibition (IC$_{50}$, μM) of novel 1,2,4-oxadiazole hydroxamate derivatives (**70a–g**).[109]

		Inhibition activity IC$_{50}$ (μM)		
Compound	R	HDAC1	HDAC2	HDAC8
70a	phenyl	0.38	1.17	2.05
70b	3-nitrophenyl	0.35	1.56	2.38
70c	4-nitrophenyl	0.07	0.23	2.56
70d	4-methoxyphenyl	2.18	>10	>10
70e	4-fluorophenyl	1.15	6.26	8.76
70f	thiophene	0.12	0.51	1.92
70g	pyridine	0.08	0.39	1.83
Vorinostat		0.15	0.28	1.68

enhanced the acetylation status of α-tubulin, confirming its target engagement.[111]

Zhang and coworkers[114] introduced the 1,2,3,4-tetrahydroisoquinoline moiety in the linker region to develop HDAC inhibitors with a more conformationally restricted structure (Table 33). They obtained four series of compounds: the first three (**73–75**) differ in the substitution both in the cap region and in the nitrogen of the tetrahydroisoquinoline ring, and the fourth series (**76**) derives from the condensation of the Cbz group in a basic medium, obtaining a hydantoin-like tricycle.

The compounds were tested against the HDAC8 isoform, and we can notice from the first two series of compounds (**73**, **74**) that, in most of the cases, the Boc substituent is preferred over the non-substituted form (compare **73a**, **73b**, and **73d** with **74a**, **74b**, and **74d**, respectively). While this is not evident for compounds bearing the naphthyl substituent, with **64c** without the Boc substitution having a lower IC$_{50}$ value (1.06 μM) than **73c** (4.25 μM). This is probably due to the interactions the naphthalene ring forms with HDAC8 without being restricted in its rotation by the large Boc group (**74c**). **75a**, the correspondent Cbz analog of **73d** and **74d**, was more potent (IC$_{50}$ = 0.58 μM) than both compounds and the most active compound in **73** series (**73b**, IC$_{50}$ = 1.0 μM). This good inhibitory activity was confirmed by docking studies, which pointed out the multiple interactions, such as π-π stacking or hydrophobic interactions, between both the tetrahydroisoquinoline ring and the substituent in the cap group. The series of **76**, instead,

Table 31. Structures, inhibition data against HDAC1, antiproliferative activity in LLC, CT-26, A549, HCT116, and HT-29 of HDAC/IDO1 dual inhibitors bearing 1,2,5-oxadiazole (**71a–h**).[110]
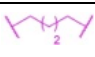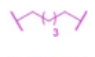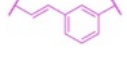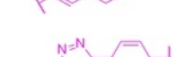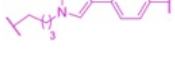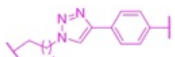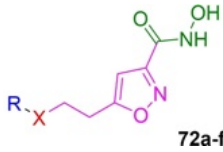
		Inhibition activity IC$_{50}$ (μM)	Antiproliferative activity IC$_{50}$ (μM)				
Compound	R	HDAC1	LLC	CT-26	A549	HCT-116	HT-29
71a		0.308	>100	>100	>100	85.37	>100
71b		0.009	90.11	95.46	40.66	17.46	28.74
71c		0.048	56.58	97.45	36-03	4.70	14.88
71d		0.070	53.30	38.94	41.66	12.44	23.31
71e		0.046	21.64	12.79	25.56	5.89	14.15
71f		0.894	>100	>100	>100	37.53	>100
71g		0.066	>100	>100	>100	>100	>100
71h		0.023	35.95	90.18	45.48	29.44	23.88
Vorinostat		0.014	9.68	5.97	2.63	3.07	1.78

ChemMedChem

Review
doi.org/10.1002/cmdc.202400194

Chemistry Europe
European Chemical
Societies Publishing

Table 32. Structures and inhibition data against HDAC1 and HDAC6 of isoxazole-3-hydroxamate derivatives (**72a–f**).[111]
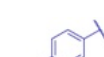

Compound	R	X	Inhibition activity IC$_{50}$ (μM)	
			HDAC1	HDAC6
72a			> 30	0.19
72b			31.5	0.075
72c			3.03	0.010
72d			2.04	0.024
72e			> 30	0.20
72f			> 30	1.98

exhibited almost no inhibition, probably due to the very rigid structure of the condensed tricycle. Furthermore, the most active compounds were evaluated for their anticancer properties against three cell lines (HCT116, SKOV3, and HL60). Compounds **73b** and **74c** exhibited better antiproliferative activity than Vorinostat, while **75a** showed a low IC$_{50}$ value, probably due to the ester hydrolysis.[114]

In order to optimize the chemical properties of a previously identified compound[115] (**R306465**, Figure 13), which exhibited potent antitumor activity but poor solubility, Angibaud *et al.*[116] explored the SAR around novel hydroxamic acids containing a 2-piperazinyl-pyrimidyl linker by synthesizing a series of novel derivatives (**77a–g**, Table 34).

Looking at Table 34, neither the substitutions on the phenyl ring nor the stereochemistry of the carbon directly linked to the nitrogen of the piperazine influence the inhibitory activity, measured using nuclear extract of HeLa cells rich in HDACs, since all the synthesized compounds have IC$_{50}$ values in the range of low nanomolar. Moreover, the substitution of the

hydroxyl group, obtaining compound **77g**, did not exhibit changes in the inhibitory activity, suggesting that the hydroxyl moiety might not interact with the hydrophobic residues in the linker region of HDACs. Of note, the compounds were more soluble than the lead compound previously identified, and their antiproliferative activity against A2780 cells correlated with their inhibitory potency, being in the low micromolar range.[116]

Rossi and coworkers[117] conducted a similar study applying a systematic approach to investigating the potential inhibitory activity of novel compounds bearing alkyl-piperazine and piperidine moieties as linkers (Table 35).

From previous results, the propyl chain connecting the ZBG and either the piperazine or the piperidine moieties resulted in the optimal length. Therefore, they synthesized 4-propylpiperidinyl (**78a–f**) or 4-propylpiperazinyl (**79a–d**) hydroxamate derivatives with different connecting units and different substituents in the cap region. It was demonstrated that the series of **79**, with the piperazine linker, inhibited the enzyme poorly. Hence, IC$_{50}$ values were determined only for the series of **78** with the piperidine linker, showing that the urea analogs (**78e,f**) were the most potent in comparison with the amide ones (**78c,d**) and sulfonamide (**78a,b**) ones. Again, **78e,f** displayed the best anticancer activity in antiproliferative assays against HCT-116 cells.[117] These data are a valuable starting point to further investigate the SAR of these compounds, for example inserting various substituents on the phenyl group, which might influence the inhibitory activity.

Figure 13. R306465 chemical structure.

ChemMedChem

Review
doi.org/10.1002/cmdc.202400194

Chemistry Europe
European Chemical
Societies Publishing

Table 33. Structures and inhibition data against HDAC8 of novel 1,2,3,4-tetrahydroisoquinoline-3-hydroxamate derivatives (**73 a–d; 74 a–d; 75 a; 76 a,b**).[114]

R=Boc (73a-d)
R=H (74a-d)
R=Cbz (75a)

76a,b
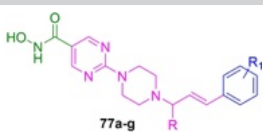
Compound	R_1	Inhibition activity IC$_{50}$ (μM) HDAC8
73 a		1.29
73 b	OCH$_3$	1.00
73 c		4.25
73 d		2.67
74 a		8.21
74 b	OCH$_3$	5.57
74 c		1.06
74 d		4.07
75 a		0.58
76 a		> 50
76 b		> 50

3.2. Benzamide–based HDAC Inhibitors

Benzamide-based inhibitors represent a vast class of molecules among the HDAC inhibitor family. These molecules contain an N-(2-aminophenyl) benzamide moiety that has a central role in the HDAC mechanism of inhibition. This moiety provides an enhanced selectivity towards HDAC1-3 inhibition compared to the lack of HDAC selectivity presented by hydroxamic acid derivatives. In particular, HDACi-bearing benzamide moieties are known for their lack of inhibition activity towards HDAC6 and HDAC8 isoforms.[118] Analyzing their binding mode is helpful to understand the selectivity of benzamide inhibitors further. The evidence of a molecular docking study done with Entinostat and histone deacetylase-like protein (HDLP) reported that the former can bind HDLP differently from the one shown by Vorinostat and TSA.[119] The results revealed that Entinostat binds the enzyme at the entrance of his active pocket. The
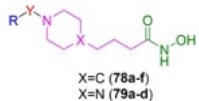
middle benzene is involved in bonds with Phe141 and Phe198 phenyl rings; the 2'-amino group is engaged in a hydrogen bond with the hydroxy group of Tyr91 or Glu92, and the pyridine nitrogen interacts with a hydrogen bond to the ionized amino group of the side chain of Lys267. The Entinostat middle benzene creates a sandwich structure with Phe141 and Phe198 aromatic rings (Figure 14) that blocks the entrance of the acetylated histone lysine in the HDAC catalytic site.
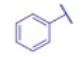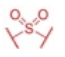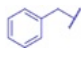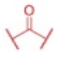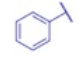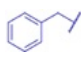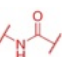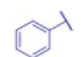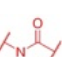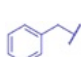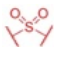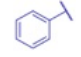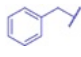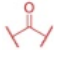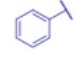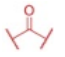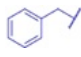
This allows us to understand that benzamide HDAC inhibitors are localized in the narrowest area of HDAC1 and −2 active pockets during their inhibition mechanism. Crystallographic analysis conducted on eutectic structures of HDAC2-inhibitor reports that the o-amino group, along with the carbonyl oxygen, is involved in Zn^{2+} chelation, allowing HDAC inhibition.[120] Thanks to the bonds with the specific residues of HDAC1 and HDAC2, it is possible to explain the benzamide inhibitor selectivity towards class I HDAC.[120–121] Considering the

ChemMedChem

Review
doi.org/10.1002/cmdc.202400194

Chemistry
Europe
European Chemical
Societies Publishing

Table 34. Structures and inhibition data of novel 2-piperazinyl-5-pyrimid-yl-hydroxamic acids (**77a–g**).[116]

Compound	R	R_1	HDAC (HeLa extract)
			Inhibition activity IC_{50} (nM)
77a[a]	—CH_2OH	—H	1.0
77b[b]	—CH_2OH	—H	1.8
77c	—CH_2OH	4-OCH_3	0.95
77d[a]	—CH_2OH	4-F	1.5
77e[b]	—CH_2OH	4-F	1.2
77f	—CH_2OH	4-Cl	1.2
77g	—CH_3	-H	1.7

[a] (+) enantiomer; [b] (−) enantiomer.

Table 35. Structures and inhibition data of novel 4-propylpiperidinyl and 4-propylpiperazinyl hydroxamate derivatives (**78a–f**; **79a–d**).[117]

Compound	Y	R	HDAC (HeLa extract)
			Inhibition activity IC_{50} (µM)
78a			0.54
78b			0.84
78c			1.39
78d			0.26
78e			0.10
78f			0.09
79a			19[a]
79b			50[a]
79c			30[a]
79d			52[a]

[a] % of inhibition using an enzymatic assay measuring total HDAC activity in HeLa cell extracts at a concentration of 50 µM.

N-(2-aminophenyl)benzamide efficacy in HDAC1 and −2 inhibition, it is clear the involvement in clinical trials of the benzamide derivatives discussed previously (Chidamide, Mocetinostat, Entinostat). Despite their selectivity, which can reduce adverse effects, bearing a free and exposed amino group can potentially be toxic *in vivo*, limiting their usage and, therefore, their clinical applications.[50a,122]

Modifying the 2-amino anilide moiety by the insertion of aryl rings has proven effectiveness in obtaining derivatives that are selective inhibitors against HDAC1/2, with no observed inhibition of HDAC3. Studies conducted by Merck have led to the discovery that conferring HDAC1/HDAC2 selectivity over HDAC3 is achievable by adding a 5-phenyl or 5-thienyl substituent to the *o*-aminoanilide zinc-binding group (ZBG) of HDAC inhibitors.[71b,c] As evident in the X-ray structure of BRD4884-HDAC2[123] (Figure 15), the aryl group interacts with the enzyme's internal cavity, explaining the high selectivity of 5-aryl aminoanilide-containing HDACi. In contrast, the corresponding internal cavity of HDAC3 contains a bulkier tyrosine residue, which obstructs access to HDAC inhibitors containing 5-aryl benzamide ZBG.

From this evidence, over the years, many research groups have dedicated their activities to optimizing the N-(2-aminophenyl) benzamide scaffold by developing many promising derivatives. Considering the known HDAC pharmacophore, to obtain more specific and potent derivatives, in the last decades, researchers have tried to achieve this aim by developing derivatives with a heterocyclic or bicycle heterocyclic structure as a linker, CAP, or CU group. Heterocyclic moieties have gained much importance in medicinal chemistry thanks to their high biocompatibility and their comprehensive therapeutic values.[124] Heterocyclic compounds, such as 5-membered and 6-membered rings, or fused ring systems, play a crucial role in optimizing new drug molecules with better potency and lowest toxicity.[125] Furthermore, rings containing an N, O, or S atom have emerged as a focal point in synthetic chemistry for developing new medicinal compounds due to their immense therapeutic potential. Hence, introducing them into the HDACi scaffold may represent a successful approach to obtaining more potent inhibitors.

Besides the hydroxamate-based HDACi discussed in paragraph 3.1, Valente *et al.* have also focused on developing 1,3,4-oxadiazole containing 2-aminoanilides. The new series of 2-aminoanilides **70a–d** and **71a,b** have been tested as HDACi to assess their capability to induce cell cycle arrest, apoptosis, and/or cytodifferentiation in human leukemia U937 cells.[106]

In the enzymatic assays, compounds **80a–d** and **81a,b** have been tested by determining their IC_{50} values against human HDAC1, HDAC4, and HDAC6 (Table 36) using Vorinostat as reference drug. The cinnamic derivative bearing 1-naphthyl ring (**80a**) displayed higher inhibitory potency than the other derivatives towards HDAC1 inhibition (IC_{50} = 1.0 µM). However, the most promising results against HDAC1 are shown by the benzoic derivatives (**81a,b**). **81a** displayed the same HDAC1 inhibitory potency as Vorinostat (IC_{50} = 0.3 µM) while **81b** displayed higher HDAC1 inhibitory potency than Vorinostat (IC_{50} = 0.2 µM). For all the derivatives (**80a–d** and **81a,b**) no

ChemMedChem

Review
doi.org/10.1002/cmdc.202400194

Chemistry Europe
European Chemical
Societies Publishing
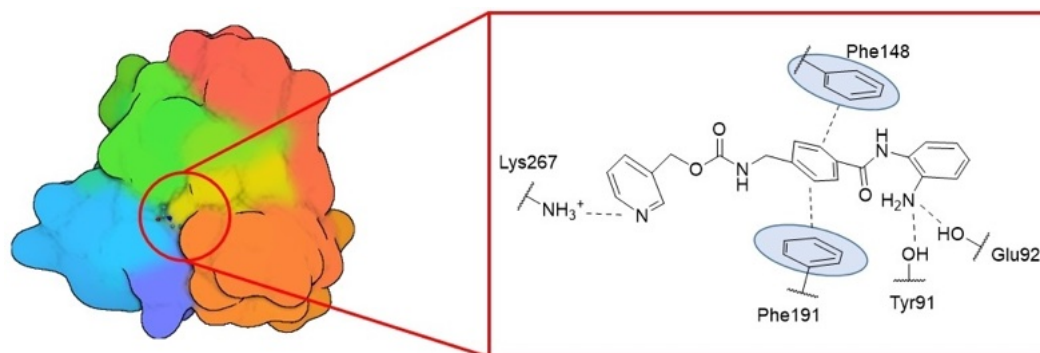
Figure 14. Representation of Entinostat's binding mode in the active site of HDAC enzyme (PDB: 1 C3S, crystal structure of an HDAC homolog, HDLP, with Vorinostat).[119]
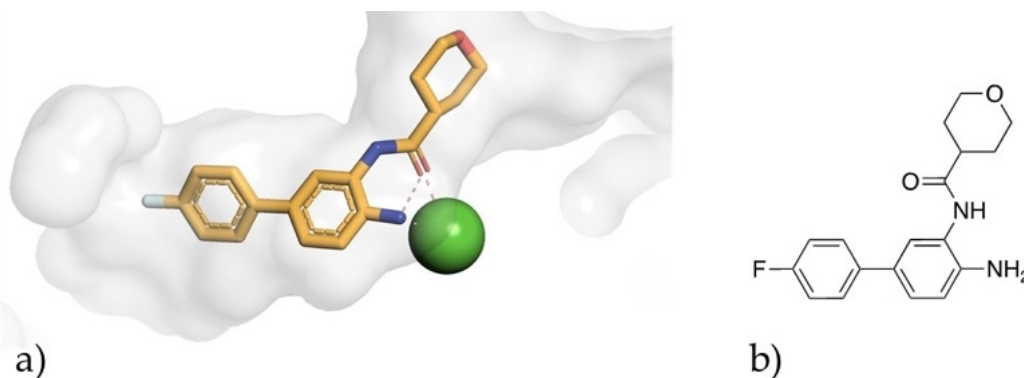
Figure 15. (a) Representation of BRD4884 binding mode in HDAC2 active site (PDB: 5IWG). The 2'-amino benzamide moiety coordinates the Zn^{2+} ion (green) while the biphenyl chain fits perfectly in the specific HDAC2 internal cavity (interactions with aminoacids not shown);[123] (b) BRD4884 chemical structure.

Table 36. Structures and inhibition data against HDAC1, −4, −6 of 1,3,4-oxadiazoles (**80 a–d**; **81 a,b**).[106]

Compound	R	n	Inhibition activity IC$_{50}$ (µM)		
			HDAC1	HDAC4	HDAC6
80 a	(naphthylmethyl)	0	1.0	> 20	> 20
80 b	(naphthylmethyl)	0	2.4	> 20	> 20
80 c	(indolylmethyl)	0	1.5	> 20	> 20
80 d	(naphthylmethyl)	1	4.1	> 20	> 20
81 a	–	0	0.3	> 20	16.1
81 b	–	1	0.2	> 20	8.9
Vorinostat			0.3	8.8	0.06

inhibitory activity was shown against HDAC4, while the benzoic derivatives (**81a,b**) showed little inhibitory effects against HDAC6. In western blot experiments, **80d**, **81a**, and **81b** displayed the most promising effects on histone H3 acetylation, and unexpectedly, the high level of α-tubulin acetylation did not correlate with the low HDAC6 inhibition potency. **81b** exhibited higher cyclin-dependent kinase inhibitor (p21) induction than Vorinostat and displayed the most promising results in U937 cells as a pro-apoptotic and/or cytodifferentiating agent exhibiting the same potency as Entinostat in cytodifferentiation. **81b** displayed single-digit micromolar antiproliferative activity against SW620 colon adenocarcinoma ($IC_{50} = 6.7 \mu M$) and against five AML cell lines (IC_{50} [U937] = 1.8 μM, IC_{50} [HL60] = 2.8 μM, IC_{50} [HEL] = 2.0 μM, IC_{50} [KG1] = 1.8 μM, IC_{50} [MOLM13] = 1.6 μM) being more potent than Vorinostat in leukemias. **81b** has been tested in combined administration with doxorubicin, being more effective than the Vorinostat-combination in inhibiting U937 cell proliferation. These results allow to correlate specific HDAC1 inhibition with induction of apoptosis, cell differentiation, and cell growth arrest.
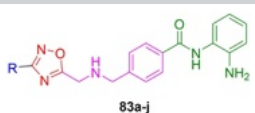
As discussed in the previous paragraph 3.1, Fang *et al.* developed a series of HDAC-indoleamine 2,3-dioxygenase 1 (IDO1) dual inhibitors by merging Mocetinostat and INCB024360. Among the synthesized compounds are **82a–d**, bearing the 2-aminoanilide as ZBG. As reported in Table 37, in the enzymatic assays, the *meta* orientation **82a** is less favored than the *para* one **82b**, which showed the highest inhibitory activity against HDAC1 ($IC_{50} = 0.0665 \mu M$), being the most promising derivative of the synthesized series. When the phenyl group of the latter compound was substituted with a thiophene (compound **82c**) or a pyridine (compound **82d**) the HDAC1 inhibiting activity decreased ($IC_{50} = 1.4 \mu M$ and $IC_{50} = 0.604 \mu M$ respectively). The antiproliferative assays were conducted in
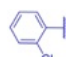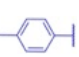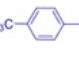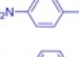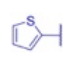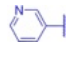
LLC (Lewis lung cancer), CT-26 (mouse colon cancer), A549 (human lung cancer), HCT-116 (human colon cancer), and HT-29 (human colon cancer) cell lines and compounds **82a–d** exhibited antitumor suppressing activities, specifically against HCT-116 cell line where compound **82b** showed a Vorinostat comparable antitumor activity ($IC_{50} = 5.12 \mu M$) establishing itself as the most promising benzamide derivative in antiproliferative assays. In an additional HCT-116 cell growth assay, **82b**-associated apoptosis was confirmed as a mechanism of cell inhibition growth. From the promising results obtained with **82b**, the research group further investigated its inhibitory potency against HDAC2, −3, −4, −6, and −8 isoforms. The IC_{50}-values against HDAC2, −3, and −6 were found to be within the submicromolar range ($IC_{50} = 0.179 \mu M$, 0.045 μM, and 0.070 μM, respectively), classifying **82b** as a *pan*-HDAC inhibitor. Furthermore, **82b** was evaluated in an *in vivo* LLC xenograft tumor model showing good antitumor potency.

As discussed before, Cai *et al.* investigated the role of 1,2,4-oxadiazole isomers in HDACi structure by synthesizing compounds **83a–j**.[108] As indicated in Table 38, all the synthesized compounds were assayed for their inhibitory potency against HDAC 1, −2, and −8 isoforms using Vorinostat and Entinostat as reference compounds. All the synthesized aminobenzamide derivatives **83a–j** exhibited submicromolar inhibitory activities against HDAC1 and −2, while no relevant HDAC8 inhibitory activity was exerted. Among them, compounds **83b** and **83e** showed HDAC1 selectivity ($IC_{50} = 0.07 \mu M$ and $IC_{50} = 0.06 \mu M$, respectively) being, respectively, 2.5-fold or 4.5-fold more selective of HDAC1 than HDAC2 ($IC_{50} = 0.150 \mu M$ and $IC_{50} = 0.320 \mu M$, respectively). In antiproliferative assays conducted against human acute monocytic myeloid leukemia cell line (U937), human lung cancer cell lines (A549 and NCI–H661), human breast cell line (MDA-MB- 231), and human colon cancer cell lines (HCT116) growth inhibitory cell activity related to the

Table 37. Structures, inhibition data against HDAC1, antiproliferative activity in LLC, CT-26, A549, HCT116, and HT-29 of HDAC/IDO1 dual inhibitors bearing 1,2,5-oxadiazole (**72a–d**).[110]

Compound	R	Inhibition activity IC_{50} (μM) HDAC1	Antiproliferative activity IC_{50} (μM) LLC	CT-26	A549	HCT-116	HT-29
82a		0.632	31.38	25.51	27.76	16.18	46.42
82b		0.066	17.62	59.84	16.73	5.12	11.71
82c		1.42	18.34	38.82	14.52	7.12	20.26
82d		0.604	15.13	23.3	20.65	6.36	12.24
Vorinostat		0.014	9.68	5.97	2.63	3.07	1.78

ChemMedChem

Review
doi.org/10.1002/cmdc.202400194

Chemistry Europe
European Chemical
Societies Publishing

Table 38. Structures, inhibition data against HDAC1, −2, −8 and antiproliferative activity in A549, NCI–H661, U937 of 1,2,4-oxadiazoles (**83 a–j**).[108]

83a-j

Compound	R	Inhibition activity IC$_{50}$ (μM)			Antiproliferative activity IC$_{50}$ (μM)		
		HDAC1	HDAC2	HDAC8	A549	NCI–H661	U937
83 a	phenyl	0.28	0.53	>10	10.83	11.79	1.63
83 b	o-Cl-phenyl	0.07	0.32	>10	7.92	3.33	0.38
83 c	p-Me-phenyl	0.21	0.56	>10	9.81	7.39	0.97
83 d	p-CF$_3$-phenyl	2.75	5.93	>10	>100	23.49	2.58
83 e	p-O$_2$N-phenyl	0.06	0.15	>10	6.39	4.73	0.52
83 f	p-H$_3$CO-phenyl	0.18	0.29	>10	7.95	5.77	1.09
83 g	p-F-phenyl	0.11	0.28	>10	10.69	4.36	1.25
83 h	p-Cl-phenyl	0.09	0.43	>10	13.52	8.00	0.43
83 i	thiophene	3.85	4.39	>10	>100	35.83	5.96
83 j	pyridine	5.26	8.37	>10	>100	>100	10.97
Vorinostat		0.15	0.28	1.68	1.65	0.13	2.83
Entinostat		0.39	0.65	>10	5.41	2.19	0.55

83 a–j diverse substitution of C3-1,2,4-oxadiazole was observed. Table 38 will report only the most significant antiproliferative data against A549, U93,7, and NCI–H661 cell lines. The introduction of an electron-withdrawing substituent at the benzene, such as *p*-nitrobenzene (**83 e**), *p*-fluorobenzene (**83 g**), *o/p*-chlorobenzene (**83 b** and **83 h**, respectively), or led to the most significant cell growth inhibition in benzamide series, in particular **83 b**, **83 e** and **83 h** exhibited more potent cytotoxic effects than Vorinostat and Entinostat, used as reference compounds, against U937 cancer cell lines. When 1,2,4-oxadiazole 3-position was substituted with benzene isoster (**83 i** and **83 j**), a decreased antiproliferative potency was observed, suggesting that (substituted)-benzene was preferred. However, all compounds showed low growth inhibitory activity against A549 and NCI–H661 lung cancer cell models. Indeed, compounds **83 b**, **83 e**, and **83 h** showed higher inhibitory activities than Vorinostat and Entinostat against human acute monocytic myeloid leukemia cell lines U937.

Among the oxa-aza heterocycles, the oxazoline introduction in HDACi was investigated. Marson and colleagues reported their library of mocetinostat derivatives where substituted unsaturated chiral oxazoline was introduced as a cap group to obtain a better solubility compared to the low solubility given by the pyrimidine of mocetinostat.[126] As shown in Table 39, among all the 2-(arylmethylamino)-4-aryl-substituted dihydrooxazole series (**84 a–o**), HDAC3 inhibition in low micromolar range was observed (IC$_{50}$ = 0.024 − 0.040 μM). However, enantiomers (*R*) and (*S*) **84 d** showed an absolute configuration-related HDAC1 inhibition, with the (4*R*)-enantiomer being 6-fold more potent than (*S*), while HDAC2 and HDAC3 inhibition was similar. An analogous example was displayed by the enantiomeric pair of 2- (arylmethylamino)-5-aryl dihydrooxazoles **84 k**, with the (5*R*)-enantiomer being 5-fold more potent than (5*S*) in HDAC1 inhibition. While (*R*)-**84 k** displayed HDAC1 inhibition in the nanomolar range (IC$_{50}$ = 0.076 μM) (*S*), **84 k** showed HDAC2 preferential inhibition (IC$_{50}$ = 0.094 μM). About the diastereoisomeric 4,5-diphenyl-4,5-dihydrooxazoles **84 m** and **84 n**, potent HDAC3 inhibition was demonstrated by **84 n**, being the most potent derivative (IC$_{50}$ = 0.006 μM) displaying a 13- and 18-fold selectivity over HDAC1 and HDAC2, respectively. A comparison between **84 n** and **84 d** highlighted the effects given by the additional phenyl group of **84 n**, which showed an increase of 5-fold in the inhibition of HDAC3. The latter results are probably related to an extended lipophilic region of HDAC3 that can accommodate the *cis*-**84 n** 1,2-diphenyl unit. Additional enzymatic assays conducted on **84 n** against HDAC4, −5, −6, −7, and −9 displayed IC$_{50}$ >100 μM, confirming its class I HDAC selectivity. SAR analysis highlighted that the introduction of the benzyl substituent (**84 c**, **84 j**) conferred better inhibition of HDAC1 (IC$_{50}$ = 0.70 μM and 0.20 μM, respectively) and HDAC2 (IC$_{50}$ = 0.2 μM and 0.13 μM, respectively) than the one given by the corresponding phenyl substituted derivatives (**84 a**, **84 d**).

ChemMedChem

Review
doi.org/10.1002/cmdc.202400194

Chemistry Europe
European Chemical
Societies Publishing

Table 39. Structures and inhibition data against HDAC1, −2, −3, −6, and −8 of 2-aminoanilide containing oxazolines (**84a–o**).[126]
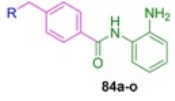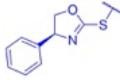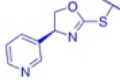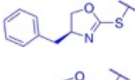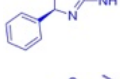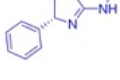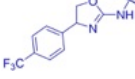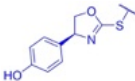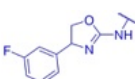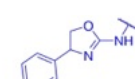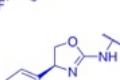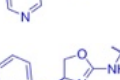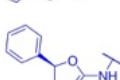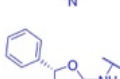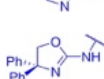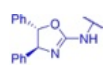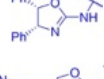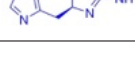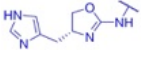
Compound	R	Inhibition activity IC$_{50}$ (µM)				% of inhibition
		HDAC1	HDAC2	HDAC3	HDAC8	HDAC6[a]
84a		1.2	0.36	0.066	9.5	54%
84b		13%[b]	0.61	0.056	112	62%
84c		0.70	0.25	0.071	88.0	60%
(*S*)−**84d**		0.53	0.18	0.040	14.7	66%
(*R*)−**84d**		0.082	0.18	0.033	80.7	69%
84e		20%[b]	0.34	0.034	82.1	67%
84f		0.29	0.23	0.018	83.3	13%
84g		0.24	0.24	0.024	52.2	70%
84h		0.19	0.15	0.034	33.9	68%
84i		0.26	0.43	0.031	111	62%
84j		0.20	0.13	0.041	63.0	72%
(*R*)−**84k**		0.076	0.192	0.011	173	74%
(*S*)−**84k**		0.39	0.094	0.035		72%
84l		21%[b]	0.40	0.055		61%
84m		28%[b]	0.28	0.12		67%
84n		0.080	0.11	0.006		71%
(*S*)-**84o**		0.078	0.16	0.021		67%

Table 39. continued						

84a–o

Compound	R	Inhibition activity IC$_{50}$ (μM)				% of inhibition
		HDAC1	HDAC2	HDAC3	HDAC8	HDAC6[a]
(R)-84o		0.13	0.29	0.018		61%
Mocetinostat		0.098	0.022	0.045		68%

[a]Percentage inhibition at 20μM;[b]Percentage inhibition at 0.2 μM.
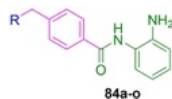
However, no advantage was achieved regarding HDAC3 inhibition. The previous trends were also observed with the 4-(1H- imidazolylmethyl)-4,5-dihydrooxazole enantiomers (R)- and (S)-**84o**. All compounds showed low inhibition of HDAC6. In biochemical assays, increased histone H3 K9 acetylation in U937 and PC-3 cancer cell lines induced by **84g**, (S)-**84k**, (R)-**84k** compounds were observed.
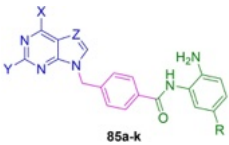
Literature evidence suggests that structural optimization of well-known benzamide-based HDACi by replacement of bicyclic heteroaryl rings as CAP group gave promising effects in inhibiting HDACs.[127]
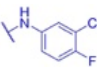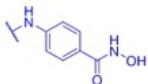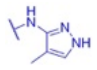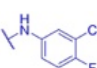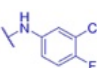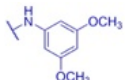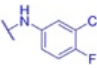
From this evidence, Nepali and colleagues focused on optimizing Entinostat and Chidamide by developing a derivative series in which their carbamate and acrylamide groups were replaced by purine/purine isostere as cap group.[128]

The synthesized compounds (**85a–k**) were assayed in vitro to assess their cytotoxic effects against triple-negative breast cancer cells (MDA-MB-231), known for their high expression of HDAC2 and HDAC3,[129] and human hepatocellular carcinomas (HCCs), characterized by an HDAC1-3 overexpression.[130] The results from these tests led the research group to conduct a structure-activity relationship (SAR) study, indicating superior antiproliferative properties for the derivatives bearing a 2-amino substituted purine (**85g, 85k**) over a 2-chlorine substituted purine (**85a, 85e**). Significant cytotoxicity was observed when a 3-chloro-4-fluoro-aniline was introduced in the 6-position of the purine core (compare **85a** to **85b**). The introduction of 4-methyl-1H-pyrazol-3-yl ring induced higher cell growth inhibition (compare **85a** and **85d**). When the purine core was replaced with his isostere (7H-pyrrolo[2,3-d]pyrimidine), lower cytotoxic effects were observed (**85e, 85f, 85j**), confirming purine core as the strongest moiety as cap group in the developed series. The most promising results were shown when 3-chloro-6-fluoro aniline (6-position) was incorporated in purine-based benzamide with an amine group in 2-position (compound **85h**). **85h** displayed the strongest cytotoxic effects against MDA-MB-231 and HCCs cell lines with IC$_{50}$ of 1.48 μM and 2.44 μM, respectively. Replacement with 3,5-dimethoxy aniline (**85i**) led to decreased antiproliferative effects. In the enzymatic assays (Table 40), the synthesized compounds showed a selective inhibiting behavior against HDAC1 and

HDAC2 isoforms. Compounds **85c, 85d, 85g, 85h, 85i**, and **85j** showed higher HDAC1 inhibition potency than Entinostat, used as reference compound. The best inhibition rate was exhibited by 3,5-dimethoxyaniline substituted compound **85i**, which displayed HDAC1 and HDAC2 inhibition in the nanomolar range (IC$_{50}$ = 0.0239 μM and 0.179 μM, respectively) even if a reduction in inhibiting MDA-MB-231 growth were shown in an antiproliferative activity assay. Compound **85h** exhibited an Entinostat-comparable inhibition potency against HDAC1 and HDAC2 (IC$_{50}$ = 0.108 μM and 0.585 μM, respectively), being 5-fold more selective towards HDAC1, probably thanks to the interaction established by its cap group as confirmed by docking study.[131] Compound **85h** was also evaluated against three leukemic cell lines, displaying IC$_{50}$ values in the low micromolar range and more cytotoxic effectiveness when compared to Vorinostat, used as reference compound. Based on this evidence, in vivo assays were conducted in a human MDA-MB-231 breast cancer xenograft model wherein compound **85h** displayed promising antitumor efficacies.
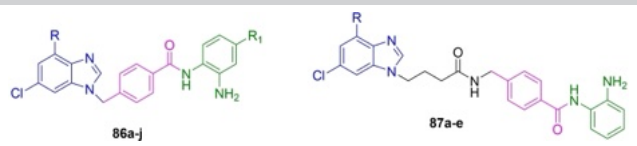
Considering the promising results obtained from 2-amino-anilide HDACi bearing purine ring, Mao et al. designed and developed a derivative series in which purine moiety was included as cap group in an Entinostat-like structure.[132] Among the synthesized compounds (**86a–j, 87a–e**), different substitutions and lengths of spacer between the linker and cap group were utilized for a SAR investigation. Total HDAC inhibitory assays were conducted, and compounds **86i, 86j**, and **87d** exhibited similar Entinostat and Vorinostat inhibitory activities (Table 41). In particular, **86j** showed the lowest IC$_{50}$ value (0.0275 μM), then being the most potent. When butylamine substitution was inserted at C6-purine position (**86b, 86d, 86f, 87d**) higher HDAC inhibition potency than the C6-homologous derivatives was displayed (IC$_{50}$ = 2.04, IC$_{50}$ = 1.01, IC$_{50}$ = 1.28 and IC$_{50}$ = 0.95 μM, respectively). Considering the aniline ring, better inhibition potency against HDAC was exhibited when no substituents were included (compare **86g–j** to **86a–f**); for example, **86j** showed 74- and 46-fold higher potency than the corresponding aniline substituted derivatives (**86b, 86d, 86f**). This SAR evidence underlines how anilide must not be substituted to obtain more potent derivatives in HDAC-inhibiting terms. Furthermore, elongation of the spacer by

ChemMedChem

Review
doi.org/10.1002/cmdc.202400194

Chemistry
Europe
European Chemical
Societies Publishing

Table 40. Structures, inhibition data against HDAC1 and −2, and antiproliferative activity in MDA-MB-231 of 2-aminoanilide bearing purine/purine isosteres (**85 a–k**).[131]

| Compound | X | Y,Z,R | Inhibition activity IC$_{50}$ (μM) | | Antiproliferative activity IC$_{50}$ (μM) |
			HDAC1	HDAC2	MDA-MB-231
85 a	−Cl	Y=Cl Z=N R=H	NA	NA	>8
85 b		Y=Cl Z=N R=H	0.685	3.78	3.24
85 c		Y=Cl Z=N R=H	0.182	1.45	>8
85 d		Y=Cl Z=N R=H	0.165	0.739	4.64
85 e	−Cl	Y=Cl Z=C R=H	0.862	6.51	7.65
85 f		Y=Cl Z=C R=H	NA	NA	>8
85 g	−Cl	Y=NH$_2$ Z=N R=H	0.271	0.761	3.08
85 h		Y=NH$_2$ Z=N R=H	0.108	0.585	1.48
85 i		Y=NH$_2$ Z=N R=H	0.024	0.179	3.17
85 j		Y=NH$_2$ Z=C R=H	0.093	1.46	5.32
85 k	−Cl	Y=NH$_2$ Z=C R=F	1.23	1.15	3.78
Entinostat		−	0.544	0.613	2.60

butanamide introduction (**87 a–e**) caused lower HDAC inhibiting potencies than the corresponding methylene-spacing derivatives (**86 a–j**). Considering the notable HDAC inhibiting properties of **86 g–j**, Mao and colleagues further evaluated their HDAC isoform specificity by doing enzymatic assays against HDAC1, −3, −8, −6, −4. The tested compounds exhibited HDAC1 selective inhibiting potency, wherein **86 j** showed the best IC$_{50}$ value (0.055 μM), being 12-fold more potent than Entinostat against HDAC1. In general, **86 g–j** also exhibited HDAC3/8 inhibiting activity in the micromolar range (IC$_{50}$≈1 μM, data not shown), but low or absent activities against HDAC6/8 were shown (IC$_{50}$ >10 μM and >100 μM, respectively; detailed data not shown). The latter evidence allows to consider **86 g–j** as

specific class I HDAC inhibitors. Compounds **86 g–j** and **87 a–e** were also evaluated in antiproliferative assays against HCT-116 (colon carcinoma), MDA-MB-231 (breast cancer), HepG2 (hepatocellular carcinoma), A549 (human pulmonary epithelial cells), SGC7901 (human gastric cancer) and K562 (leukemia). Here, we will focus on breast cancer cell lines antiproliferative data (Table 41). 4-fold to 40-fold higher cytotoxic activity than Entinostat and Vorinostat was exhibited by compounds **86 g–j** against the MDA-MB-231 cancer cell line with IC$_{50}$ values in the low micromolar range, wherein compound **86 j** displayed the most promising antiproliferative activity among the developed series. Compounds **86 g–j** exhibited low cytotoxic effects, thus confirming the previous evaluation obtained from the HDACs

Table 41. Structures, inhibition data against total HDACs and HDAC1, and antiproliferative activity in MDA-MB-231 of 2-aminoanilides bearing purines (**86a–j; 87a–e**).[132]

Compound	R	R_1	Inhibition activity IC$_{50}$ (μM)		
			Total HDACs	HDAC1	MDA-MB-231
86a	$-NH(CH_2)_2CH_3$	$-Br$	9.26	–	–
86b	$-NH(CH_2)_3CH_3$	$-Br$	2.04	–	–
86c	$-NH(CH_2)_2CH_3$	$-CH_3$	3.13	–	–
86d	$-NH(CH_2)_3CH_3$	$-CH_3$	1.01	–	–
86e	$-NH(CH_2)_2CH_3$	$-F$	4.41	–	–
86f	$-NH(CH_2)_3CH_3$	$-F$	1.28	–	–
86g	$-NHCH_3$	$-H$	1.48	0.077	0.24
86h	$-NHCH_2CH_3$	$-H$	1.64	0.093	0.06
86i	$-NH(CH_2)_2CH_3$	$-H$	0.574	0.309	0.05
86j	$-NH(CH_2)_3CH_3$	$-H$	0.027	0.055	0.50
87a	$-NHCH_3$	$-H$	5.02	–	15.46
87b	$-NHCH_2CH_3$	$-H$	2.31	–	17.48
87c	$-NH(CH_2)_2CH_3$	$-H$	1.26	–	28.39
87d	$-NH(CH_2)_3CH_3$	$-H$	0.95	–	5.64
87e	$-NH(CH_2CH_3)_2$	$-H$	3.91	–	11.06
Entinostat	–	–	0.524	0.686	4.63
Vorinostat	–	–	0.104	0.060	1.54

inhibitory assays. These data confirmed the previously discussed data about the higher HDAC inhibition that purine introduction in benzamide inhibitors confers.
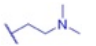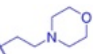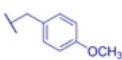
As mentioned in the previous paragraph 3.1, quinazoline ring has been used to develop heterocycle-bearing HDAC inhibitors. Vaisburg *et al.* further investigated quinazoline-based HDAC inhibitors by creating a series of N-(2-amino-phenyl)-4-(heteroarylmethyl)-benzamides (**88a–h, 89a–c**). Initially, this research group devised a series of 4-quinazolinone derivatives to explore the potential of this ring as a cap group (compounds **88a** and **88b**).[133] Subsequently, they synthesized a derivative series incorporating 2,4-quinazolindione (compounds **88c–h**). All compounds exhibited recombinant HDAC1 inhibition activity within the (sub)micromolar range (IC$_{50}$ 0.1–1.0 μM), demonstrating substantial *in vitro* antiproliferative activities in HCT116 cancer cell lines (Table 42). Moreover, these compounds induced the expression of the cyclin-dependent kinase inhibitor p21$^{WAF1/Cip1}$ and caused apoptosis in the HCT116 human colon cancer cell line (data not shown).

The research efforts of Vaisburg and collaborators also extended to developing thienopyrimidine-based HDAC inhibitors (compounds **88a–c**). These compounds displayed similar in vitro inhibitory potencies compared to their quinazolinone analogs (compounds **88a, 88c**, and **88e**). However, the most promising profile emerged with compound **89b**, which exhibited HDAC1 inhibiting potency in the dual-digit nanomolar

range (IC$_{50}$ = 0.06 μM) and demonstrated significant antitumoral activity in *in vivo* A549, DU145, and HCT116 human tumor xenograft models showing tumor growth inhibition of 55%, 67%, and 61%, respectively.

Among the diverse substitutions investigated as cap groups, the integration of thioquinazolinone onto the 2-aminoanilide HDACi moiety was explored. Converso's research group reported the cell cycle checkpoint kinase 1 (Chk1) inhibiting properties of thioquinazolinones.[134] Given the scientific evidence surrounding the cancer-related effects linked to compromised Chk1 function, Cheng *et al.* developed promising derivatives of 2-aminoanilide, incorporating the thioquinazolinone pharmacophore as a cap group (**90a–i, 91a–f**).[135] Here, we discuss the cytotoxic activity of derivatives bearing the thioquinazolinone group that was assayed for their antiproliferative activity across five human cancer cell lines: malignant melanoma (A375), cervical cancer (HeLa), lung cancer (A549), colorectal cancer (HCT116), and hepatocellular carcinoma (SMMC7721). Compound **90a** exhibited cytotoxic effects exclusively against SMMC7721 cell lines. Variations in the R_1 alkyl chain's length, as in the compounds **90a, 90d–f** and **9i,h**, resulted in different cytotoxicity, with the shorter carbon chain in compound **90b** displaying the highest antiproliferative activity. **90c**, containing a 2-chlorophenyl group, demonstrated higher cytotoxicity than its 4-chlorophenyl analog (**90d**). Regarding the R substitution, it was observed that the 7-

ChemMedChem

Review
doi.org/10.1002/cmdc.202400194

Chemistry
Europe
European Chemical
Societies Publishing
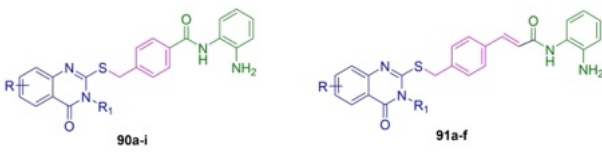
Table 42. Structures, inhibition against HDAC1 and antiproliferative activity in HCT116 of N-(2-amino-phenyl)-4-(heteroarylmethyl)-benzamides (**88 a–h; 89 a–c**).[133]

Compound	R	R_1	Inhibition activity IC_{50} (µM) HDAC1	Antiproliferative activity IC_{50} (µM) HCT116
88 a	—H	–	0.1	0.4
88 b	—CH$_3$	–	0.08	0.6
88 c	–	—H	0.06	0.8
88 d	–	—CH$_3$	0.1	0.7
88 e	–	—CH$_2$CH$_3$	0.2	0.4
88 f	–	(N,N-dimethylaminopropyl)	0.3	1
88 g	–	(morpholinopropyl)	0.4	1
88 h	–	(4-methoxybenzyl)	0.1	0.8
89 a	–	–	0.2	0.7
89 b	–	—H	0.06	0.4
89 c	–	—CH$_2$CH$_3$	0.3	0.8

methoxy substitution (**90 b**) led to higher antiproliferative activity than the corresponding electron-withdrawing substituents 7-fluoro (**90 e**), 7-chloro (**90 h**), and 7-bromo (**90 i**). Within the **91 a–f** series carrying a phenylacrylamide group, all compounds except for compound **91 b** exhibited no cytotoxic effects. Here, we present the IC_{50} values (Table 43) of compounds **90 c**, **90 i**, **90 b**, and **91 b**, which demonstrated promising antiproliferative effects in the single to double-digit micromolar range against A375, A549, and SMMC7721 cell lines. Antiproliferative activity data (% of growth inhibition) of the previously discussed compounds against A375, A549, and SMMC7721 are reported in Table 43. Given the notably high cytotoxicity exhibited by these compounds (**90 b**, **90 c**, **90 i**, and **91 b**), further evaluations were conducted to assess their activity against the HDAC1, HDAC2, and HDAC6 isoforms. Compound **90 b**, containing a methyl group in N2-thioquinazolone, displayed excellent inhibitory activity against HDAC1 and HDAC2 ($IC_{50} = 0.01$ µM and $IC_{50} = 0.16$ µM respectively), exhibiting a 4000-fold selectivity towards HDAC1 compared to HDAC6. Similarly, compound **91 b** demonstrated 400-fold and 222-fold inhibition potency against HDAC1 and HDAC2, respectively, compared to HDAC6, while compounds **90 c** and **90 i** showed inhibition potencies similar to Entinostat against HDAC1 and HDAC2 (IC_{50} [HDAC1] $= 0.38$ µM and 0.29 µM, IC_{50} [HDAC2] $= 0.61$ µM and 0.53 µM respectively).

Furthermore, compounds **90 b**, **90 c**, **90 i**, and **91 b** exhibited suppression of cell migration and reduced colony formation in SMMC7721 cell lines. Additionally, these compounds promoted cell apoptosis more effectively than Entinostat in the same cell lines. Among the developed derivatives, compound **90 b** garnered significant attention due to its potent in vivo antitumor efficacy and low toxicity demonstrated in A549 xenograft mice models.

The research group led by Zhang investigated the quinazolinyl ring as a substitution for benzamide in HDACi. They designed and developed a derivative series of HDACi, where quinazoline was incorporated as a cap group. Specifically, the research team modified the Entinostat structure by replacing its pyridinyl carbamate moiety with a substituted 4-aminoquinazoline.[136] The developed series (**92 a–n**) underwent enzymatic assays against the HDAC1 isoform. The resulting data were evaluated via an in-depth SAR analysis. As reported in Table 44, the C2-quinazoline substituted derivatives (**92 a–d**) displayed lower HDAC1 inhibiting potency compared to the reference compound Entinostat. For instance, compounds **92 a**, **92 c**, and **92 d** were inactive with IC_{50} values over 500 µM, while compound **92 b** was 5-fold less potent than Entinostat (IC_{50} $= 3.26$ µM and 0.668 µM, respectively). The absence of quinazoline substitutions (**92 e**) resulted in more potent HDAC1 inhibitory activity ($IC_{50} = 0.212$ µM) than Entinostat. Upon learn-

ChemMedChem

Review
doi.org/10.1002/cmdc.202400194

Chemistry Europe
European Chemical
Societies Publishing
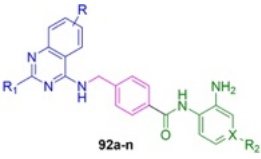
Table 43. Structures, inhibition data against HDAC1, −2, and −6 and antiproliferative activity in A375, A549, and SMMC7721 of 2-aminoanilide bearing thioquinazolinone (**90 a–i**; **91 a–f**).[135]
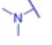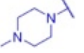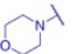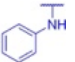
Compound	R	R$_1$	Inhibition activity IC$_{50}$ (μM)			% antiproliferative activity at 2μM		
			HDAC1	HDAC2	HDAC6	A375	A549	SMMC7721
90 a	5-CH$_3$	CH$_3$	–	–	–	35.6%	34.7%	59.2%
90 b	7-OCH$_3$	CH$_3$	0.01	0.16	>40	52.2%	38.0%	68.8%
90 c	7-OCH$_3$	Ph-2Cl	0.38	0.61	>40	41.8%	52.5%	50.4%
90 d	7-OCH$_3$	Ph-4Cl	–	–	–	21.7%	20.9%	21.3%
90 e	7-F	CH$_3$	–	–	–	30.0%	21.3%	52.5%
90 f	7-F	CH$_2$CH$_3$	–	–	–	8.4%	54.4%	0.8%
90 g	7-F	(CH$_2$)$_3$CH$_3$	–	–	–	18.0%	41.1%	9.1%
90 h	7-Cl	CH$_3$	–	–	–	44.5%	21.8%	38.9%
90 i	7-Br	CH$_3$	0.29	0.53	>40	34.5%	37.5%	35.6%
91 a	7-OCH$_3$	CH$_3$	–	–	–	2.5%	54.3%	3.6%
91 b	7-OCH$_3$	CH$_2$CH$_3$	0.1	0.18	>40	55.0%	18.6%	56.8%
91 c	7-F	CH$_3$	–	–	–	1.6%	2.9%	12.3%
91 d	7-Cl	CH$_3$	–	–	–	2.4%	15.5%	7.8%
91 e	7-Cl	(CH$_2$)$_2$CH$_3$	–	–	–	20.5%	34.3%	6.6%
91 f	7-Br	CH$_3$	–	–	–	4.0%	1.9%	13.2%
Entinostat	–	–	0.35	0.67	4.12	–	–	–

ing that the C2 position of quinazoline should remain unsubstituted and considering the promising data from **92 e**, Zhang *et al.* developed a series where C6 and C7 substitutions were explored (**92 f–n**). Table 44 demonstrates that the HDAC1 inhibitory potency was directly correlated with the position and size of the substituents within the synthesized series. Introducing halogens (**92 h**, **92 i**, **92 l**) resulted in slightly lower inhibitory potency compared to the most potent compound **92 e**, with compound **92 l** displaying an IC$_{50}$ value (0.396 μM) closer to the best compound in the developed series (**92 e**). A similar trend of significantly reduced inhibitory potency was observed when bulkier substituents (**92 m**, **92 n**) were used. The research group also investigated the 2-amino-4-fluorophenyl group or 2-amino-4-pyridyl group as ZBG (compounds **92 f**, **92 g**, **92 j**, and **92 k**) but lower potency than the corresponding derivatives with 2-aminophenyl substitution at the same positions was observed (compounds **92 e** and **92 i**). Based on the HDAC1 inhibition data, Zhang *et al.* selected **92 e** and **92 f** for evaluation in an antiproliferative assay against a panel of human cancer cells (Hut78, K562, Jurkat E6-1, Hep3B, A549, and HCT-116) and human fetal lung fibroblast normal cell lines (MRC-5). **92 e** exhibited cytotoxic effects against the tested cancer cell lines, particularly against Hut78, K562, Hep3B, and HCT116 cells, with lower micromolar IC$_{50}$ values than Entinostat. Interestingly, both **92 e** and **92 f** showed weak cytotoxic effects against MRC5 cell lines (IC$_{50}$ > 100 μM), demonstrating selectivity towards cancer

cells' cytotoxicity over normal human cells. Based on enzymatic and antiproliferative assay data, **92 e** was further evaluated for HDAC isoform selectivity by conducting in vitro assays against HDAC1, −2, −8, and −6 isoforms. The tested compound **92 e** exhibited good selectivity against HDAC1 over HDAC2 (IC$_{50}$ [HDAC2] = 2.50 μM), while inactivity against both HDAC8 (IC$_{50}$ > 10 μM) and HDAC6 (IC$_{50}$ > 10 μM) was shown. Subsequent docking evaluations confirmed the strong binding of **92 e** to HDAC1. Consequently, this compound underwent further testing in an A549 non-small cell lung cancer mouse xenograft model study, displaying significant inhibition of tumor growth.

The exploration of CAP substitution with heterocyclic groups in HDACi structure resulted in an increased inhibition potency against HDAC1 and HDAC2. In line with this, Gerokinstantis *et al.* aimed to synthesize a series of novel N-(2-aminophenyl)-benzamide inhibitors incorporating amino acids like pyroglutamic (**93 a–e**) or proline (**94 a–f**), as well as various heterocyclic carboxylic acids as cap groups (**95 a–c**), to investigate their roles in antiproliferative and antifibrotic terms.[137] In enzymatic assays, all compounds were analyzed against human HDAC1, HDAC2, and HDAC6 isoforms (see Table 45). Compound **93 a** possesses an HDAC1 IC$_{50}$ value of 0.430 μ and no HDAC2 inhibiting activity, highlighting the 4-((4-(aminomethyl)phenoxy) methyl)benzoyl group as detrimental for HDAC1 selectivity. Compounds with an additional methylene spacer, such as **93 b** and **93 c**, were analyzed as

Table 44. Structures and inhibition data against HDAC1 of quinazolinyl substituted 2-aminoanilides (**92a–n**).[136]

Compound	R	R$_1$	R$_2$	X	Inhibition activity IC$_{50}$ (μM) HDAC1
92a	H	(dimethylamino)	H	C	>500
92b	H	(N-methylpiperazinyl)	H	C	3.26
92c	H	(morpholinyl)	H	C	>500
92d	H	(N-phenylamino)	H	C	>500
92e	H	−H	H	C	0.212
92f	H	−H	–	N	3.44
92g	H	−H	F	C	7.32
92h	5-Cl	−H	H	C	0.441
92i	6-F	−H	H	C	1.14
92j	6-F	−H	–	N	–
92k	6-F	−H	F	C	–
92l	6-Cl	−H	H	C	0.396
92m	6,7-OCH$_3$	−H	H	C	–
92n	6,7-O(CH$_2$)$_2$OCH$_3$	−H	H	C	3.23
Entinostat	–	–	–	–	0.668

enantiomeric pair possessing an N-benzyl-pyroglutamic acid as the cap group. They inhibited HDAC1 and HDAC2 with IC$_{50}$ values (0.1 μM and 0.116 μM for HDAC1; 0.092 μM and 0.143 μM for HDAC2, respectively). Interestingly, the stereochemistry of the cap group had no effect on their performance. Compound **93d**, exhibiting a fluorine atom at the *para* position of the benzyl group, exhibited reduced inhibitory potency (IC$_{50}$ = 0.216 μM for HDAC1; IC$_{50}$ = 0.348 μM for HDAC2). However, compound **93e**, with a bromine atom at the same position, showed more potent inhibition (IC$_{50}$ = 0.051 μM for HDAC1; IC$_{50}$ = 0.082 μM for HDAC2). Among the benzamide derivatives featuring N-benzyl-pyroglutamic acid as the cap group, they demonstrated inhibiting selectivity for class I HDACs without inhibiting HDAC6 isoform (IC$_{50}$ > 100 μM). Furthermore, compounds **93b** and **93c** exhibited antiproliferative activity against A549 human epithelial lung cancer cells with promising inhibitory values (IC$_{50}$ = 6.8 μM and 3.9 μM, respectively). This research group also developed a series of benzamide derivatives with proline as the cap group while retaining the 4-((4-(aminomethyl)-phenoxy)methyl)benzoyl group as linker. Compound **94a**, featuring a free proline as the cap group, exhibited stronger inhibition (IC$_{50}$ = 0.055 μM against HDAC1; IC$_{50}$ = 0.072 μM against HDAC2) than the corresponding (R) enantiom-er **94b**, which showed an IC$_{50}$ of 0.259 μM against HDAC1. The enantiomeric pair, compounds **94c** and **94d** showed similar inhibition potencies (IC$_{50}$ = 0.113 μM and 0.093 μM for HDAC1; IC$_{50}$ = 0.192 μM and 0.083 μM for HDAC2, respectively), affirming the prior findings indicating no effect due to the stereo-chemistry of the N-protected cap group. Compounds **94e** and **94f** replacing the N-benzyl group with benzyloxycarbonyl or benzoyl group, respectively, led to a reduction in inhibitor potency against HDAC1 (IC$_{50}$ = 0.215 μM and 0.202 μM, respectively), while no HDAC2 inhibitory activity was detected. Similar to the previous series, proline-based benzamide inhibitors displayed inhibitory activity against class I HDACs without affecting HDAC6. As previously mentioned, these compounds exhibited antiproliferative effects against A549 human epithelial lung cancer cell lines, with compounds **94c** and **94d** showing higher antiproliferative activity (IC$_{50}$ = 3.7 μM and 4.7 μM, respectively). Additionally, heterocyclic carboxylic acids were investigated as cap groups in benzamide-based HDAC inhibitors. Compounds **95a**, **95b**, and **95c**, featuring furan-2-carboxylic acid, 2-picolinic acid, and indole-2-carboxylic acid, exhibited HDAC1 inhibiting potency in the high nanomolar range (IC$_{50}$ = 0.111 μM, IC$_{50}$ = 0.200 μM and IC$_{50}$ = 0.182 μM, respectively). However, they displayed minor effects in terms of

ChemMedChem

Review
doi.org/10.1002/cmdc.202400194

Chemistry Europe
European Chemical
Societies Publishing

Table 45. Structures and inhibition data against HDAC1, −2, −6 of N-(2-aminophenyl)-benzamide inhibitors bearing pyroglutamic aminoacid (**93 a–e**), proline aminoacid (**94 a–f**) and various heterocyclic carboxylic acids (**95 a–c**).[137]

Compound	R	Stereochemistry	Inhibition activity IC$_{50}$ (µM)		
			HDAC1	HDAC2	HDAC6
93 a	(n=0)	(S)	0.430	ND	>10
93 b	(n=1)	(S)	0.100	0.116	>100
93 c	(n=1)	(R)	0.092	0.143	>100
93 d	(F, n=1)	(S)	0.216	0.348	>100
93 e	(Br, n=1)	(S)	0.051	0.082	>100
94 a	—H 2HCl	(S)	0.055	0.072	>100
94 b	—H 2HCl	(R)	0.259	ND	>10
94 c		(S)	0.113	0.192	>100
94 d		(R)	0.093	0.083	>100
94 e		(S)	0.216	ND	>10
94 f		(S)	0.202	ND	>10
95 a		–	0.111	ND	>10
95 b		–	0.200	ND	>10
95 c		–	0.182	ND	>10

ND = not detected.

antiproliferative activity, confirming that the proline and pyroglutamic acid-based HDACi are preferred cap groups in the reported benzamide derivative series. Notably, compounds **93 c** and **94 c** showed a reduction in EGFR gene expression, indicating a correlation between HDAC1 inhibition and relative EGFR protein expression. In additional enzymatic assays, compounds **93 b**, **93 c**, and **94 a–c**, were tested against human HDAC3, HDAC4, and HDAC8 isoforms. These compounds did not show inhibitory effects against HDAC4 and HDAC8. However, the latter compounds displayed HDAC3 inhibitory activity in the micromolar range (data not shown), with compound **94 a** being the strongest inhibitor of HDAC3 (IC$_{50}$ = 0.061 µM).

ChemMedChem

Review
doi.org/10.1002/cmdc.202400194

Chemistry Europe
European Chemical
Societies Publishing

As discussed before, the pyridine group was involved in developing 2-aminoanilide HDACi. Zwergel and colleagues developed, in parallel to the hydroxamates **35a–f** and **36a–f** (Table 8), a novel 2-acylamino-5-(3-oxoprop-1-en-1-yl)pyridine 2-aminoanilide series (**96a–f**) and a corresponding nicotinic derivative series (**97a–f**) to be tested in enzymatic and antiproliferative assays.[72] As displayed in Table 46, all the synthesized compounds were assayed against HDAC1, −3,−4,−6, and −8 isoforms to evaluate their inhibitory capability. Both the pyridylacrylic and nicotinic derivative series exhibited inhibitory activity against HDAC1 and HDAC3 iso-

forms in the single-digit to micromolar range, highlighting a selectivity towards HDAC3 over HDAC1. Specifically, compound **96e**, featuring 1-naphthylacetamide C2 substitution, and compound **87d**, bearing a 3-methyl-2-phenylbutanamide moiety at C2, demonstrated the highest inhibitory potency against HDAC3 (IC$_{50}$ = 0.187 μM and 0.113 μM, respectively). In granulocytic differentiation assays conducted in human U937 leukemia cell lines, compounds **96b**, **96e**, and **97c** exhibited potent cytodifferentiating effects, although less effective than Entinostat. However, these compounds underwent further evaluation in antiproliferative assays against human chronic myelogenous

Table 46. Structures and inhibition data against HDAC1, −3, −6,–8 of 2-acylamino-5-(3-oxoprop-1-en-1-yl)pyridine 2-aminoanilide (**96a–f**) and the related nicotinic derivative series (**97a–f**).[72]

| Compound | R | Inhibition activity IC$_{50}$ (μM) | | | | |
		HDAC1	HDAC2	HDAC3	HDAC6	HDAC8
96a		5.89	0.206	NA	NA	135
96b		3.43	0.426	NA	98.3	86.8
96c		5.77	0.681	NA	115.8	98.5
96d		3.18	0.406	NA	NA	181
96e		0.366	0.187	NA	NA	140
96f		2.57	0.694	NA	309	NA
97a		1.41	0.202	NA	NA	NA
97b		1.13	0.176	NA	NA	103
97c		1.27	0.185	NA	NA	136
97d		0.379	0.113	NA	NA	NA
97e		1.42	0.389	NA	NA	78
97f		2.36	0.752	NA	NA	96
Vorinostat	-	0.31	0.13	8.8	0.06	0.31

NA = not active.

ChemMedChem

Review
doi.org/10.1002/cmdc.202400194

Chemistry
Europe
European Chemical
Societies Publishing
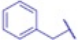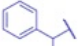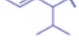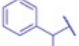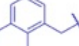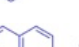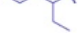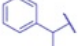
leukemia K562, colorectal carcinoma HCT116, and lung adeno-carcinoma A549 cell lines, demonstrating IC$_{50}$ values ranging from single-digit to micromolar levels.

Considering the previous work,[72] Di Bello *et al.* designed and developed the corresponding regioisomer series (**98a–f, 99a–f**).[73] The molecules were evaluated against HDAC1, −3, −4, −6, and −8, and the related IC$_{50}$ values are reported in Table 47. Within the pyridylacrylic series, an increase in alkyl substituents at Cα (**98a–c**) led to a slight decrease in inhibitory activity against HDAC1, −3, and −8 as the substituents grew. The introduction of a benzyl group (**98d**) and a 2-naphthylace-

tyl moiety (**98f**) resulted in a loss of potency against HDAC1, −3, and a complete loss of activity against HDAC8. Conversely, the 1-naphthylacetyl derivative (**99e**) displayed high potency against HDAC1 (IC$_{50}$ = 0.063 μM), gaining a 4-fold selectivity over HDAC3. All the IC$_{50}$ values are reported in Table 47.

The picolinic derivatives exhibited inhibitory potency against HDAC1 and HDAC3 in the submicromolar range. Replacement of the phenylacetyl group of **98a** by 1- and 2-naphthylacetyl moieties (**97e** and **97f**, respectively) resulted in observed activity against HDAC1. Surprisingly, compounds **93d** and **93f** showed inhibitory activities against HDAC10 (IC$_{50}$ =

Table 47. Structures and inhibition data against HDAC1, −3, −6, −8 of 5-acylamino-2-pyridylacrylic 2-aminoanilides (**98a–f**) and 5-acylamino-2- picolinic 2-aminoanilides (**99a–f**).[73]

| Compound | R | Inhibition activity IC$_{50}$ (μM) | | | | | |
		HDAC1	HDAC3	HDAC4	HDAC6	HDAC8	HDAC10
98a		0.108	0.224	NA	NA	31.4	–
98b		0.143	0.268	NA	NA	35.6	–
98c		0.151	0.319	NA	NA	43.1	–
98d		0.496	0.603	NA	NA	NA	–
98e		0.063	0.264	NA	NA	NA	–
98f		0.203	0.414	NA	NA	77.1	–
99a		0.201	0.248	NA	NA	77.1	–
99b		0.321	0.433	NA	NA	66.2	–
99c		0.330	0.488	NA	NA	75.2	–
99d		0.353	0.515	NA	NA	NA	0.320
99e		0.129	0.289	NA	NA	98.4	–
99f		0.189	0.440	NA	NA	NA	0.446
Vorinostat	-	0.077	0.064	76.0	0.010	0.306	0.198

NA = not active.

0.320 μM and 0.446 μM, respectively). None of the synthesized compounds were active against HDAC6. Moreover, compounds **98 c–f** and **99 a**, **99 d**, and **99 f** underwent testing in antiproliferative assays to assess their potential to impair cell differentiation in human chronic myelogenous leukemia K562, colorectal carcinoma HCT116, and lung adenocarcinoma A549 cells. All the tested compounds demonstrated single-digit to submicromolar potency against the three cancer cell lines. Notably, compounds **99 a**, **99 d**, and **99 f** exhibited IC_{50} values ranging from 0.32-0.56 μM against HCT116 and K562 cells and 1.28-1.51 μM against A549 cells, showing 3.3-fold greater potency than Entinostat, used as a reference compound.
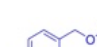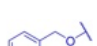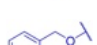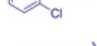
As previously discussed, the coumarin moiety gained much importance in pharmaceutical applications. Abdizadeh and colleagues reported a study in which new coumarin-based benzamides derivatives have been designed and synthesized in order to replace the benzyl carbamate moiety of Entinostat or the (E)-3-(pyridin-3-yl)acrylamide moiety of Chidamide as cap group.[138] The total HDAC inhibitory activity of compounds **100 a–u** was assessed in human colon cancer (HCT116) and ovarian cancer (A2780) cell lines, with Entinostat used as the reference compound (Table 48). The SAR data highlighted a strong relationship between the HDAC inhibitor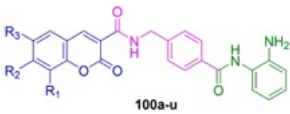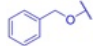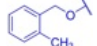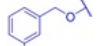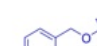y activity of the synthesized compounds and the length and position of the alkoxy group used as a substitution for the coumarin moiety. The introduction of C7-methoxy or C7-ethoxy (**100 c,d**) resulted in higher cytotoxicity against the tested cell lines compared to the related 8-alkoxy derivatives (**100 t** and **100 u**). Notably, compound **100 i**, bearing a p-tolyloxy moiety, exhibited the most potent inhibitory activity against HCT116 and A2780 cell lines ($IC_{50}=0.25$ μM and $IC_{50}=2.06$ μM, respectively), thus being more potent than Entinostat. Additionally, compounds **100 p** and **100 s** demonstrated significant HDAC inhibitory activity in the tested cell lines ($IC_{50}=0.42$ μM and $IC_{50}=0.80$ μM, respectively, in HCT116; $IC_{50}=5.41$ μM and $IC_{50}=4.90$ μM, respectively, in A2780). Considering **100 a** as the simplest derivative bearing no substitution along the coumarin ring and displaying modest activity against HDAC in HCT116 and A2780 ($IC_{50}=11.41$ μM and $IC_{50}=54.92$ μM, respectively), further substitution in different positions of the coumarin ring led to higher inhibition activity. For instance, compound **100 b**, with a C6-bromo substituent on the coumarin ring, along with compounds **100 c–e**, **100 t**, and **100 u** containing various alkoxyl or benzyl groups at C8 or C7 positions, exhibited higher HDAC inhibitory potency than the reference compound **100 a**. These findings suggested that bulky R groups contributed to increased HDAC inhibitory activity, potentially related to the lipophilicity of the cap groups, enabling better penetration into the tested cell lines. The introduction of an O-benzyl substituent (**100 f**) displayed significant potency ($IC_{50}=2.49$ μM in HCT116 and $IC_{50}=12.82$ μM in A2780). Furthermore, the potency of O-benzyl substituted derivatives increased upon introducing electron-donating or electron-withdrawing groups onto the benzene ring. Compounds **100 g–i**, bearing o-, m-, or p-methyl groups on the O-benzyl moiety, exhibited high inhibitory potency. Among the halogen-substituted series (**100 k–p**), the highest potency was observed with a bromo substituent (**100 p**). Generally, *ortho*

substitution led to lower HDAC inhibitory potency compared to the corresponding *meta/para*-substituted derivatives (**100 g** vs. **100 h**; **100 k** vs **100 l** and **100 m**; **100 n** vs **100 o**). The introduction of the O-benzyl moiety at the 7-position of coumarin resulted in higher HDAC inhibition potency in HCT116 and A2780 cell lines compared to the corresponding O-alkoxy groups, in line with the previously discussed SAR data. Here, we review enzymatic assay data of selected benzyloxy coumarin derivatives (**100 e**, **100 j**, **100 p**, and **100 s**), which showed strong HDAC inhibitory activity in cellular total HDAC inhibition assay conducted on the HCT116 colon cancer cell lines and A2780 cancer cell lines. Compound **100 s** exhibited higher IC_{50} values against HDAC1 ($IC_{50}=0.47$ μM) showing a very similar effect to Entinostat ($IC_{50}=0.41$ μM) while also compounds **100 e**, **100 j** and **100 s** exhibited significant inhibitory activity ($IC_{50}=0.87$ μM, $IC_{50}=0.50$ μM and $IC_{50}=0.71$ μM; respectively). The research team utilized molecular docking studies to investigate the binding role of the coumarin structure within the active site. Compounds **100 e**, **100 j**, **100 p**, and **100 s** exhibited successful docking to HDAC1, binding in a similar manner to Entinostat. This suggests that the coumarin structure could be regarded as a valuable moiety for inclusion in HDACi structures.

4. Conclusions and Future Perspectives

To date, several compounds as potential HDAC inhibitors have been developed and can be classified by their zinc-binding group in major classes, which have different characteristics and, therefore, different potencies and selectivity over the various HDAC isoforms. As stated above in this review, changes in the cap and the linker regions cannot only influence the selectivity towards HDAC isoforms but also improve the inhibitory potency of the resulting compounds Therefore, various studies regarding the investigation of the cap and the linker areas have been pursued in order to achieve selective compounds, which can thus overcome both cancer resistance to drugs and tumor recurrence, which are still serious problems nowadays. The replacement of the known moieties of HDAC pharmacophore with heterocycles, or the hybridization with heterocyclic moieties known as anticancer ag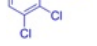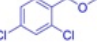ents, can be valuable options to fulfill this aim. Changes to HDACi are, however, not only carried out to improve potency and/or selectivity, but also intellectual properties such as patents might play a role. However, we focused in the present work on a summary of the very ample academic scientific literature. Indeed, many heterocyclic rings, such as quinolines, quinolones, and coumarins, have been largely studied for their therapeutic potential and, in combination with HDAC inhibitory moiety, might be more effective in counteracting cancer progression. As seen above, numerous compounds have been synthesized and tested showing promising inhibitory activity, as well as antiproliferative results. For instance, novel HDAC inhibitors bearing nitrogen atoms containing heterocycles, such as tetrahydroisoquinoline, pyridine, indazole, or tetrazole, showed promising inhibitory activity in the range of low nanomolar, and some of them

Table 48. Structures and inhibition data against cells extract HDACs (HCT116 and A2780) and against HDAC1 of new coumarin-based benzamides derivatives (**100 a–u**).[138]

Compound	R$_1$	R$_2$	R$_3$	Inhibition activity IC$_{50}$ (µM)		
				HDAC (HCT116 extract)	HDAC (A2780 extract)	HDAC1
100 a	–H	–H	–H	11.41	54.92	–
100 b	–H	–H	–Br	6.64	27.52	–
100 c	–H	–CH$_3$O	–H	3.08	21.62	–
100 d	–H	–CH$_3$CH$_2$O	–H	2.31	17.04	–
100 e	–H	–CH$_3$CH$_2$CH$_2$O	–H	1.09	14.81	0.87
100 f	–H	(benzyloxy)	–H	2.49	12.82	–
100 g	–H	(2-methylbenzyloxy)	–H	1.40	20.84	–
100 h	–H	(3-methylbenzyloxy)	–H	1.31	10.10	–
100 i	–H	(4-methylbenzyloxy)	–H	0.25	2.06	–
100 j	–H	(4-methoxybenzyloxy)	–H	1.00	6.52	0.71
100 k	–H	(2-fluorobenzyloxy)	–H	9.32	17.33	–
100 l	–H	(3-fluorobenzyloxy)	–H	3.73	15.77	–
100 m	–H	(4-fluorobenzyloxy)	–H	2.46	9.72	–
100 n	–H	(2-chlorobenzyloxy)	–H	4.76	10.09	–
100 o	–H	(4-chlorobenzyloxy)	–H	1.77	6.04	–
100 p	–H	(4-bromobenzyloxy)	–H	0.42	5.41	0.50
100 q	–H	(2,3-dichlorobenzyloxy)	–H	6.14	29.33	–
100 r	–H	(2,4-dichlorobenzyloxy)	–H	4.26	23.86	–
100 s	–H	(3,4-dichlorobenzyloxy)	–H	0.80	4.90	0.47
100 t	–CH$_3$O	–H	–H	5.17	40.09	–
100 u	–CH$_3$CH$_2$O	–H	–H	2.04	32.86	–
Entinostat	–	–	–	1.96	3.15	0.41

resulted in highly isoform-selective HDACi. Moreover, the presence of heteroatoms within the molecule often helps in creating additional interactions in the outer area of the enzyme and in the linker region as well, as demonstrated in several studies reported in this review.[57a,139] However, it remains challenging for medicinal chemists to turn these further interactions into more isoform-selective compounds, which remain difficult to achieve. Nonetheless, in the present review, we highlighted some studies that reached this goal, developing new highly selective molecules, particularly over HDAC6. These compounds might give rise to new possibilities for treating the multiple diseases in which HDAC6 is involved, besides cancer. Furthermore, incorporating a known heterocyclic moiety, such as β-carboline or quinazoline moieties, which have been studied for their safety and pharmacokinetic profile, could accelerate the developing process, and give medicinal chemists some hints for molecular optimization. In conclusion, this review provides a comprehensive summary of the main heterocycles containing HDAC inhibitors over the last fifteen years, analyzing the heterocycles' roles in modulating HDAC inhibition potency. Moreover, it can be a valuable summary for medicinal chemists who want to explore the chemical space around heterocycles towards more potent and selective HDAC-inhibiting compounds for the application in various HDAC-driven diseases with a favorable safety profile.

Author Contributions

Conceptualization, S.V., and C.Z.; formal analysis, A.R. and C.C.; A.R. and C.C.; writing-original draft preparation, A.R. and C. C.; writing-review and editing, A.M. S.V. and C.Z.; visualization, A.R. and C.C.; supervision, S.V. and C.Z.; funding acquisition, A.M., S.V. and C.Z. All authors have read and agreed to the published version of the manuscript.

Acknowledgements

Conflict of Interests

The authors declare no conflict of interest.

Data Availability Statement

The raw data supporting the conclusions of this article will be made available by the authors upon request.

Keywords: Epigenetics · HDAC inhibition · Heterocycles · Cancer

[1] a) T. Jenuwein, C. D. Allis, *Science* **2001**, *293*, 1074–1080; b) A. Gaspar-Maia, A. Alajem, E. Meshorer, M. Ramalho-Santos, *Nat. Rev. Mol. Cell Biol.* **2011**, *12*, 36–47.

[2] a) R. Margueron, P. Trojer, D. Reinberg, *Curr. Opin. Genet. Dev.* **2005**, *15*, 163–176; b) K. P. Nightingale, L. P. O'Neill, B. M. Turner, *Curr. Opin. Genet. Dev.* **2006**, *16*, 125–136.

[3] J. Choudhary, S. G. Grant, *Nat. Neurosci.* **2004**, *7*, 440–445.

[4] T. Kouzarides, *Curr. Opin. Genet. Dev.* **1999**, *9*, 40–48.

[5] a) K. Struhl, *Genes Dev.* **1998**, *12*, 599–606; b) O. Witt, H. E. Deubzer, T. Milde, I. Oehme, *Cancer Lett.* **2009**, *277*, 8–21.

[6] M. A. Glozak, N. Sengupta, X. Zhang, E. Seto, *Gene* **2005**, *363*, 15–23.

[7] M. Yoshida, N. Kudo, S. Kosono, A. Ito, *Proc Jpn Acad Ser B Phys Biol Sci* **2017**, *93*, 297–321.

[8] F. Fiorentino, C. Castiello, A. Mai, D. Rotili, *J. Med. Chem.* **2022**, *65*, 9580–9606.

[9] Y. Zhang, H. Fang, J. Jiao, W. Xu, *Curr. Med. Chem.* **2008**, *15*, 2840–2849.

[10] a) R. N. Saha, K. Pahan, *Cell Death Differ.* **2006**, *13*, 539–550; b) I. F. Harrison, D. T. Dexter, *Pharmacol. Ther.* **2013**, *140*, 34–52; c) J. Graff, D. Rei, J. S. Guan, W. Y. Wang, J. Seo, K. M. Hennig, T. J. Nieland, D. M. Fass, P. F. Kao, M. Kahn, S. C. Su, A. Samiei, N. Joseph, S. J. Haggarty, I. Delalle, L. H. Tsai, *Nature* **2012**, *483*, 222–226.

[11] a) L. Zhang, X. Qin, Y. Zhao, L. Fast, S. Zhuang, P. Liu, G. Cheng, T. C. Zhao, *J. Pharmacol. Exp. Ther.* **2012**, *341*, 285–293; b) H. J. Kee, I. S. Sohn, K. I. Nam, J. E. Park, Y. R. Qian, Z. Yin, Y. Ahn, M. H. Jeong, Y. J. Bang, N. Kim, J. K. Kim, K. K. Kim, J. A. Epstein, H. Kook, *Circulation* **2006**, *113*, 51–59; c) Y. Chen, J. Du, Y. T. Zhao, L. Zhang, G. Lv, S. Zhuang, G. Qin, T. C. Zhao, *Cardiovasc Diabetol* **2015**, *14*, 99.

[12] a) Y. Hu, B. A. Suliman, in *Regulation of Inflammatory Signaling in Health and Disease*, **2017**, pp. 91–110; b) F. Leoni, A. Zaliani, G. Bertolini, G. Porro, P. Pagani, P. Pozzi, G. Dona, G. Fossati, S. Sozzani, T. Azam, P. Bufler, G. Fantuzzi, I. Goncharov, S. H. Kim, B. J. Pomerantz, L. L. Reznikov, B. Siegmund, C. A. Dinarello, P. Mascagni, *Proc. Natl. Acad. Sci. USA* **2002**, *99*, 2995–3000.

[13] a) A. Mai, S. Massa, D. Rotili, I. Cerbara, S. Valente, R. Pezzi, S. Simeoni, R. Ragno, *Med. Res. Rev.* **2005**, *25*, 261–309; b) M. Biel, V. Wascholowski, A. Giannis, *Angew. Chem. Int. Ed. Engl.* **2005**, *44*, 3186–3216.

[14] T. C. S. Ho, A. H. Y. Chan, A. Ganesan, *J. Med. Chem.* **2020**, *63*, 12460–12484.

[15] M. S. Finnin, J. R. Donigian, A. Cohen, V. M. Richon, R. A. Rifkind, P. A. Marks, R. Breslow, N. P. Pavletich, *Nature* **1999**, *401*, 188–193.

[16] a) M. Paris, M. Porcelloni, M. Binaschi, D. Fattori, *J. Med. Chem.* **2008**, *51*, 1505–1529; b) X. Hou, J. Du, R. Liu, Y. Zhou, M. Li, W. Xu, H. Fang, *J. Chem. Inf. Model.* **2015**, *55*, 861–871; c) P. Bertrand, *Eur. J. Med. Chem.* **2010**, *45*, 2095–2116.

[17] S. Clive, M. M. Woo, T. Nydam, L. Kelly, M. Squier, M. Kagan, *Cancer Chemother. Pharmacol.* **2012**, *70*, 513–522.

[18] M. Dokmanovic, C. Clarke, P. A. Marks, *Mol. Cancer Res.* **2007**, *5*, 981–989.

[19] a) K. Chen, L. Xu, O. Wiest, *J. Org. Chem.* **2013**, *78*, 5051–5055; b) D. Wang, P. Helquist, O. Wiest, *J. Org. Chem.* **2007**, *72*, 5446–5449.

[20] A. D. Bondarev, M. M. Attwood, J. Jonsson, V. N. Chubarev, V. V. Tarasov, H. B. Schioth, *Br. J. Clin. Pharmacol.* **2021**, *87*, 4577–4597.

[21] a) J. E. Bradner, N. West, M. L. Grachan, E. F. Greenberg, S. J. Haggarty, T. Warnow, R. Mazitschek, *Nat. Chem. Biol.* **2010**, *6*, 238–243; b) P. Jones, in *Epigenetic Targets in Drug Discovery*, **2009**, pp. 185–223.

[22] J. J. McClure, X. Li, C. J. Chou, **2018**, pp. 183–211.

[23] L. Santo, T. Hideshima, A. L. Kung, J. C. Tseng, D. Tamang, M. Yang, M. Jarpe, J. H. van Duzer, R. Mazitschek, W. C. Ogier, D. Cirstea, S. Rodig, H. Eda, T. Scullen, M. Canavese, J. Bradner, K. C. Anderson, S. S. Jones, N. Raje, *Blood* **2012**, *119*, 2579–2589.

[24] P. Huang, I. Almeciga-Pinto, M. Jarpe, J. H. van Duzer, R. Mazitschek, M. Yang, S. S. Jones, S. N. Quayle, *Oncotarget* **2017**, *8*, 2694–2707.

ChemMedChem

Review

doi.org/10.1002/cmdc.202400194

Chemistry
Europe

European Chemical
Societies Publishing

[25] a) A. Ganesan, *ChemMedChem* **2016**, *11*, 1227–1241; b) A. R. de Lera, A. Ganesan, *Curr. Opin. Chem. Biol.* **2020**, *57*, 135–154.

[26] a) X. Cai, H. X. Zhai, J. Wang, J. Forrester, H. Qu, L. Yin, C. J. Lai, R. Bao, C. Qian, *J. Med. Chem.* **2010**, *53*, 2000–2009; b) T. J. Galloway, L. J. Wirth, A. D. Colevas, J. Gilbert, J. E. Bauman, N. F. Saba, D. Raben, R. Mehra, A. W. Ma, R. Atoyan, J. Wang, B. Burtness, A. Jimeno, *Clin. Cancer Res.* **2015**, *21*, 1566–1573.

[27] T. Mehrling, Y. Chen, *Anti-Cancer Agents Med. Chem.* **2016**, *16*, 20–28.

[28] R. Furumai, A. Matsuyama, N. Kobashi, K. H. Lee, M. Nishiyama, H. Nakajima, A. Tanaka, Y. Komatsu, N. Nishino, M. Yoshida, S. Horinouchi, *Cancer Res.* **2002**, *62*, 4916–4921.

[29] P. Atadja, L. Perez, in *Successful Drug Discovery*, **2016**, pp. 59–88.

[30] a) P. Atadja, *Cancer Lett.* **2009**, *280*, 233–241; b) P. Revill, N. Mealy, N. Serradell, J. Bolos, E. Rosa, *Drugs Future* **2007**, *32*, 315–322.

[31] R. M. Poole, *Drugs* **2014**, *74*, 1543–1554.

[32] S. Mandl-Weber, F. G. Meinel, R. Jankowsky, F. Oduncu, R. Schmidmaier, P. Baumann, *Br. J. Haematol.* **2010**, *149*, 518–528.

[33] M. Bitzer, M. Horger, E. G. Giannini, T. M. Ganten, M. A. Worns, J. T. Siveke, G. M. Dollinger, G. Gerken, M. E. Scheulen, H. Wege, V. Zagonel, U. Cillo, F. Trevisani, A. Santoro, V. Montesarchio, N. P. Malek, J. Holzapfel, T. Herz, A. S. Ammendola, S. Pegoraro, B. Hauns, A. Mais, U. M. Lauer, S. W. Henning, B. Hentsch, *J. Hepatol.* **2016**, *65*, 280–288.

[34] a) V. Novotny-Diermayr, K. Sangthongpitag, C. Y. Hu, X. Wu, N. Sausgruber, P. Yeo, G. Greicius, S. Pettersson, A. L. Liang, Y. K. Loh, Z. Bonday, K. C. Goh, H. Hentze, S. Hart, H. Wang, K. Ethirajulu, J. M. Wood, *Mol. Cancer Ther.* **2010**, *9*, 642–652; b) H. Wang, N. Yu, D. Chen, K. C. Lee, P. L. Lye, J. W. Chang, W. Deng, M. C. Ng, T. Lu, M. L. Khoo, A. Poulsen, K. Sangthongpitag, X. Wu, C. Hu, K. C. Goh, X. Wang, L. Fang, K. L. Goh, H. H. Khng, S. K. Goh, P. Yeo, X. Liu, Z. Bonday, J. M. Wood, B. W. Dymock, E. Kantharaj, E. T. Sun, *J. Med. Chem.* **2011**, *54*, 4694–4720.

[35] L. Catley, E. Weisberg, Y. T. Tai, P. Atadja, S. Remiszewski, T. Hideshima, N. Mitsiades, R. Shringarpure, R. LeBlanc, D. Chauhan, N. C. Munshi, R. Schlossman, P. Richardson, J. Griffin, K. C. Anderson, *Blood* **2003**, *102*, 2615–2622.

[36] J. M. Wagner, B. Hackanson, M. Lubbert, M. Jung, *Clin Epigenetics* **2010**, *1*, 117–136.

[37] A. Mullard, *Nat. Rev. Drug Discovery* **2024**, *23*, 88–95.

[38] S. Consalvi, C. Mozzetta, P. Bettica, M. Germani, F. Fiorentini, F. Del Bene, M. Rocchetti, F. Leoni, V. Monzani, P. Mascagni, P. L. Puri, V. Saccone, *Mol. Med.* **2013**, *19*, 79–87.

[39] P. Bettica, S. Petrini, V. D'Oria, A. D'Amico, M. Catteruccia, M. Pane, S. Sivo, F. Magri, S. Brajkovic, S. Messina, G. L. Vita, B. Gatti, M. Moggio, P. L. Puri, M. Rocchetti, G. De Nicolao, G. Vita, G. P. Comi, E. Bertini, E. Mercuri, *Neuromuscul Disord* **2016**, *26*, 643–649.

[40] a) X. Lu, Z. Ning, Z. Li, H. Cao, X. Wang, *Intractable Rare Dis Res* **2016**, *5*, 185–191; b) M. Yoshimitsu, K. Ando, T. Ishida, S. Yoshida, I. Choi, M. Hidaka, Y. Takamatsu, M. Gillings, G. T. Lee, H. Onogi, K. Tobinai, *Jpn. J. Clin. Oncol.* **2022**, *52*, 1014–1020.

[41] C. J. Chou, D. Herman, J. M. Gottesfeld, *J. Biol. Chem.* **2008**, *283*, 35402–35409.

[42] Q. C. Ryan, D. Headlee, M. Acharya, A. Sparreboom, J. B. Trepel, J. Ye, W. D. Figg, K. Hwang, E. J. Chung, A. Murgo, G. Melillo, Y. Elsayed, M. Monga, M. Kalnitskiy, J. Zwiebel, E. A. Sausville, *J. Clin. Oncol.* **2005**, *23*, 3912–3922.

[43] M. Fournel, C. Bonfils, Y. Hou, P. T. Yan, M. C. Trachy-Bourget, A. Kalita, J. Liu, A. H. Lu, N. Z. Zhou, M. F. Robert, J. Gillespie, J. J. Wang, H. Ste-Croix, J. Rahil, S. Lefebvre, O. Moradei, D. Delorme, A. R. Macleod, J. M. Besterman, Z. Li, *Mol. Cancer Ther.* **2008**, *7*, 759–768.

[44] A. C. Bretz, U. Parnitzke, K. Kronthaler, T. Dreker, R. Bartz, F. Hermann, A. Ammendola, T. Wulff, S. Hamm, *J Immunother Cancer* **2019**, *7*, 294.

[45] J. Jampilek, *Molecules* **2019**, *24*.

[46] A. Citarella, D. Moi, L. Pinzi, D. Bonanni, G. Rastelli, *ACS Omega* **2021**, *6*, 21843–21849.

[47] J. R. Somoza, R. J. Skene, B. A. Katz, C. Mol, J. D. Ho, A. J. Jennings, C. Luong, A. Arvai, J. J. Buggy, E. Chi, J. Tang, B. C. Sang, E. Verner, R. Wynands, E. M. Leahy, D. R. Dougan, G. Snell, M. Navre, M. W. Knuth, R. V. Swanson, D. E. McRee, L. W. Tari, *Structure* **2004**, *12*, 1325–1334.

[48] a) I. S. Ignatyev, M. Montejo, P. G. Rodriguez Ortega, J. J. Gonzalez, *J. Mol. Model.* **2013**, *19*, 1819–1834; b) N. J. Porter, A. Mahendran, R. Breslow, D. W. Christianson, *Proc. Natl. Acad. Sci. USA* **2017**, *114*, 13459–13464.

[49] S. Geurs, D. Clarisse, K. De Bosscher, M. D'Hooghe, *J. Med. Chem.* **2023**, *66*, 7698–7729.

[50] a) L. Zhang, J. Zhang, Q. Jiang, L. Zhang, W. Song, *J. Enzyme Inhib. Med. Chem.* **2018**, *33*, 714–721; b) A. G. Kazantsev, L. M. Thompson, *Nat. Rev. Drug Discovery* **2008**, *7*, 854–868.

[51] S. Tasneem, M. M. Alam, M. Amir, M. Akhter, S. Parvez, G. Verma, L. M. Nainwal, A. Equbal, T. Anwer, M. Shaquiquzzaman, *Mini-Rev. Med. Chem.* **2022**, *22*, 1648–1706.

[52] M. Mottamal, S. Zheng, T. L. Huang, G. Wang, *Molecules* **2015**, *20*, 3898–3941.

[53] A. Hameed, M. Al-Rashida, M. Uroos, S. A. Ali, Arshia, M. Ishtiaq, K. M. Khan, *Expert Opin. Ther. Pat.* **2018**, *28*, 281–297.

[54] a) T. Liu, F. Peng, X. Cao, F. Liu, Q. Wang, L. Liu, W. Xue, *ACS Omega* **2021**, *6*, 30826–30833; b) H.-X. Wang, H.-Y. Liu, W. Li, S. Zhang, Z. Wu, X. Li, C.-W. Li, Y.-M. Liu, B.-Q. Chen, *Med. Chem. Res.* **2018**, *28*, 203–214.

[55] Q. Zhang, Y. Li, B. Zhang, B. Lu, J. Li, *Bioorg. Med. Chem. Lett.* **2017**, *27*, 4885–4888.

[56] I. Raji, K. Ahluwalia, A. K. Oyelere, *Bioorg. Med. Chem. Lett.* **2017**, *27*, 744–749.

[57] a) D. T. Hieu, D. T. Anh, N. M. Tuan, P. T. Hai, L. T. Huong, J. Kim, J. S. Kang, T. K. Vu, P. T. P. Dung, S. B. Han, N. H. Nam, N. D. Hoa, *Bioorg. Chem.* **2018**, *76*, 258–267; b) D. T. Hieu, D. T. Anh, P. T. Hai, L. T. Huong, E. J. Park, J. C. Choi, J. S. Kang, P. T. P. Dung, S. B. Han, N. H. Nam, *Chem. Biodiversity* **2018**, *15*, e1800027.

[58] M. Patel, R. J. McHugh, Jr., B. C. Cordova, R. M. Klabe, S. Erickson-Viitanen, G. L. Trainor, J. D. Rodgers, *Bioorg. Med. Chem. Lett.* **2000**, *10*, 1729–1731.

[59] D. Gupta, N. N. Ghosh, R. Chandra, *Bioorg. Med. Chem. Lett.* **2005**, *15*, 1019–1022.

[60] O. I. El-Sabbagh, M. E. El-Sadek, S. M. Lashine, S. H. Yassin, S. M. El-Nabtity, *Med. Chem. Res.* **2009**, *18*, 782–797.

[61] A. Carta, P. Sanna, L. Gherardini, D. Usai, S. Zanetti, *Farmaco* **2001**, *56*, 933–938.

[62] M. A. Ali, M. S. Yar, *J. Enzyme Inhib. Med. Chem.* **2007**, *22*, 183–189.

[63] D. T. Hieu, D. T. Anh, P. T. Hai, N. T. Thuan, L. T. Huong, E. J. Park, A. Young Ji, J. Soon Kang, P. T. Phuong Dung, S. B. Han, N. H. Nam, *Chem. Biodiversity* **2019**, *16*, e1800502.

[64] Z. Yang, T. Wang, F. Wang, T. Niu, Z. Liu, X. Chen, C. Long, M. Tang, D. Cao, X. Wang, W. Xiang, Y. Yi, L. Ma, J. You, L. Chen, *J. Med. Chem.* **2016**, *59*, 1455–1470.

[65] J. Chen, Z. Sang, Y. Jiang, C. Yang, L. He, *Chem. Biol. Drug Des.* **2019**, *93*, 232–241.

[66] a) J. Dhuguru, O. A. Ghoneim, *Molecules* **2022**, *27*; b) Y. Pan, H. Hou, B. Zhou, J. Gao, F. Gao, *Eur. J. Med. Chem.* **2023**, *262*, 115879.

[67] G. Balasubramanian, N. Kilambi, S. Rathinasamy, P. Rajendran, S. Narayanan, S. Rajagopal, *J. Enzyme Inhib. Med. Chem.* **2014**, *29*, 555–562.

[68] a) R. E. Hawtin, D. E. Stockett, J. A. Byl, R. S. McDowell, T. Nguyen, M. R. Arkin, A. Conroy, W. Yang, N. Osheroff, J. A. Fox, *PLoS One* **2010**, *5*, e10186; b) U. Hoch, J. Lynch, Y. Sato, S. Kashimoto, F. Kajikawa, Y. Furutani, J. A. Silverman, *Cancer Chemother. Pharmacol.* **2009**, *64*, 53–65.

[69] N. Relitti, A. P. Saraswati, G. Chemi, M. Brindisi, S. Brogi, D. Herp, K. Schmidtkunz, F. Saccoccia, G. Ruberti, C. Ulivieri, F. Vanni, F. Sarno, L. Altucci, S. Lamponi, M. Jung, S. Gemma, S. Butini, G. Campiani, *Eur. J. Med. Chem.* **2021**, *212*, 112998.

[70] A. Bracken, A. Pocker, H. Raistrick, *Biochem. J.* **1954**, *57*, 587–595.

[71] a) C. L. Hamblett, L. J. Methot, D. M. Mampreian, D. L. Sloman, M. G. Stanton, A. M. Kral, J. C. Fleming, J. C. Cruz, M. Chenard, N. Ozerova, A. M. Hitz, H. Wang, S. V. Deshmukh, N. Nazef, A. Harsch, B. Hughes, W. K. Dahlberg, A. A. Szewczak, R. E. Middleton, R. T. Mosley, J. P. Secrist, T. A. Miller, *Bioorg. Med. Chem. Lett.* **2007**, *17*, 5300–5309; b) J. L. Methot, P. K. Chakravarty, M. Chenard, J. Close, J. C. Cruz, W. K. Dahlberg, J. Fleming, C. L. Hamblett, J. E. Hamill, P. Harrington, A. Harsch, R. Heidebrecht, B. Hughes, J. Jung, C. M. Kenific, A. M. Kral, P. T. Meinke, R. E. Middleton, N. Ozerova, D. L. Sloman, M. G. Stanton, A. A. Szewczak, S. Tyagarajan, D. J. Witter, J. P. Secrist, T. A. Miller, *Bioorg. Med. Chem. Lett.* **2008**, *18*, 973–978; c) J. L. Methot, D. M. Hoffman, D. J. Witter, M. G. Stanton, P. Harrington, C. Hamblett, P. Siliphaivanh, K. Wilson, J. Hubbs, R. Heidebrecht, A. M. Kral, N. Ozerova, J. C. Fleming, H. Wang, A. A. Szewczak, R. E. Middleton, B. Hughes, J. C. Cruz, B. B. Haines, M. Chenard, C. M. Kenific, A. Harsch, J. P. Secrist, T. A. Miller, *ACS Med. Chem. Lett.* **2014**, *5*, 340–345.

[72] C. Zwergel, E. Di Bello, R. Fioravanti, M. Conte, A. Nebbioso, R. Mazzone, G. Brosch, C. Mercurio, M. Varasi, L. Altucci, S. Valente, A. Mai, *ChemMedChem* **2021**, *16*, 989–999.

[73] E. Di Bello, V. Sian, G. Bontempi, C. Zwergel, R. Fioravanti, B. Noce, C. Castiello, S. Tomassi, D. Corinti, D. Passeri, R. Pellicciari, C. Mercurio, M.

ChemMedChem

Review

doi.org/10.1002/cmdc.202400194

Chemistry
Europe

European Chemical
Societies Publishing

Varasi, L. Altucci, M. Tripodi, R. Strippoli, A. Nebbioso, S. Valente, A. Mai, *Eur. J. Med. Chem.* **2023**, *247*, 115022.

[74] D. T. Oanh, H. V. Hai, S. H. Park, H. J. Kim, B. W. Han, H. S. Kim, J. T. Hong, S. B. Han, V. T. Hue, N. H. Nam, *Bioorg. Med. Chem. Lett.* **2011**, *21*, 7509–7512.

[75] a) D. A. Erlanson, R. S. McDowell, T. O'Brien, *J. Med. Chem.* **2004**, *47*, 3463–3482; b) E. R. Zartler, M. J. Shapiro, *Curr. Opin. Chem. Biol.* **2005**, *9*, 366–370.

[76] J. Liu, J. Zhou, F. He, L. Gao, Y. Wen, L. Gao, P. Wang, D. Kang, L. Hu, *Eur. J. Med. Chem.* **2020**, *192*, 112189.

[77] a) J. M. Llovet, R. K. Kelley, A. Villanueva, A. G. Singal, E. Pikarsky, S. Roayaie, R. Lencioni, K. Koike, J. Zucman-Rossi, R. S. Finn, *Nat Rev Dis Primers* **2021**, *7*, 6; b) A. Huang, X. R. Yang, W. Y. Chung, A. R. Dennison, J. Zhou, *Signal Transduct Target Ther* **2020**, *5*, 146.

[78] Z. Lai, H. Ni, X. Hu, S. Cui, *J. Med. Chem.* **2023**, *66*, 10791–10807.

[79] M. E. Riveiro, A. Moglioni, R. Vazquez, N. Gomez, G. Facorro, L. Piehl, E. R. de Celis, C. Shayo, C. Davio, *Bioorg. Med. Chem.* **2008**, *16*, 2665–2675.

[80] Y. Shikishima, Y. Takaishi, G. Honda, M. Ito, Y. Takfda, O. K. Kodzhimatov, O. Ashurmetov, K. H. Lee, *Chem Pharm Bull (Tokyo)* **2001**, *49*, 877–880.

[81] A. Asadipour, M. Alipour, M. Jafari, M. Khoobi, S. Emami, H. Nadri, A. Sakhteman, A. Moradi, V. Sheibani, F. Homayouni Moghadam, A. Shafiee, A. Foroumadi, *Eur. J. Med. Chem.* **2013**, *70*, 623–630.

[82] D. A. Ostrov, J. A. Hernandez Prada, P. E. Corsino, K. A. Finton, N. Le, T. C. Rowe, *Antimicrob. Agents Chemother.* **2007**, *51*, 3688–3698.

[83] J. Dandriyal, R. Singla, M. Kumar, V. Jaitak, *Eur. J. Med. Chem.* **2016**, *119*, 141–168.

[84] M. Kaur, S. Kohli, S. Sandhu, Y. Bansal, G. Bansal, *Anti-Cancer Agents Med. Chem.* **2015**, *15*, 1032–1048.

[85] F. Yang, N. Zhao, J. Song, K. Zhu, C. S. Jiang, P. Shan, H. Zhang, *Molecules* **2019**, *24*.

[86] Y. Ling, C. Xu, L. Luo, J. Cao, J. Feng, Y. Xue, Q. Zhu, C. Ju, F. Li, Y. Zhang, Y. Zhang, X. Ling, *J. Med. Chem.* **2015**, *58*, 9214–9227.

[87] M. Zhao, L. Bi, W. Wang, C. Wang, M. Baudy-Floc'h, J. Ju, S. Peng, *Bioorg. Med. Chem.* **2006**, *14*, 6998–7010.

[88] J. Wu, M. Zhao, K. Qian, K. H. Lee, S. Morris-Natschke, S. Peng, *Eur. J. Med. Chem.* **2009**, *44*, 4153–4161.

[89] Y. Ling, J. Guo, Q. Yang, P. Zhu, J. Miao, W. Gao, Y. Peng, J. Yang, K. Xu, B. Xiong, G. Liu, J. Tao, L. Luo, Q. Zhu, Y. Zhang, *Eur. J. Med. Chem.* **2018**, *144*, 398–409.

[90] N. H. Nam, T. L. Huong, T. M. Dung do, P. T. Dung, D. T. Oanh, D. Quyen, T. Thao le, S. H. Park, K. R. Kim, B. W. Han, J. Yun, J. S. Kang, Y. Kim, S. B. Han, *Eur. J. Med. Chem.* **2013**, *70*, 477–486.

[91] D. T. Anh, P. T. Hai, D. T. M. Dung, P. T. P. Dung, L. T. Huong, E. J. Park, H. W. Jun, J. S. Kang, J. H. Kwon, T. T. Tung, S. B. Han, N. H. Nam, *Bioorg. Med. Chem. Lett.* **2020**, *30*, 127537.

[92] a) M. Aldeghi, S. Malhotra, D. L. Selwood, A. W. Chan, *Chem. Biol. Drug Des.* **2014**, *83*, 450–461; b) D. F. Veber, S. R. Johnson, H. Y. Cheng, B. R. Smith, K. W. Ward, K. D. Kopple, *J. Med. Chem.* **2002**, *45*, 2615–2623.

[93] M. Brindisi, J. Senger, C. Cavella, A. Grillo, G. Chemi, S. Gemma, D. M. Cucinella, S. Lamponi, F. Sarno, C. Iside, A. Nebbioso, E. Novellino, T. B. Shaik, C. Romier, D. Herp, M. Jung, S. Butini, G. Campiani, L. Altucci, S. Brogi, *Eur. J. Med. Chem.* **2018**, *157*, 127–138.

[94] A. P. Saraswati, N. Relitti, M. Brindisi, J. D. Osko, G. Chemi, S. Federico, A. Grillo, S. Brogi, N. H. McCabe, R. C. Turkington, O. Ibrahim, J. O'Sullivan, S. Lamponi, M. Ghanim, V. P. Kelly, D. Zisterer, R. Amet, P. Hannon Barroeta, F. Vanni, C. Ulivieri, D. Herp, F. Sarno, A. Di Costanzo, F. Saccoccia, G. Ruberti, M. Jung, L. Altucci, S. Gemma, S. Butini, D. W. Christianson, G. Campiani, *ACS Med. Chem. Lett.* **2020**, *11*, 2268–2276.

[95] R. De Vreese, Y. Depetter, T. Verhaeghe, T. Desmet, V. Benoy, W. Haeck, L. Van Den Bosch, M. D'Hooghe, *Org. Biomol. Chem.* **2016**, *14*, 2537–2549.

[96] L. Van Helleputte, V. Benoy, L. Van Den Bosch, *Research and Reports in Biology* **2014**.

[97] M. R. Shakespear, M. A. Halili, K. M. Irvine, D. P. Fairlie, M. J. Sweet, *Trends Immunol.* **2011**, *32*, 335–343.

[98] R. De Vreese, L. Galle, Y. Depetter, J. Franceus, T. Desmet, K. Van Hecke, V. Benoy, L. Van Den Bosch, M. D'Hooghe, *Chemistry* **2017**, *23*, 128–136.

[99] N. Ressing, M. Sonnichsen, J. D. Osko, A. Scholer, J. Schliehe-Diecks, A. Skerhut, A. Borkhardt, J. Hauer, M. U. Kassack, D. W. Christianson, S. Bhatia, F. K. Hansen, *J. Med. Chem.* **2020**, *63*, 10339–10351.

[100] Y. Depetter, S. Geurs, R. De Vreese, S. Goethals, E. Vandoorn, A. Laevens, J. Steenbrugge, E. Meyer, P. de Tullio, M. Bracke, M. D'Hooghe, O. De Wever, *Int. J. Cancer* **2019**, *145*, 735–747.

[101] a) A. Rau, W. S. Lieb, O. Seifert, J. Honer, D. Birnstock, F. Richter, N. Aschmoneit, M. A. Olayioye, R. E. Kontermann, *Mol. Cancer Ther.* **2020**, *19*, 1474–1485; b) E. M. Huber, M. Groll, *Angew. Chem. Int. Ed. Engl.* **2012**, *51*, 8708–8720.

[102] P. Guan, F. Sun, X. Hou, F. Wang, F. Yi, W. Xu, H. Fang, *Bioorg. Med. Chem.* **2012**, *20*, 3865–3872.

[103] B. Vergani, G. Sandrone, M. Marchini, C. Ripamonti, E. Cellupica, E. Galbiati, G. Caprini, G. Pavich, G. Porro, I. Rocchio, M. Lattanzio, M. Pezzuto, P. Skorupska, P. Cordella, P. Pagani, P. Pozzi, R. Pomarico, D. Modena, F. Leoni, R. Perego, C. Steinkuhler, A. Stevenazzi, *J. Med. Chem.* **2019**, *62*, 10711–10739.

[104] V. Simon, S. Cavalu, S. Simon, H. Mocuta, E. Vanea, M. Prinz, M. Neumann, *Solid State Ionics* **2009**, *180*, 764–769.

[105] K. Bhat, K. Sufeera, S. K. Chaitanya, *J Young Pharm* **2011**, *3*, 310–314.

[106] S. Valente, D. Trisciuoglio, T. De Luca, A. Nebbioso, D. Labella, A. Lenoci, C. Bigogno, G. Dondio, M. Miceli, G. Brosch, D. Del Bufalo, L. Altucci, A. Mai, *J. Med. Chem.* **2014**, *57*, 6259–6265.

[107] S. Valente, M. Tardugno, M. Conte, R. Cirilli, A. Perrone, R. Ragno, S. Simeoni, A. Tramontano, S. Massa, A. Nebbioso, M. Miceli, G. Franci, G. Brosch, L. Altucci, A. Mai, *ChemMedChem* **2011**, *6*, 698–712.

[108] J. Cai, H. Wei, K. H. Hong, X. Wu, M. Cao, X. Zong, L. Li, C. Sun, J. Chen, M. Ji, *Eur. J. Med. Chem.* **2015**, *96*, 1–13.

[109] J. Cai, H. Wei, K. H. Hong, X. Wu, X. Zong, M. Cao, P. Wang, L. Li, C. Sun, B. Chen, G. Zhou, J. Chen, M. Ji, *Bioorg. Med. Chem.* **2015**, *23*, 3457–3471.

[110] K. Fang, G. Dong, Y. Li, S. He, Y. Wu, S. Wu, W. Wang, C. Sheng, *ACS Med. Chem. Lett.* **2018**, *9*, 312–317.

[111] S. Shen, M. Hadley, K. Ustinova, J. Pavlicek, T. Knox, S. Noonepalle, M. T. Tavares, C. A. Zimprich, G. Zhang, M. B. Robers, C. Barinka, A. P. Kozikowski, A. Villagra, *J. Med. Chem.* **2019**, *62*, 8557–8577.

[112] I. N. Gaisina, W. Tueckmantel, A. Ugolkov, S. Shen, J. Hoffen, O. Dubrovskyi, A. Mazar, R. A. Schoon, D. Billadeau, A. P. Kozikowski, *ChemMedChem* **2016**, *11*, 81–92.

[113] Y. Zhang, J. B. Ying, J. J. Hong, F. C. Li, T. T. Fu, F. Y. Yang, G. X. Zheng, X. J. Yao, Y. Lou, Y. Qiu, W. W. Xue, F. Zhu, *ACS Chem. Neurosci.* **2019**, *10*, 2467–2480.

[114] Y. Zhang, J. Feng, C. Liu, L. Zhang, J. Jiao, H. Fang, L. Su, X. Zhang, J. Zhang, M. Li, B. Wang, W. Xu, *Bioorg. Med. Chem.* **2010**, *18*, 1761–1772.

[115] J. Arts, P. Angibaud, A. Marien, W. Floren, B. Janssens, P. King, J. van Dun, L. Janssen, T. Geerts, R. W. Tuman, D. L. Johnson, L. Andries, M. Jung, M. Janicot, K. van Emelen, *Br. J. Cancer* **2007**, *97*, 1344–1353.

[116] P. Angibaud, K. Van Emelen, L. Decrane, S. van Brandt, P. Ten Holte, I. Pilatte, B. Roux, V. Poncelet, D. Speybrouck, L. Queguiner, S. Gaurrand, A. Marien, W. Floren, L. Janssen, M. Verdonck, J. van Dun, J. van Gompel, E. Gilissen, C. Mackie, M. Du Jardin, J. Peeters, M. Noppe, L. Van Hijfte, E. Freyne, M. Page, M. Janicot, J. Arts, *Bioorg. Med. Chem. Lett.* **2010**, *20*, 294–298.

[117] C. Rossi, M. Porcelloni, P. D'Andrea, C. I. Fincham, A. Ettorre, S. Mauro, A. Squarcia, M. Bigioni, M. Parlani, F. Nardelli, M. Binaschi, C. A. Maggi, D. Fattori, *Bioorg. Med. Chem. Lett.* **2011**, *21*, 2305–2308.

[118] P. Karagianni, J. Wong, *Oncogene* **2007**, *26*, 5439–5449.

[119] X. Ai-Hua, L. Bo–Yu, L. Chen-Zhong, L. Zhi-Bin, L. Xian-Ping, S. Le-Ming, Z. Jia-Ju, *Acta Physico-Chimica Sinica* **2004**, *20*, 569–572.

[120] C. Bressi, M. Porcellana, P. M. Marinaccio, E. P. Nocito, L. Magri, *J. Nerv. Ment. Dis.* **2010**, *198*, 647–652.

[121] B. E. Lauffer, R. Mintzer, R. Fong, S. Mukund, C. Tam, I. Zilberleyb, B. Flicke, A. Ritscher, G. Fedorowicz, R. Vallero, D. F. Ortwine, J. Gunzner, Z. Modrusan, L. Neumann, C. M. Koth, P. J. Lupardus, J. S. Kaminker, C. E. Heise, P. Steiner, *J. Biol. Chem.* **2013**, *288*, 26926–26943.

[122] L. Verna, J. Whysner, G. M. Williams, *Pharmacol. Ther.* **1996**, *71*, 83–105.

[123] F. F. Wagner, M. Weiwer, M. Steinbacher, A. Schomburg, P. Reinemer, J. P. Gale, A. J. Campbell, S. L. Fisher, W. N. Zhao, S. A. Reis, K. M. Hennig, M. Thomas, P. Muller, M. R. Jefson, D. M. Fass, S. J. Haggarty, Y. L. Zhang, E. B. Holson, *Bioorg. Med. Chem.* **2016**, *24*, 4008–4015.

[124] T. Lee, M. Cho, S. Y. Ko, H. J. Youn, D. J. Baek, W. J. Cho, C. Y. Kang, S. Kim, *J. Med. Chem.* **2007**, *50*, 585–589.

[125] D. Kumar, V. Kumar, R. Marwaha, G. Singh, *Current Bioactive Compounds* **2019**, *15*, 271–279.

[126] C. M. Marson, C. J. Matthews, S. J. Atkinson, N. Lamadema, N. S. Thomas, *J. Med. Chem.* **2015**, *58*, 6803–6818.

[127] Y. Li, Y. Wang, N. Xie, M. Xu, P. Qian, Y. Zhao, S. Li, *Eur. J. Med. Chem.* **2015**, *100*, 270–276.

[128] S. Sharma, J. Singh, R. Ojha, H. Singh, M. Kaur, P. M. S. Bedi, K. Nepali, *Eur. J. Med. Chem.* **2016**, *112*, 298–346.

[129] B. M. Muller, L. Jana, A. Kasajima, A. Lehmann, J. Prinzler, J. Budczies, K. J. Winzer, M. Dietel, W. Weichert, C. Denkert, *BMC Cancer* **2013**, *13*, 215.

[130] R. Buurman, E. Gurlevik, V. Schaffer, M. Eilers, M. Sandbothe, H. Kreipe, L. Wilkens, B. Schlegelberger, F. Kuhnel, B. Skawran, *Gastroenterology* **2012**, *143*, 811–820 e815.

[131] K. Nepali, T. Y. Chang, M. J. Lai, K. C. Hsu, Y. Yen, T. E. Lin, S. B. Lee, J. P. Liou, *Eur. J. Med. Chem.* **2020**, *196*, 112291.

[132] P. T. Mao, W. B. He, X. Mai, L. H. Feng, N. Li, Y. J. Liao, C. S. Zhu, J. Li, T. Chen, S. H. Liu, Q. M. Zhang, L. He, *Bioorg. Med. Chem.* **2022**, *56*, 116599.

[133] A. Vaisburg, I. Paquin, N. Bernstein, S. Frechette, F. Gaudette, S. Leit, O. Moradei, S. Raeppel, N. Zhou, G. Bouchain, S. H. Woo, Z. Jin, J. Gillespie, J. Wang, M. Fournel, P. T. Yan, M. C. Trachy-Bourget, M. F. Robert, A. Lu, J. Yuk, J. Rahil, A. R. Macleod, J. M. Besterman, Z. Li, D. Delorme, *Bioorg. Med. Chem. Lett.* **2007**, *17*, 6729–6733.

[134] A. Converso, T. Hartingh, R. M. Garbaccio, E. Tasber, K. Rickert, M. E. Fraley, Y. Yan, C. Kreatsoulas, S. Stirdivant, B. Drakas, E. S. Walsh, K. Hamilton, C. A. Buser, X. Mao, M. T. Abrams, S. C. Beck, W. Tao, R. Lobell, L. Sepp-Lorenzino, J. Zugay-Murphy, V. Sardana, S. K. Munshi, S. M. Jezequel-Sur, P. D. Zuck, G. D. Hartman, *Bioorg. Med. Chem. Lett.* **2009**, *19*, 1240–1244.

[135] C. Cheng, F. Yun, J. He, S. Ullah, Q. Yuan, *Eur. J. Med. Chem.* **2019**, *173*, 185–202.

[136] Z. Zhang, Q. Zhang, H. Zhang, M. Jiao, Z. Guo, X. Peng, L. Fu, J. Li, *Bioorg. Chem.* **2021**, *117*, 105407.

[137] D. T. Gerokonstantis, C. Mantzourani, D. Gkikas, K. C. Wu, H. N. Hoang, I. Triandafillidi, I. Barbayianni, P. Kanellopoulou, A. C. Kokotos, P. Moutevelis-Minakakis, V. Aidinis, P. K. Politis, D. P. Fairlie, G. Kokotos, *J. Med. Chem.* **2023**, *66*, 14357–14376.

[138] T. Abdizadeh, M. R. Kalani, K. Abnous, Z. Tayarani-Najaran, B. Z. Khashyarmanesh, R. Abdizadeh, R. Ghodsi, F. Hadizadeh, *Eur. J. Med. Chem.* **2017**, *132*, 42–62.

[139] a) Q. Zhang, B. Lu, J. Li, *Bioorg. Med. Chem. Lett.* **2017**, *27*, 3162–3166; b) F. Zhu, X. Meng, H. Liang, C. Sheng, G. Dong, D. Liu, S. Wu, *Bioorg. Chem.* **2022**, *122*, 105702; c) X. H. Zhang, M. Qin, H. P. Wu, M. Y. Khamis, Y. H. Li, L. Y. Ma, H. M. Liu, *J. Med. Chem.* **2021**, *64*, 1362–1391; d) D. Chen, C. K. Soh, W. H. Goh, Z. Wang, H. Wang, *Bioorg. Chem.* **2020**, *98*, 103724.